

GWs for cosmology

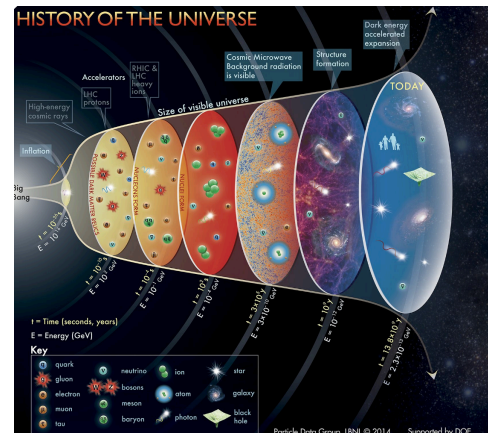
Lecture 2

Danièle Steer



- Lecture 1: – **Overview** on early- and late-time cosmology with GWs; current and future experiments, – **orders of magnitude**
- Lecture 2: – Late-time cosmology: GWs and $d_L(z)$
 - GWs in theories beyond GR, $d_L^{GW}(z)$
 - **standard sirens I**: Measuring H_0 with GWs and O3 results of LVK
 - Back to early-time universe: an example of what physics we can probe.
- Lecture 3 (Chiara Caprini):
 - *cosmological* stochastic GW background: **early-universe cosmology with GWs**
Solutions of the GW propagation equation in FLRW; its calculation for different sources (inflation, topological defects, first order phase transitions)
- Lecture 4 (Nicola Tamanini):
 - **Standard sirens II**: more details, statistical methods, future prospects
- Lecture 5 (Tania Regimbau):
 - **astrophysical stochastic GW background**: Definition/statistical properties, pulsar timing arrays and background from supermassive BH binaries, LVK results, prospects for the future.

Gravitational waves for cosmology



late-time universe



Individual resolvable astrophysical sources and populations of sources

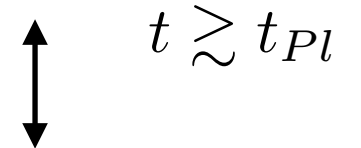
at cosmological distances

e.g. binary neutron stars (BNS),
binary black holes (BBH),
neutron star-black-hole binary (NS-BH)
Rotating asymmetric neutron stars
supernova explosions...



- Expansion rate $H(z)$
- Hubble constant H_0
- Ω_m
- beyond Λ CDM, dark energy $w(z)$
- late-time modified gravity (modified GW propagation)
- astrophysics; eg populations of BBHs
-

Very early universe until today



Stochastic GW background
astrophysical and cosmological origin

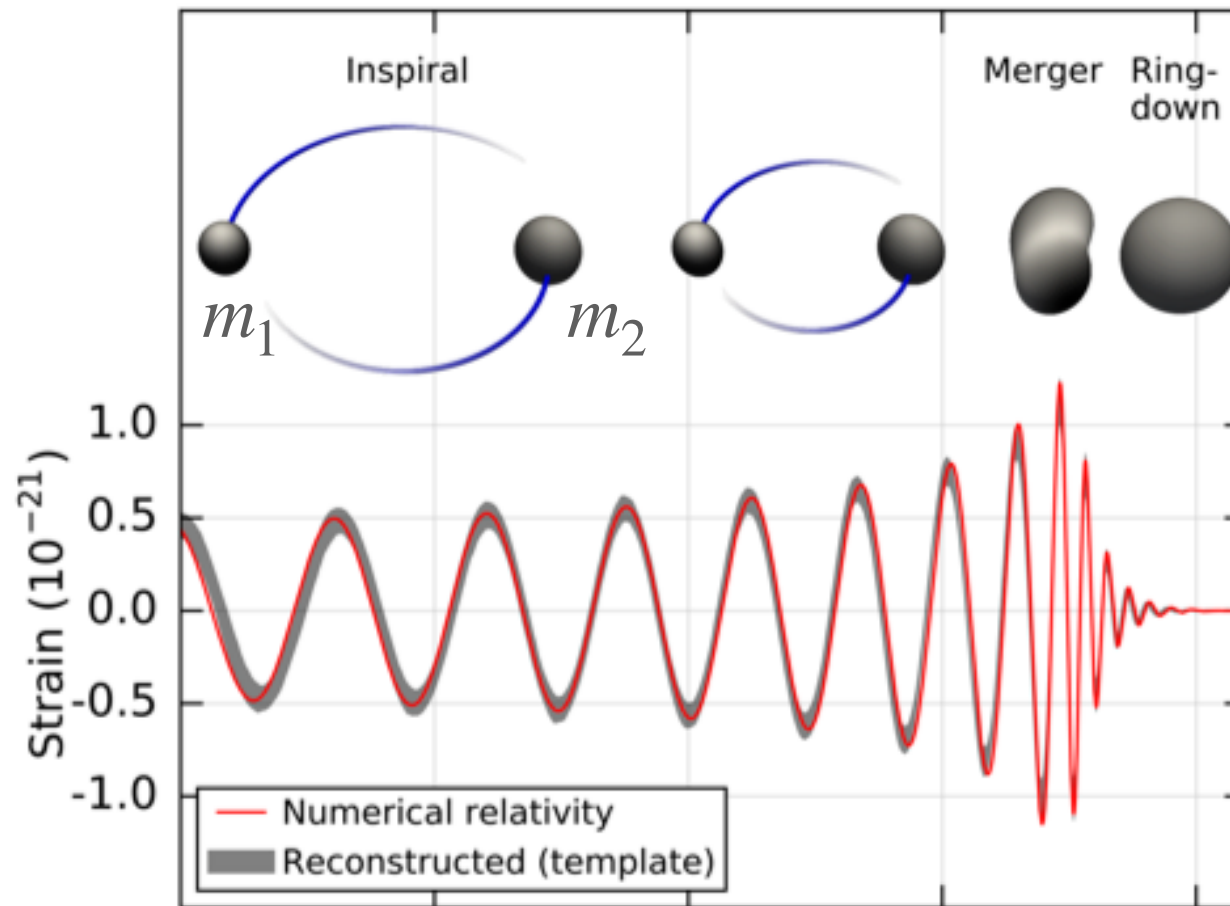


$$\Omega_{\text{gw}}(t_0, f) = \frac{f}{\rho_c} \frac{d\rho_{\text{gw}}}{df}(t_0, f)$$



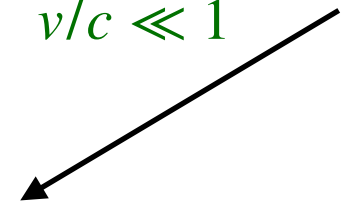
- population of BH, white dwarfs..
- inflationary GWs
- 1st order Phase transitions
- topological defects
- scalar induced GWs
- primordial black holes
- axions
- early modified gravity...

More speculative. Early universe sources beyond standard model of particle physics!



$$g_{\mu\nu} = \eta_{\mu\nu} + h_{\mu\nu} + \dots$$

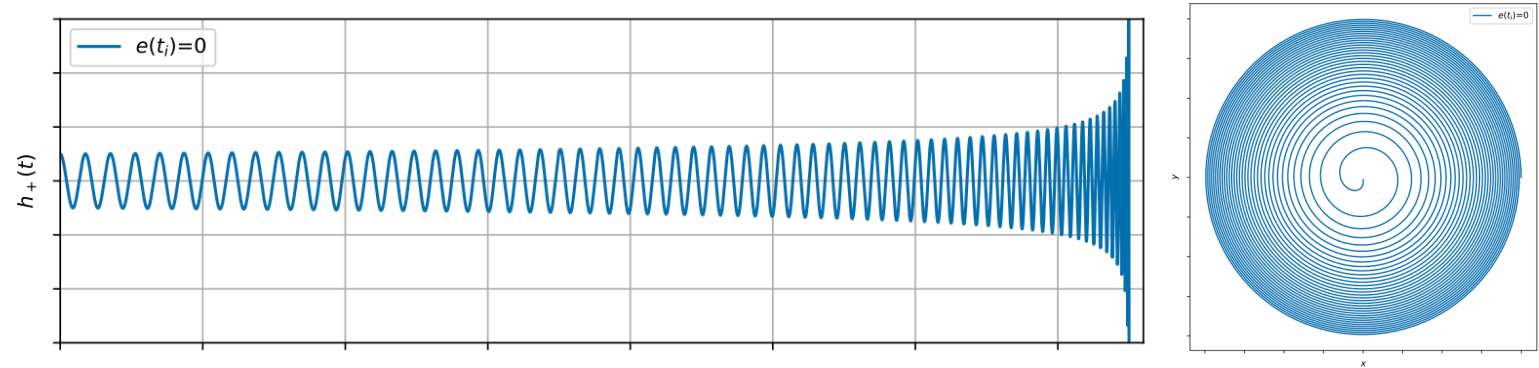
$$v/c \ll 1$$



- The *inspiral phase* can be understood with perturbation theory (the “post-Newtonian (PN) expansion” of the Einstein equations) presented below, more details in (Thorne 1980 ; Blanchet 2006 ; Poisson and Will 2014).
- The *merger phase* generally requires numerical relativity other other techniques such as effective one-body techniques, see e.g. (Deruelle and Uzan 2018) for an introduction.
- The *ringdown phase* can also be approached with perturbative methods, namely BH perturbation theory, see e.g. (Kokkotas and Schmidt 1999 ; Santoni 2024).

We estimated orders of magnitude for the *inspiral phase*

[assumptions (i) lowest order PN expansion; (ii) point particles of mass m_1 and m_2 , no tidal effects, (iii) no spins, (iv) Circular orbits, (v) and **ignoring cosmology** (assumed a flat space-time)]



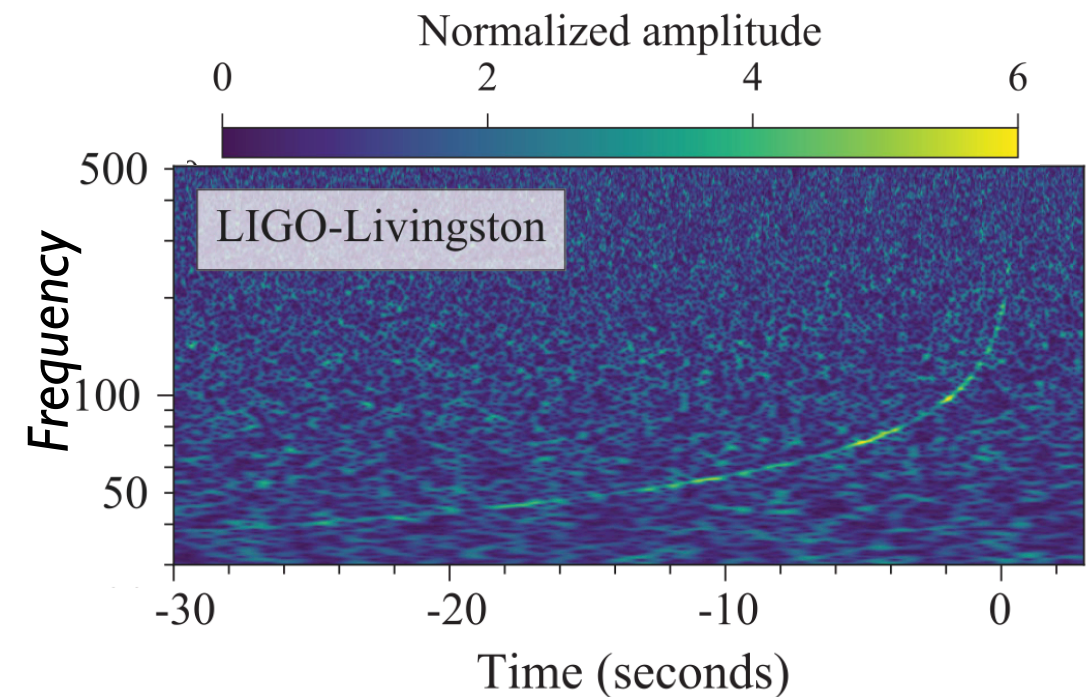
– Frequency:
$$f_{\text{GW}}(t) = \frac{1}{\pi} \left(\frac{G\mathcal{M}}{c^3} \right)^{-5/8} \left(\frac{5}{256} \right)^{3/8} (t - t_c)^{-3/8}$$

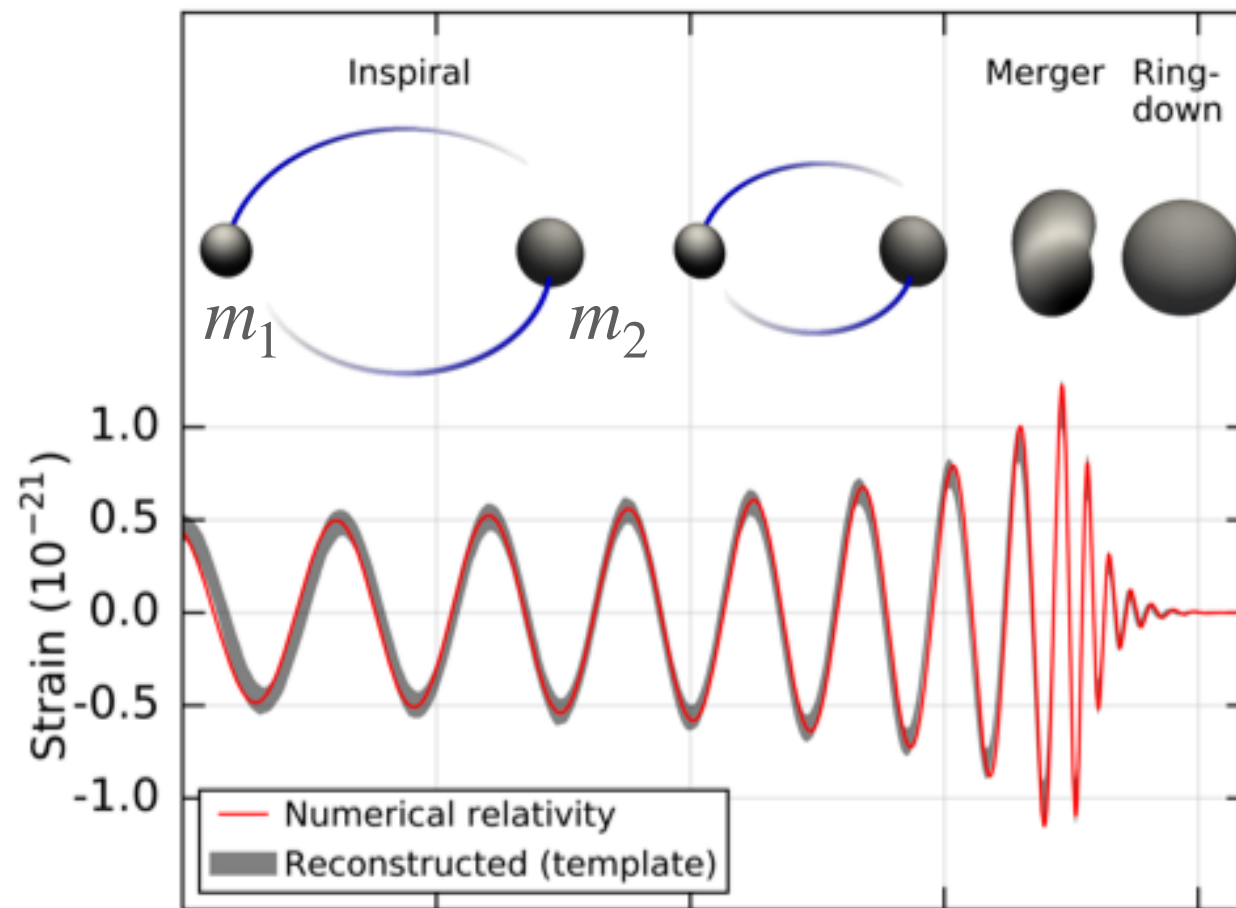
with chirp mass $\mathcal{M} \equiv \frac{(m_1 m_2)^{3/5}}{(m_1 + m_2)^{1/5}}$

– merger frequency:
$$f_{\text{merger}} \simeq \frac{1}{6^{3/2}} \left(\frac{c^3}{G(m_1 + m_2)} \right)$$

– Time in detector band f_{low} :
$$T \sim 10^{-3} f_{\text{low}}^{-8/3} \left(\frac{c^3}{G\mathcal{M}} \right) \quad (\text{assuming } f_{\text{low}} \ll f_{\text{merger}})$$

– gravitational wave polarisations:
$$h_{+, \times} \sim \frac{4}{R} \left(\frac{G\mathcal{M}}{c^2} \right)^{5/3} \left(\frac{\pi f_{\text{GW}}}{c} \right)^{2/3}$$



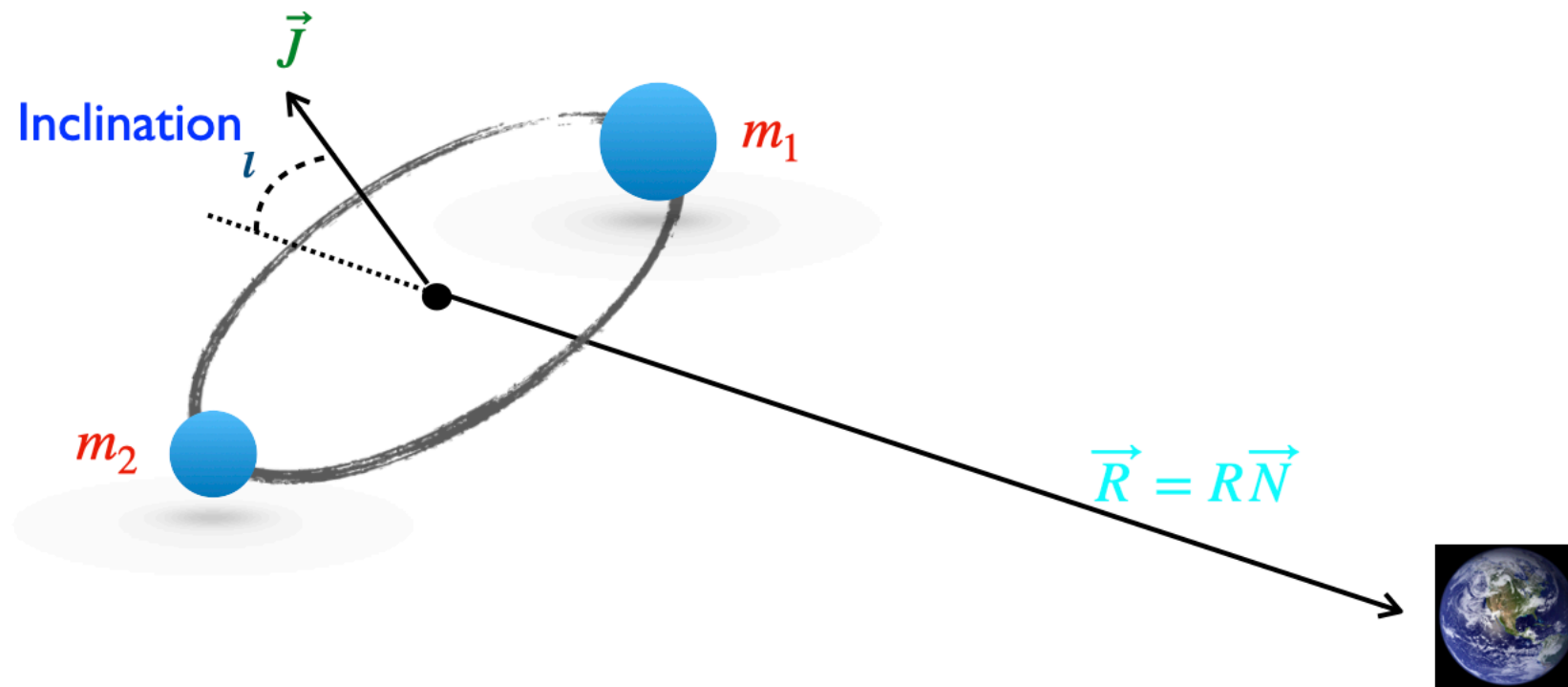


different phenomenological waveform models, calibrated to numerical-relativity simulations, including spins, eccentricity, higher order modes, ringdown....

- The *inspiral phase* can be understood with perturbation theory (the “post-Newtonian (PN) expansion” of the Einstein equations) presented below, more details in (Thorne 1980 ; Blanchet 2006 ; Poisson and Will 2014).
- The *merger phase* generally requires numerical relativity other other techniques such as effective one-body techniques, see e.g. (Deruelle and Uzan 2018) for an introduction.
- The *ringdown phase* can also be approached with perturbative methods, namely BH perturbation theory, see e.g. (Kokkotas and Schmidt 1999 ; Santoni 2024).

We estimated orders of magnitude for the *inspiral phase*

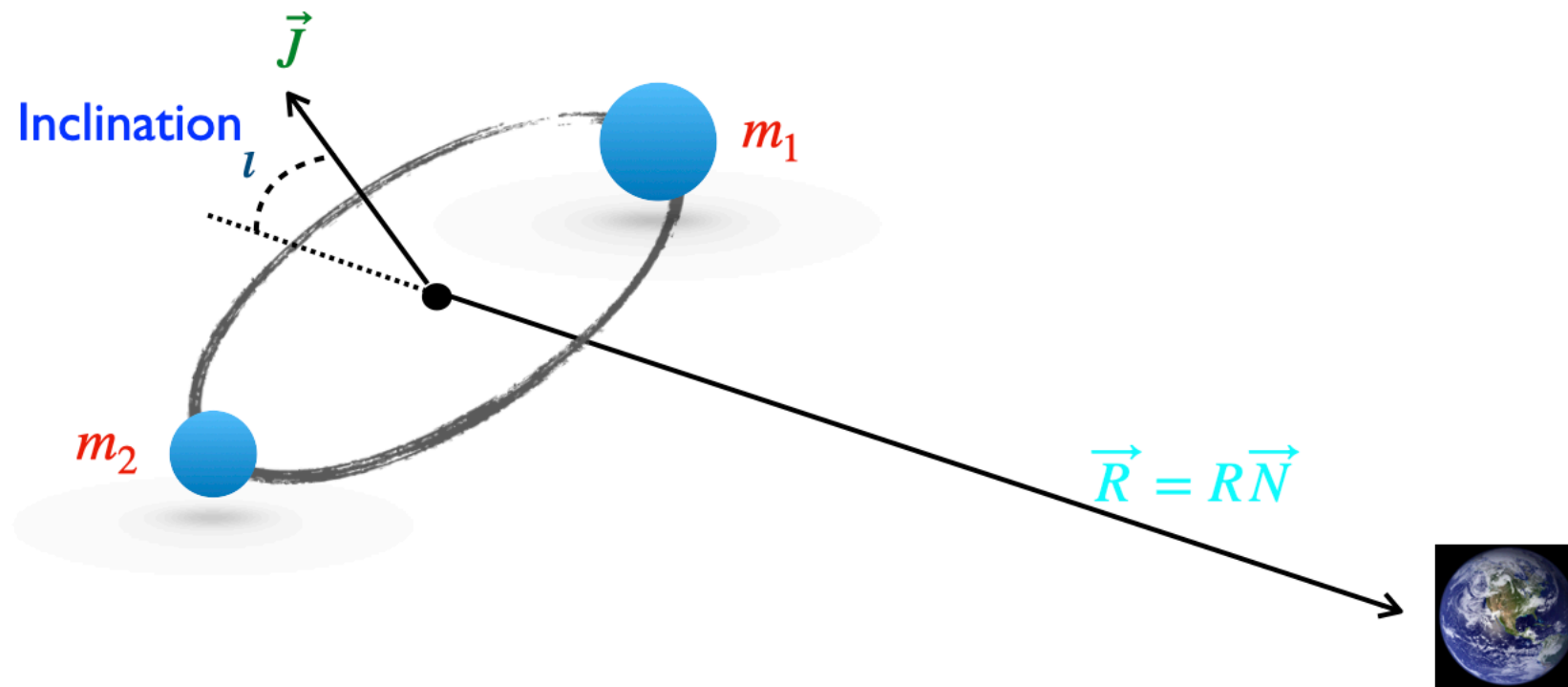
[assumptions (i) lowest order PN expansion; (ii) point particles of mass m_1 and m_2 , no tidal effects, (iii) no spins, (iv) Circular orbits, (v) and **ignoring cosmology** (assumed a flat space-time)]



– gravitational wave polarisations : $h_{+, \times} \sim \frac{4}{R} \left(\frac{G \mathcal{M}}{c^2} \right)^{5/3} \left(\frac{\pi f_{\text{GW}}}{c} \right)^{2/3} \cdot (\text{inclination angle factors})$

We estimated orders of magnitude for the *inspiral phase*

[assumptions (i) lowest order order PN expansion; (ii) point particles of mass m_1 and m_2 , no tidal effects, (iii) no spins, (iv) Circular orbits, (v) and **ignoring cosmology** (assumed a flat space-time)]



$$h_+ = \frac{4}{R} \left(\frac{G\mathcal{M}}{c^2} \right)^{5/3} \left(\frac{\pi f_{\text{GW}}(t_R)}{c} \right)^{2/3} \frac{1 + \cos^2 i}{2} \cdot \cos(2\Phi(t_R))$$

$$h_\times = \frac{4}{R} \left(\frac{G\mathcal{M}}{c^2} \right)^{5/3} \left(\frac{\pi f_{\text{GW}}(t_R)}{c} \right)^{2/3} \cos i \cdot \cos(2\Phi(t_R))$$

with $\Phi(t) = \int_{t_c}^t 2\pi f_{\text{GW}}(t') dt' + \Phi(t_c)$

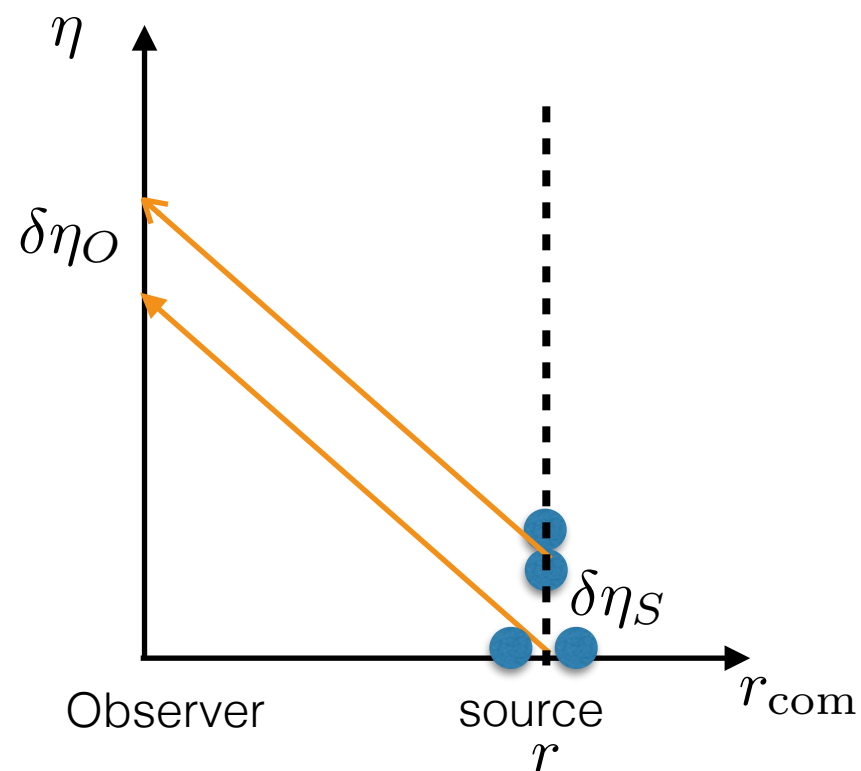
$$= -2 \left(\frac{t_R}{5G\mathcal{M}} \right)^{5/8} + \Phi(t_c)$$

– gravitational wave polarisations : $h_{+,\times} \sim \frac{4}{R} \left(\frac{G\mathcal{M}}{c^2} \right)^{5/3} \left(\frac{\pi f_{\text{GW}}}{c} \right)^{2/3} \cdot (\text{inclination angle factors})$

Inspiral of compact binaries at cosmological distances

Turn on expansion, FRWL universe.

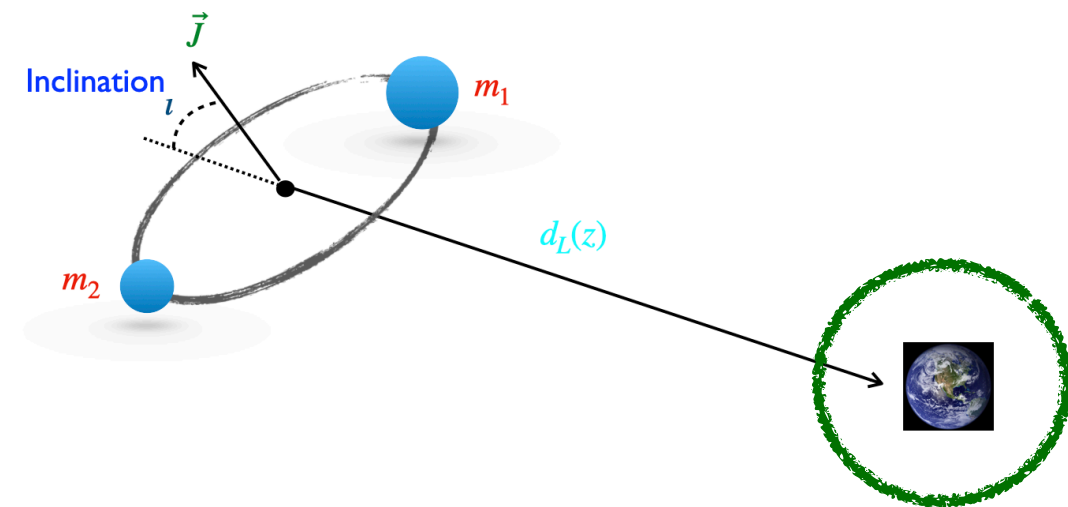
$$ds^2 = -dt^2 + a^2(t)d\vec{x}^2 = a^2(\eta)[-d\eta^2 + d\vec{x}^2]$$



Idea:

- in local wave-zone of the source (scales large relative to source, small relative to Hubble), have previous solution

- then propagate it in FRWL space-time to observer



– Standard time dilation

$$dt = \frac{a(t_0)}{a(t_s)} dt_s = (1 + z) dt_s$$

$$f = \frac{f_s}{1 + z}$$

– GW amplitude scales as a^{-1} : why?

From source to observer:

- Perturbed FRWL metric (ignoring scalars and vectors):

$$ds^2 = -dt^2 + a^2(t) \left[(\delta_{ij} + h_{ij}^{\text{TT}}) dx^i dx^j \right]$$

$$|h_{ij}| \ll 1$$

$$h^i_i = \partial_j h^j_i = 0$$

- Linearised Einstein equations $\square h_{ij}^{\text{TT}} = \bar{\nabla}_\mu \bar{\nabla}^\mu h_{ij}^{\text{TT}} = 0$, away from the source

$$\ddot{h}_{ij}^{\text{TT}}(t, \vec{x}) + 3H\dot{h}_{ij}^{\text{TT}}(t, \vec{x}) - \frac{\bar{\nabla}^2}{a^2} h_{ij}^{\text{TT}}(t, \vec{x}) = 0$$

- In conformal time ($' = d/d\eta$) and Fourier space

$$h_{ij}^{\prime\prime\text{TT}}(\eta, \vec{k}) + 2\mathcal{H}h_{ij}^{\prime\text{TT}}(\eta, \vec{k}) - k^2 h_{ij}^{\text{TT}}(\eta, \vec{k}) = 0 \quad \text{with } \mathcal{H} = \frac{a'}{a}$$

- Change of variable

$$h = \frac{Q}{a} \Rightarrow Q'' + \left(k^2 - \frac{a''}{a} \right) Q = 0$$

- On subHubble scales $Q'' + k^2 Q \sim 0 \Rightarrow Q \sim e^{\pm ik\eta}$

- Thus for sub-Hubble modes

$$h(\vec{k}, \eta) = \frac{A(\vec{k})}{a(\eta)} e^{ik\eta} + \frac{B(\vec{k})}{a(\eta)} e^{-ik\eta}$$

Redshifting amplitude

at source

$$h_+(t_s, \vec{x}) = \frac{4}{R} \left(\frac{G\mathcal{M}}{c^2} \right)^{5/3} \left(\frac{\pi f_{\text{GW}}(t_R^s)}{c} \right)^{2/3} \frac{1 + \cos^2 \iota}{2} \cdot \cos(2\Phi(t_R^s))$$

$$h_\times(t_s, \vec{x}) = \frac{4}{R} \left(\frac{G\mathcal{M}}{c^2} \right)^{5/3} \left(\frac{\pi f_{\text{GW}}(t_R^s)}{c} \right)^{2/3} \cos \iota \cdot \cos(2\Phi(t_R^s))$$

$$\Phi(t_R^s) = -2 \left(\frac{t_R^s}{5G\mathcal{M}} \right)^{5/8} + \Phi(t_c)$$

Becomes at the observer

$$h_+(t, \vec{x}) = \frac{4}{d_L} \left(\frac{G\mathcal{M}_z}{c^2} \right)^{5/3} \left(\frac{\pi f_{\text{GW}}(t_R)}{c} \right)^{2/3} \frac{1 + \cos^2 \iota}{2} \cdot \cos(2\Phi(t_R))$$

$$h_\times(t, \vec{x}) = \frac{4}{d_L} \left(\frac{G\mathcal{M}_z}{c^2} \right)^{5/3} \left(\frac{\pi f_{\text{GW}}(t_R)}{c} \right)^{2/3} \cos \iota \cdot \cos(2\Phi(t_R))$$

$$\Phi(t_R^s) = -2 \left(\frac{t_R}{5G\mathcal{M}_z} \right)^{5/8} + \Phi(t_c)$$

- Phase depends on **redshifted chirp mass**

Amplitude depends on the **luminosity distance**

$$d_L = a(t_0)R(1+z)$$

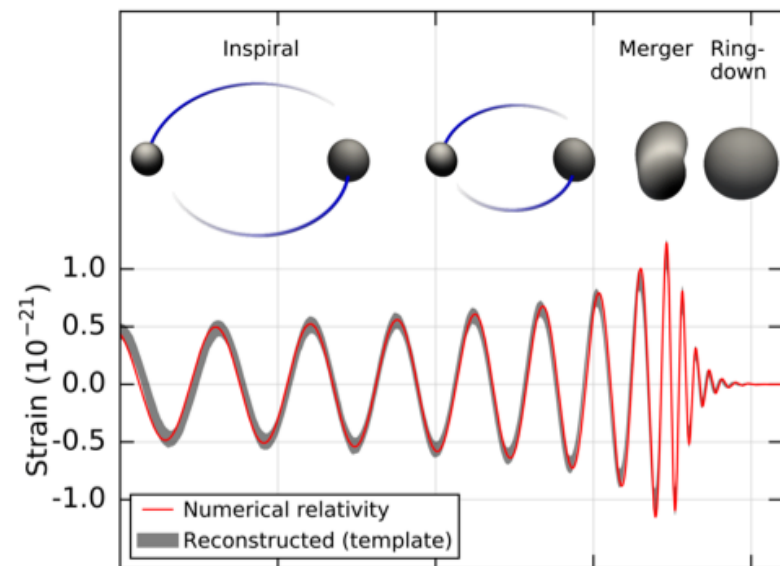
$$d_L(z) = \frac{c(1+z)}{H_0} \int_0^z \frac{dz'}{[\Omega_m(1+z')^3 + \Omega_\Lambda(1+z')^{3(1+w(z'))}]^{1/2}}$$

$$m_{1,2}^{\text{det}}(z) = (1+z)m_{1,2}$$

$$\mathcal{M}_z = (1+z)\mathcal{M}$$

redshifted / detector frame masses

Cosmological setting



→ $\text{fn}(t; \mathcal{M}_z)$

$\text{fn}(d_L; \mathcal{M}_z)$

• Phase:

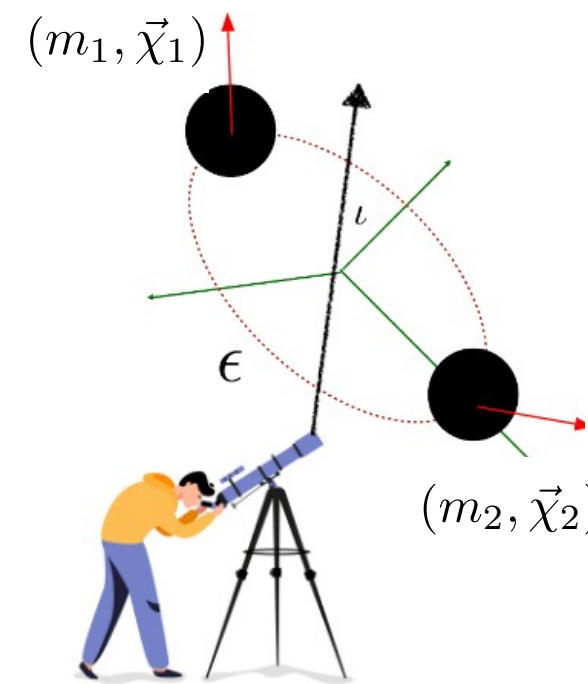
$$m_{1,2}^{\text{det}}(z) = (1+z)m_{1,2}$$

$$\mathcal{M}_z = (1+z)\mathcal{M}$$

• Amplitude:

$$d_L, \mathcal{M}_z, \iota, \dots$$

dominant quadrupole mode: degeneracy between distance and inclination gives *large*, even up to 40% errors on luminosity distance.

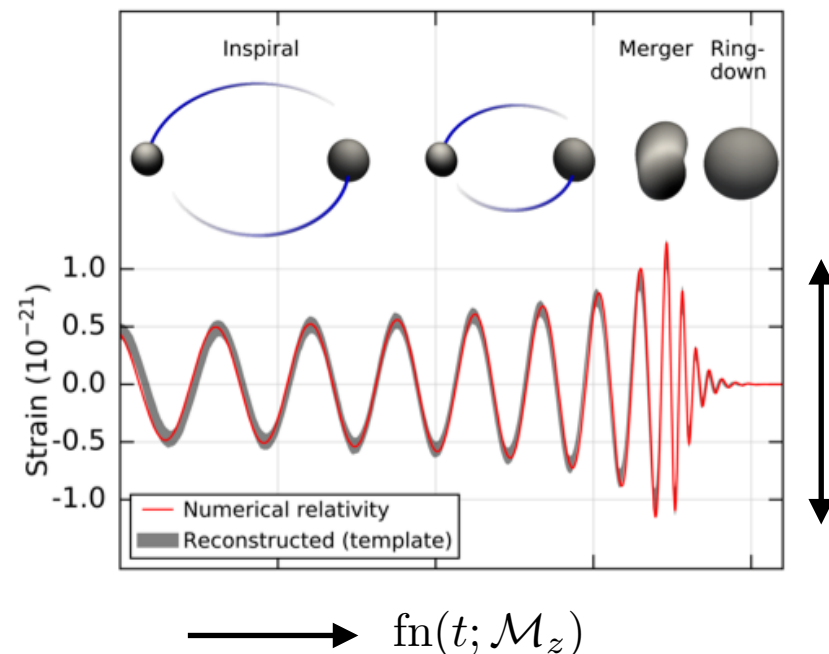


Fisher matrix analysis

$$\frac{\Delta \mathcal{A}}{\mathcal{A}} \sim 0.1 \left(\frac{10}{\rho} \right)$$

$$\frac{\Delta \mathcal{M}_z}{\mathcal{M}_z} \sim 10^{-5} \left(\frac{10}{\rho} \right) \left(\frac{\mathcal{M}_z}{M_\odot} \right)^{5/3}.$$

Cosmological setting



dominant quadrupole mode: degeneracy between distance and inclination gives *large*, up to -40% errors on luminosity distance.

- Phase:

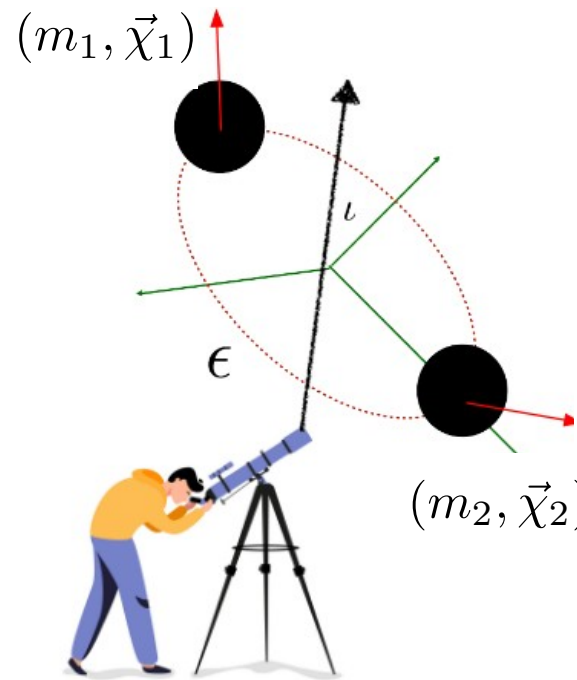
$$m_{1,2}^{\text{det}}(z) = (1+z)m_{1,2}$$

$$\mathcal{M}_z = (1+z)\mathcal{M}$$

chirp mass $\mathcal{M} = \frac{(m_1 m_2)^{3/5}}{(m_1 + m_2)^{1/5}}$

- Amplitude:

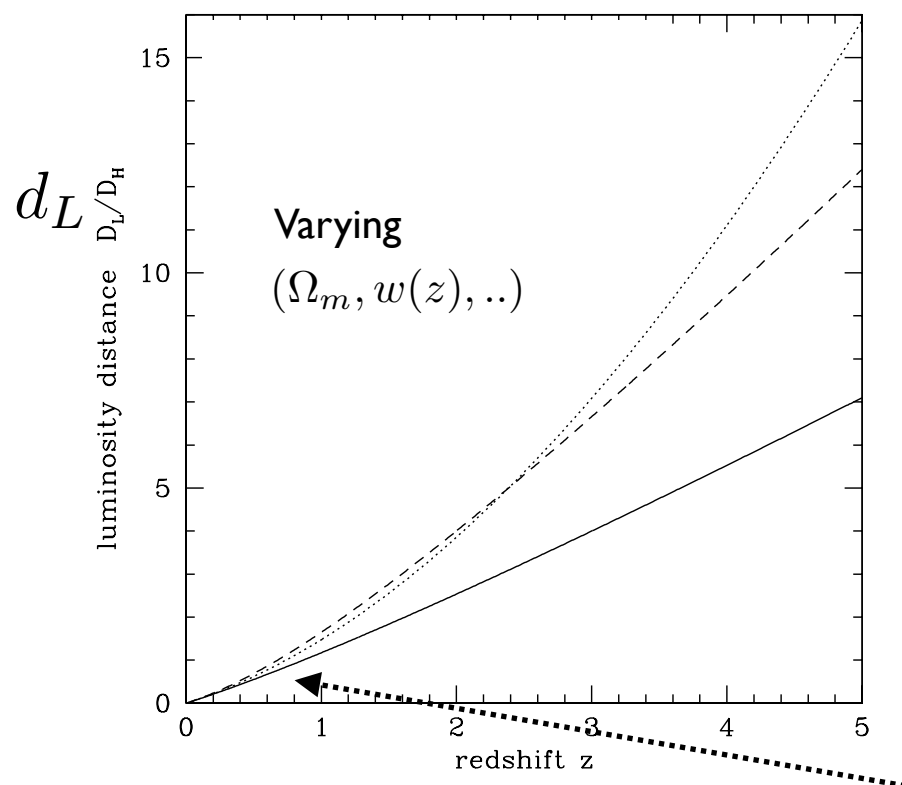
$$d_L, \mathcal{M}_z, l, \dots$$



Fisher matrix analysis

$$\frac{\Delta \mathcal{A}}{\mathcal{A}} \sim 0.1 \left(\frac{10}{\rho} \right)$$

$$\frac{\Delta \mathcal{M}_z}{\mathcal{M}_z} \sim 10^{-5} \left(\frac{10}{\rho} \right) \left(\frac{\mathcal{M}_z}{M_\odot} \right)^{5/3}$$



$$d_L(z) = \frac{c(1+z)}{H_0} \int_0^z \frac{dz'}{[\Omega_m(1+z')^3 + \Omega_\Lambda(1+z')^{3(1+w(z'))}]^{1/2}}$$

- But for point sources, perfect degeneracy between source masses, redshift, spins. Some extra non gravitational information necessary to determine z .

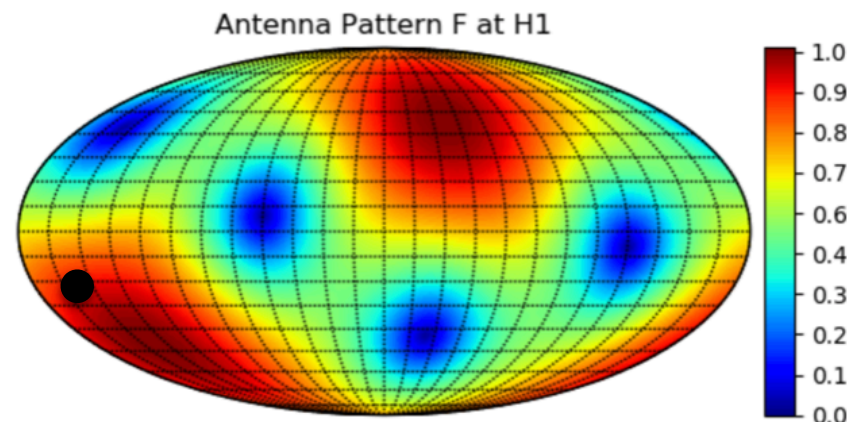
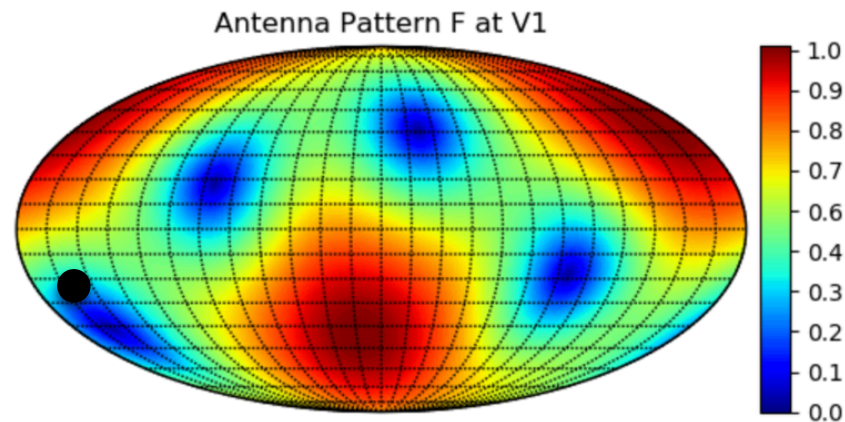
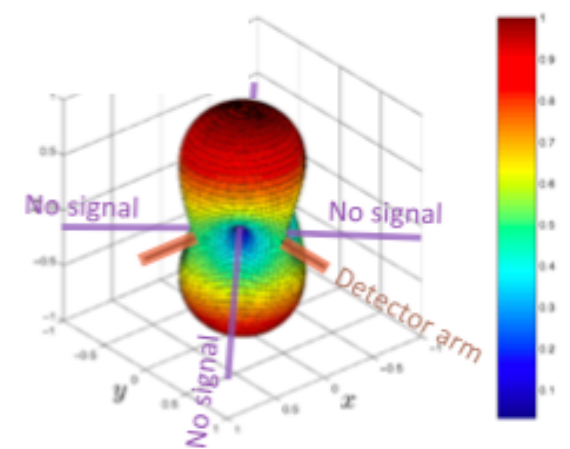
$$d_L = \frac{cz}{H_0}$$

$$\frac{\Delta H_0}{H_0} \sim \frac{\Delta z}{z} + \frac{\Delta D_L}{D_L}$$

Crux of doing late-time cosmology with GWs is to determine *redshift* of the sources.

Reminder..

$$h(t, \alpha, \delta, \dots) = F_+(t, \alpha, \delta, \psi)h_+(t) + F_x(t, \alpha, \delta, \psi)h_x(t)$$

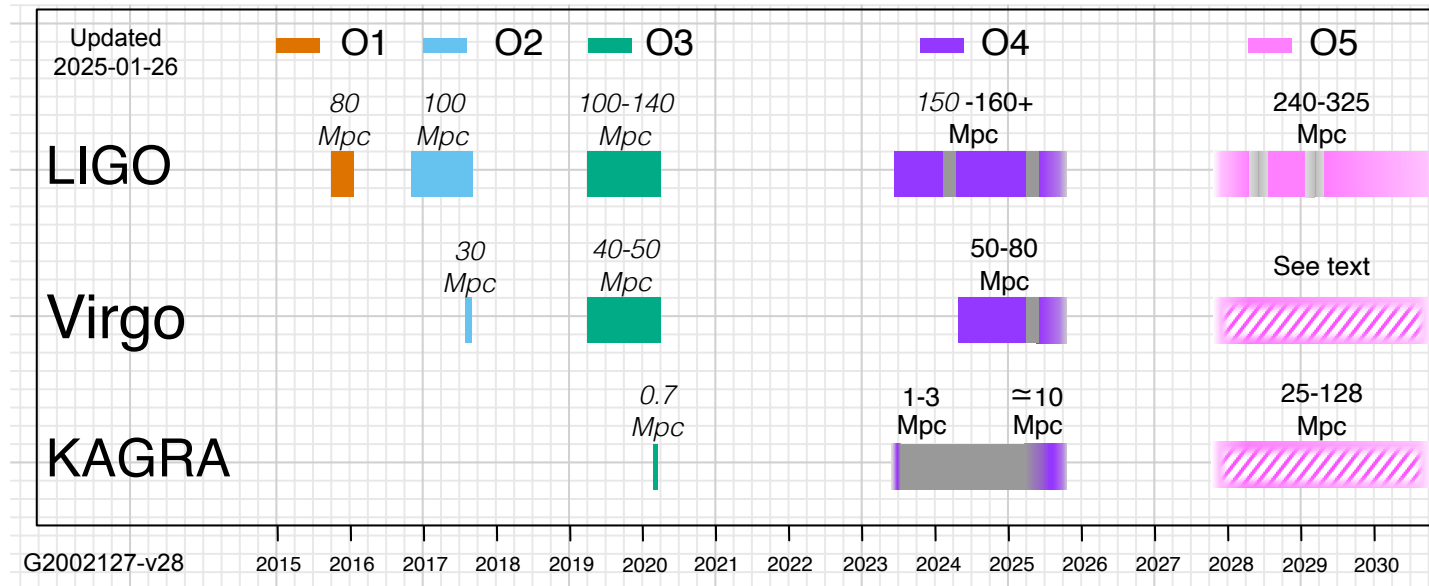


•=GW170817

$$\theta = \left[\begin{array}{l} \alpha \\ \delta \\ d_L \\ t_{\oplus} \\ \iota \\ \psi \\ \phi_c \\ \hline m_1 \\ m_2 \\ \mathbf{S}_1 \\ \mathbf{S}_2 \end{array} \right] \left\{ \begin{array}{l} \text{right ascension} \\ \text{declination} \\ \text{distance} \\ \text{arrival time at geocenter} \\ \text{inclination angle} \\ \text{polarization angle} \\ \text{coalescence phase} \\ \hline \text{first component's mass} \\ \text{second component's mass} \\ \text{first component's spin} \\ \text{second component's spin} \end{array} \right\} \left\{ \begin{array}{l} \text{extrinsic} \\ \text{parameters,} \\ \hline \text{intrinsic} \\ \text{parameters,} \end{array} \right.$$

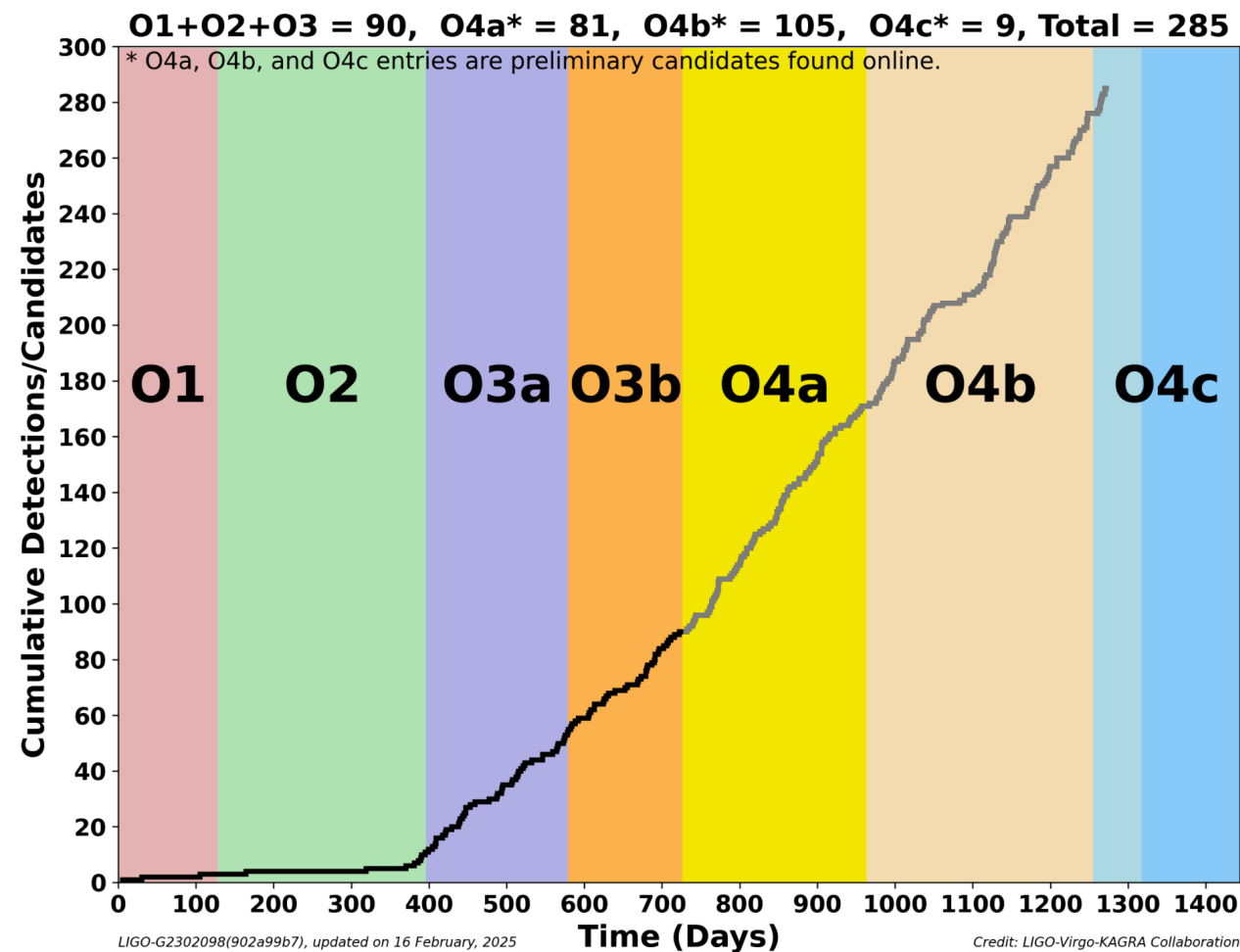
Position and orientation,
amplitude of waveform
(plus e, \dots)

physical properties on
which the *phase* of the
waveform depends
(For NS, equation of state..)



- **O1** ○ 3 BBHs
- **O2** ○ 7 BBHs
 - 1 BNS with EM counterpart GWI70817
- **O3** ○ 4 events compatible with NSBH masses
 - 2 events compatible with BNS masses
 - ~80 BBHs.
- **O4a ; O4b** and since end January **O4c**

Public alerts: <https://gracedb.ligo.org/>
<https://emfollow.docs.ligo.org/>
<https://gwosc.org/>



For all of these events LVK provides the SNR and posterior distributions for the different parameters
redshifted masses,
luminosity distances,
sky localisation,
 spins...

GWTC-I catalogue events

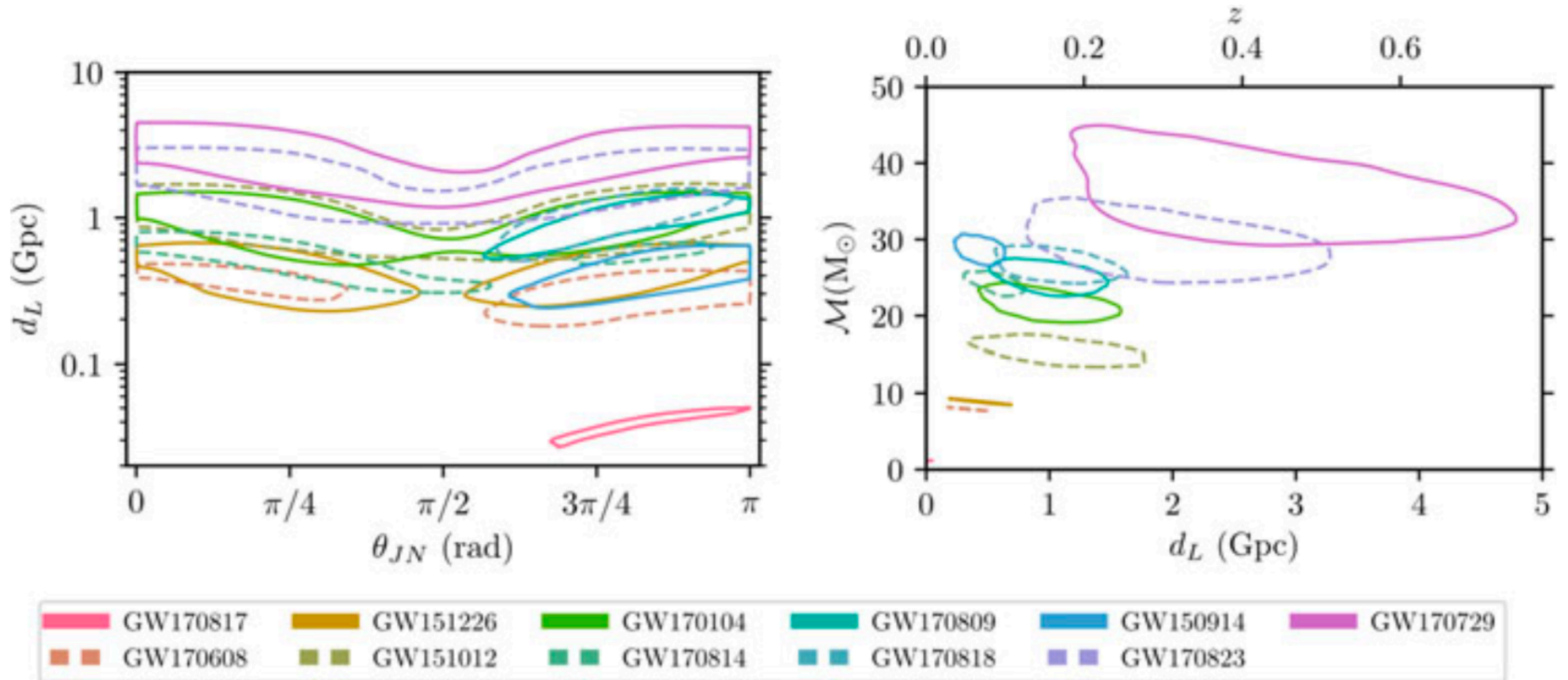
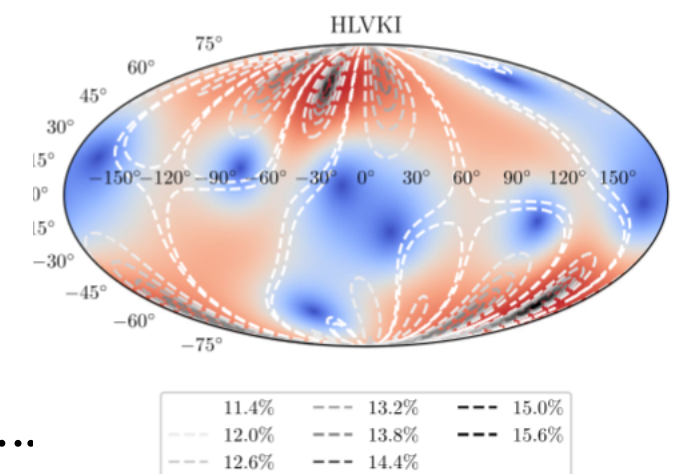


Fig. 3 *Left panel:* 90% confidence level intervals for luminosity distance and ι (indicated as θ_{jn}) for the ten BBH events in [32]. *Right panel:* 90% confidence level intervals for luminosity distance and chirp mass for the ten BBH events in [32]

- Typically have 10-40% error on the distance measurement due to degeneracy with inclination. Reduces marginally by having more detectors, but even for very loud sources and with HLVKI the minimum is $\sim 10\%$ depending on position on the skyunless.....

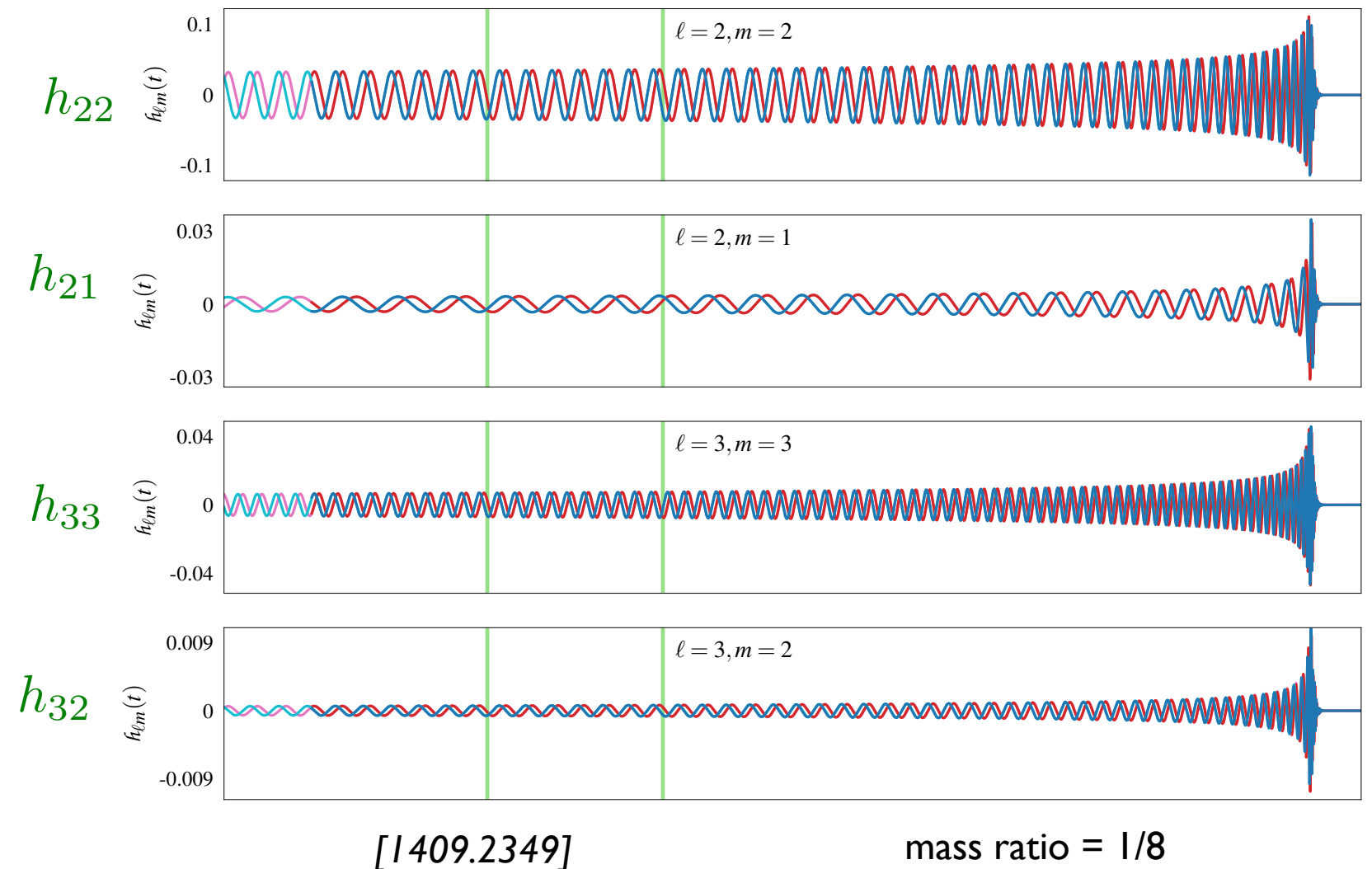


e.g. can measure higher order modes

- Two polarisation modes generally decomposed into spin -2 weighted spherical harmonics:
- So far discussed the dominant quadrupolar mode.
- Higher order modes generally depend on the **mass difference**, and **scale differently with inclination**.

$$h_+ - ih_\times = \sum_{\ell=2}^{\infty} \sum_{m=-\ell}^{\ell} Y_{\ell m}(i, \varphi) h_{\ell m},$$

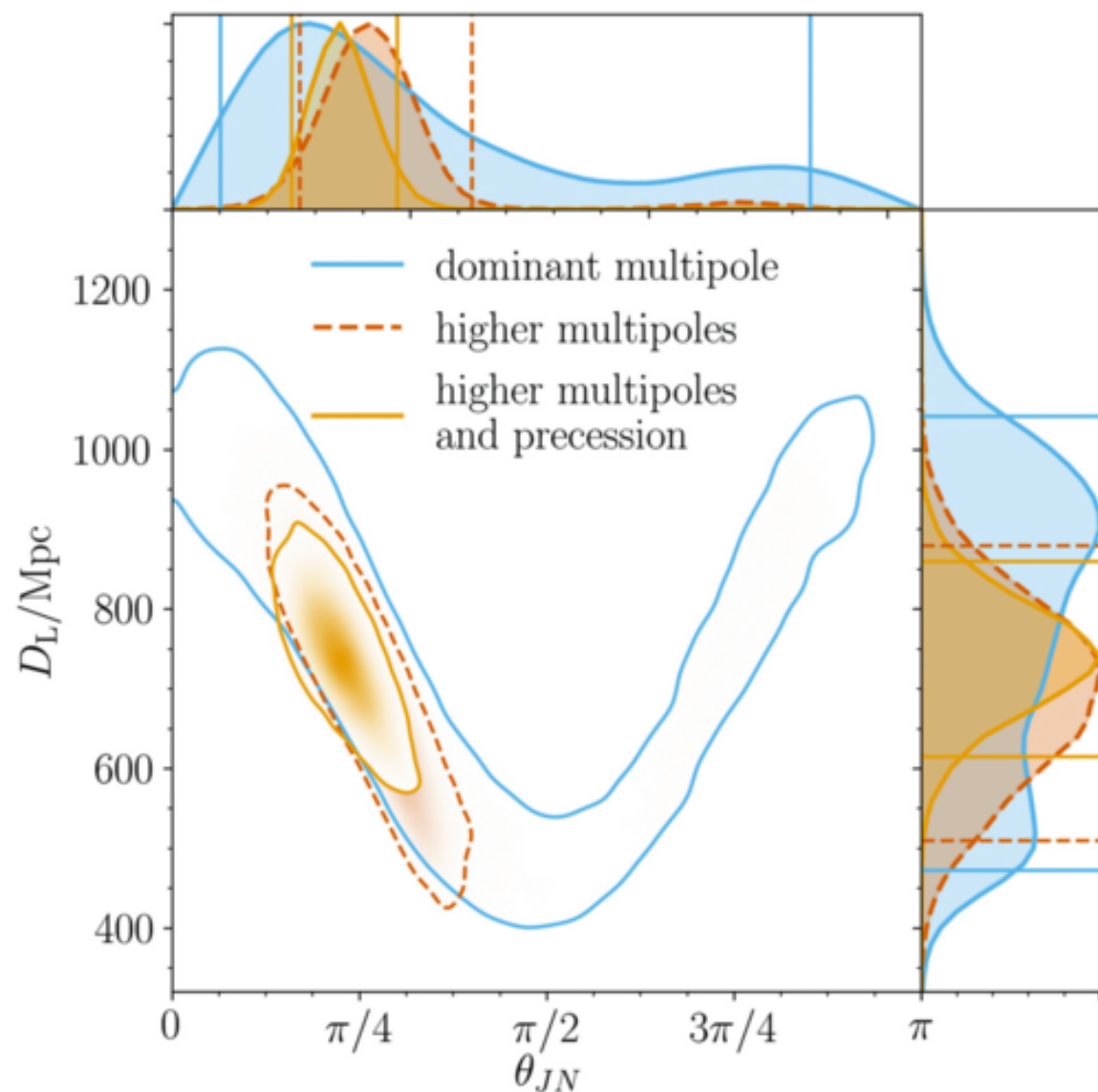
$$\Delta = \frac{(m_1 - m_2)}{(m_1 + m_2)},$$



e.g. can measure higher order modes

- Two polarisation modes generally decomposed into spin -2 weighted spherical harmonics:
- So far discussed the dominant quadrupolar mode.
- **Higher order modes generally depend on the mass difference, and scale differently with inclination.**

$$h_+ - ih_\times = \sum_{\ell=2}^{\infty} \sum_{m=-\ell}^{\ell} Y_{\ell m}(i, \varphi) h_{\ell m},$$

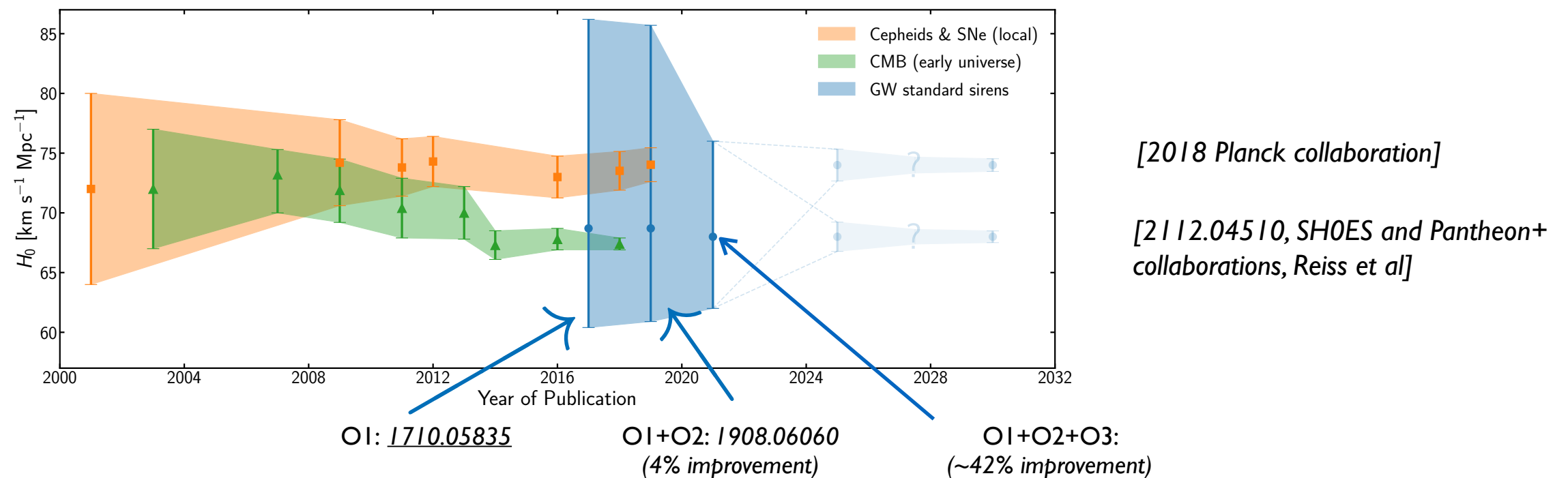


$$m_1 \sim 30M_{\odot}, m_2 \sim 8M_{\odot}$$

Fig. 4 GW190412: Posterior distribution for the luminosity distance and inclination. The central plot shows the 90% confidence level for different waveform approximants namely: the dominant multipole (and no precession), higher multipoles and no precession; and higher multipoles and precession. The impact of higher multipoles on constraining the inclination and distance is clear. The top and side plots show the marginal posteriors of ι and d_L respectively. Figure from [37]

Late time cosmology (H_0, Ω_m) with GWs: results + future

- The hope: GWs can say something about the ~ 5 -sigma tension between measurements that calculate the sound horizon at decoupling (+assumption of Lambda CDM) and those that do not?



GW results with LVK observations

Determining the redshift

Reminder: for point sources, there's a perfect degeneracy between source masses, redshift, spins.
Some extra non gravitational information necessary to determine z .

– **Bright siren** method, requires **EM counterparts**. [B.Schutz, '86]

Potentially most accurate for cosmological parameters.

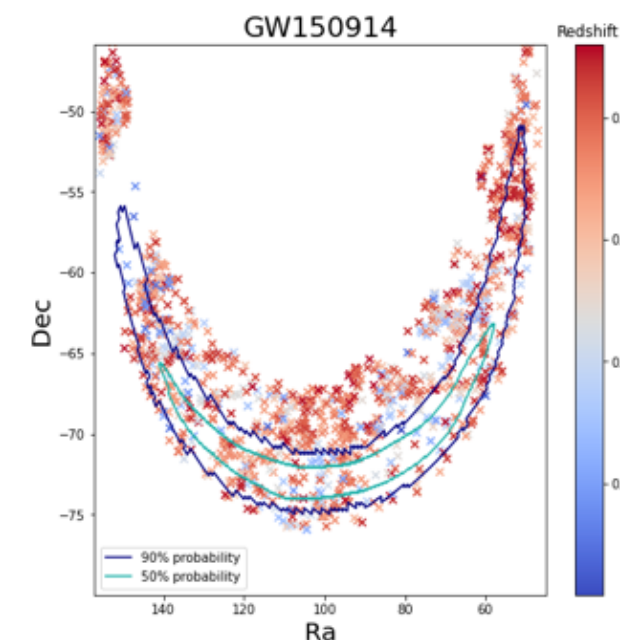
- **LVK**: only one seen so far, GW170817, with optical identification of host galaxy.
- **ET**: how many are expected?
- **LISA**. SMBHB mergers may be accompanied by an electromagnetic counterpart (generated by gas accreting on the binary or on the remnant BH). Expected rate: $\sim 7\text{-}20$ per year! [Mangiagli et al 2207.16078]

– **Spectral siren** method

Requires knowledge of underlying **astrophysical properties of sources** (mass distribution)

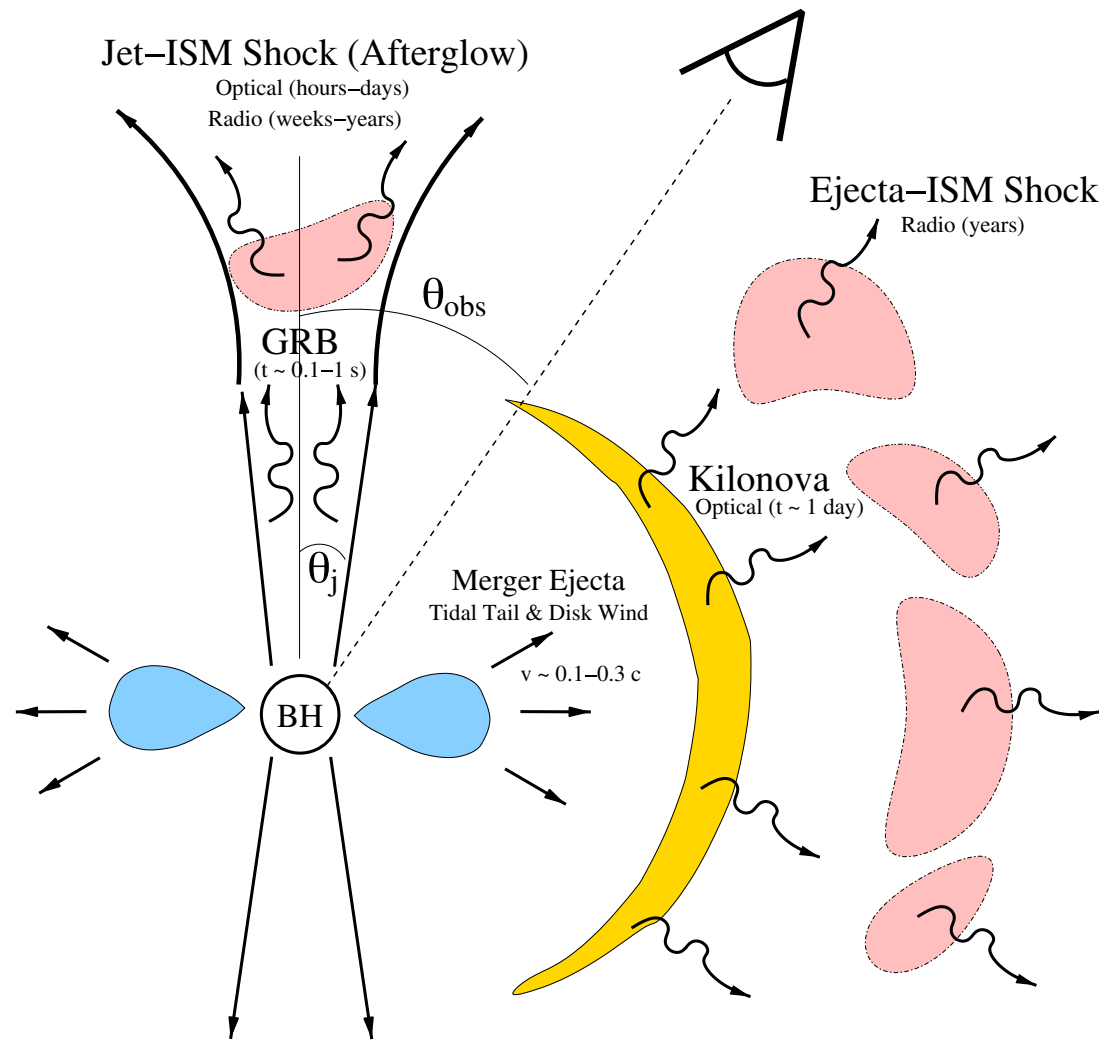
– **Dark siren** method = spectral sirens + information from **galaxy catalogues**.
(But often these may not be complete, and will definitely not be at larger z .)

– **NS**, a measure of the tidal deformability + equation of state



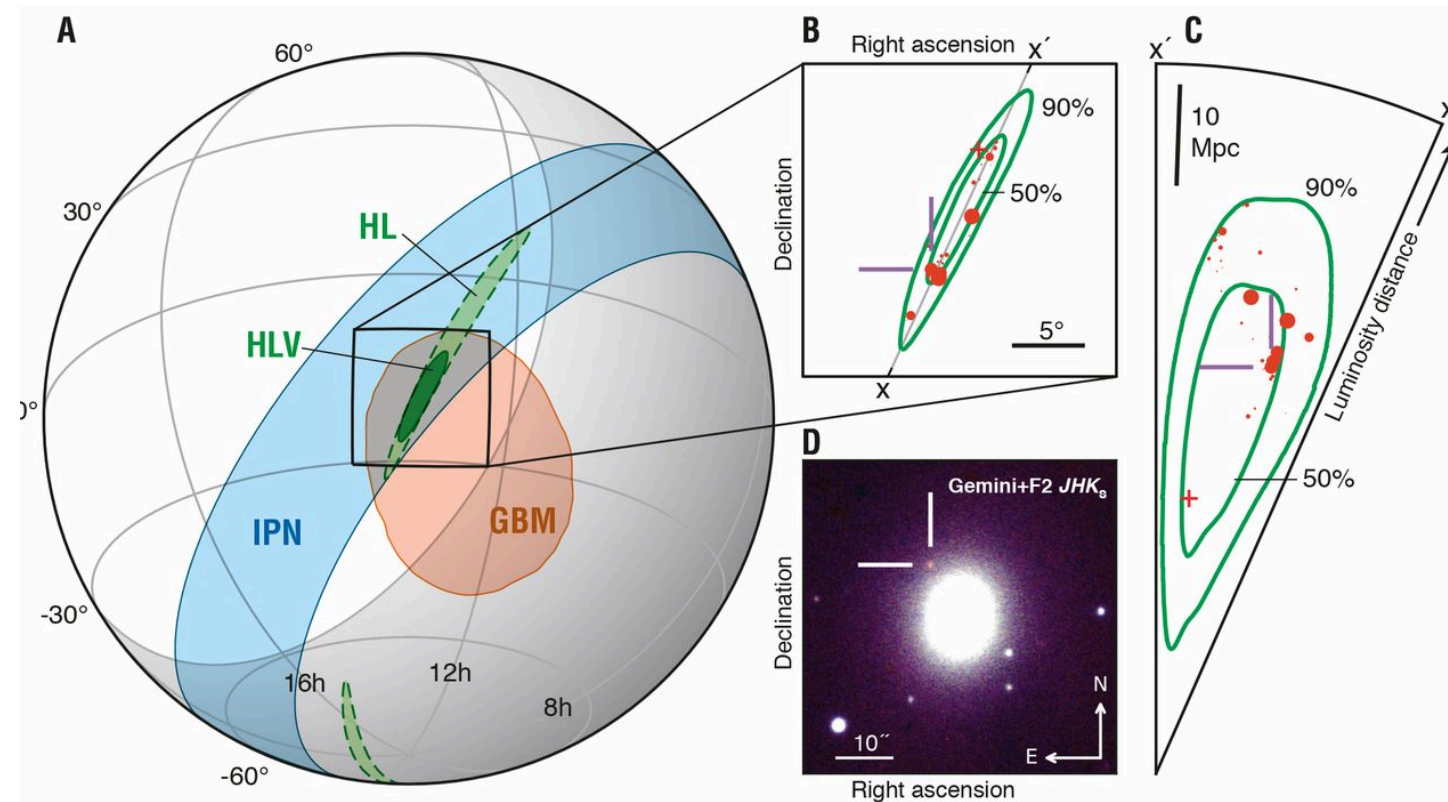
Bright sirens

(NS-NS or NS-BH mergers).



For GW170817:

- 30 deg² localisation area, SNR ~ 30
- measure redshift from optical identification of the host galaxy (NGC4993 in the Hydra constellation)



[LVC+, ApJL (2017)]

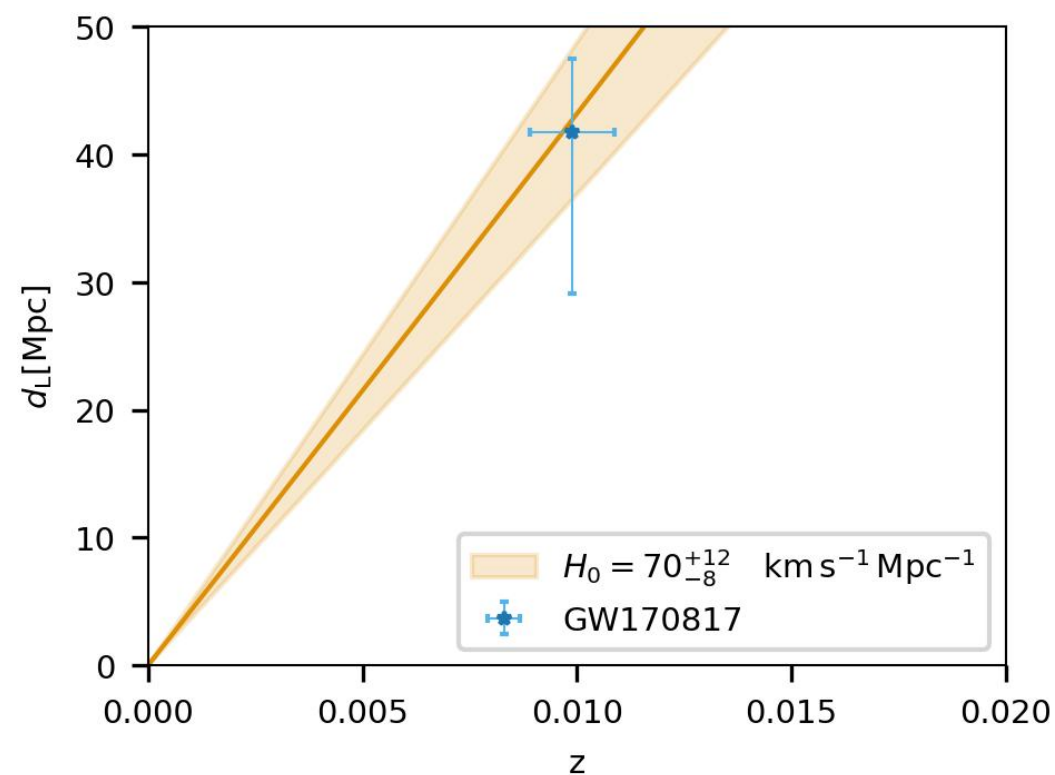
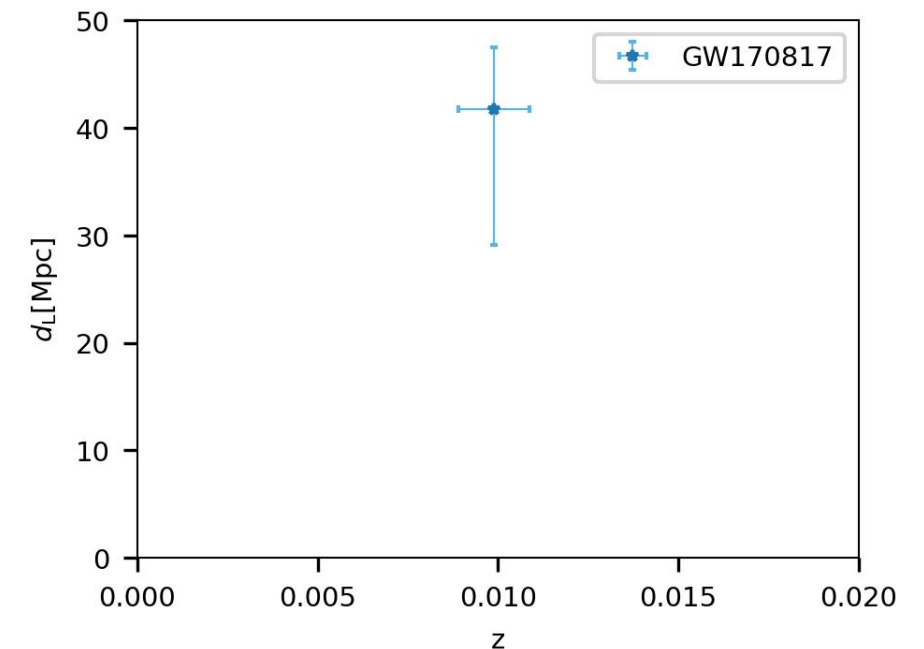
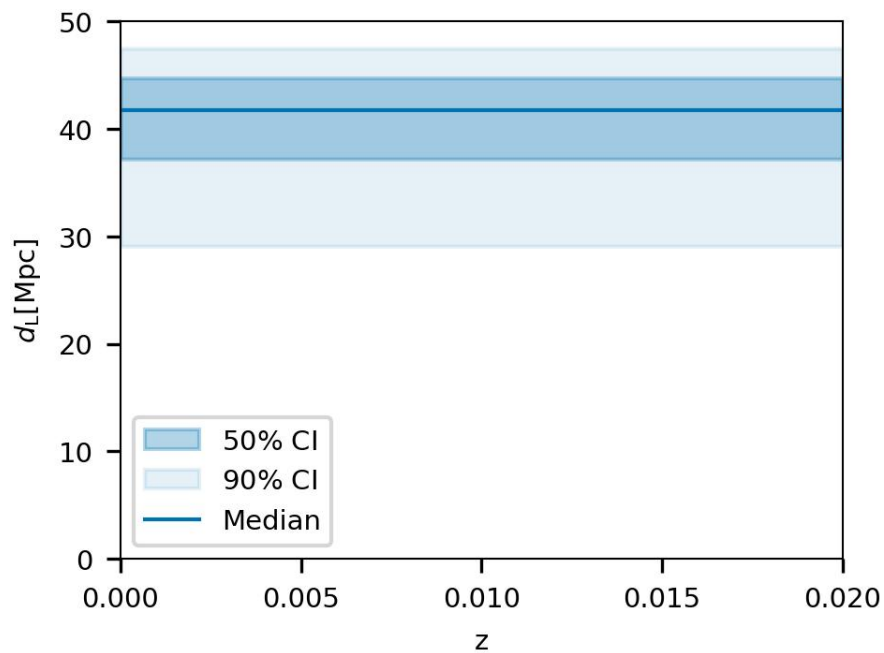
[Metzger&Berger, ApJ (2012)]

Figure 1. Summary of potential electromagnetic counterparts of NS-NS/NS-BH mergers discussed in this paper, as a function of the observer angle, θ_{obs} . Following the merger a centrifugally supported disk (blue) remains around the central compact object (usually a BH). Rapid accretion lasting $\lesssim 1$ s powers a collimated relativistic jet, which produces a short-duration gamma-ray burst (Section 2). Due to relativistic beaming, the gamma-ray emission is restricted to observers with $\theta_{\text{obs}} \lesssim \theta_j$, the half-opening angle of the jet. Non-thermal afterglow emission results from the interaction of the jet with the surrounding circumburst medium (pink). Optical afterglow emission is observable on timescales up to \sim days-weeks by observers with viewing angles of $\theta_{\text{obs}} \lesssim 2\theta_j$ (Section 3.1). Radio afterglow emission is observable from all viewing angles (isotropic) once the jet decelerates to mildly relativistic speeds on a timescale of weeks-months, and can also be produced on timescales of years from sub-relativistic ejecta (Section 3.2). Short-lived isotropic optical emission lasting \sim few days (kilonova; yellow) can also accompany the merger, powered by the radioactive decay of heavy elements synthesized in the ejecta (Section 4).

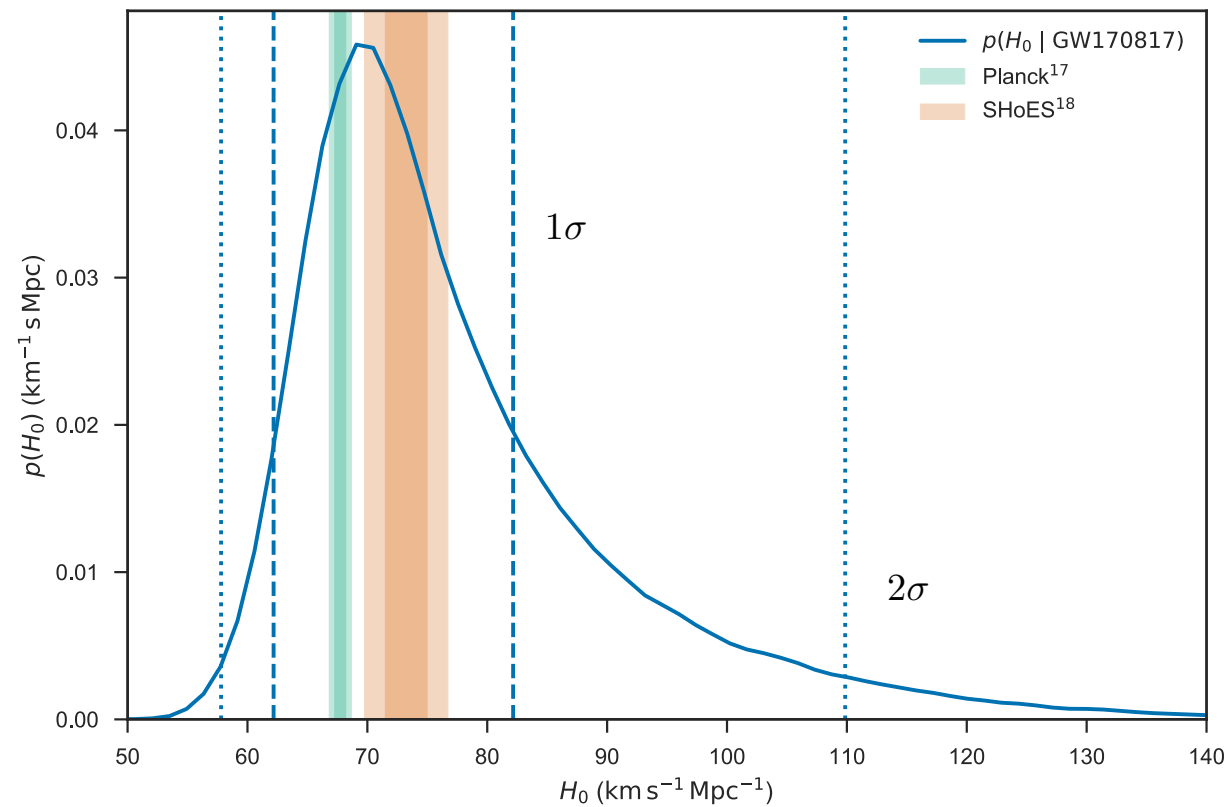
Bright sirens: Cosmology with GW170817

- BNS detected by LIGO and Virgo.
source distance ~ 40 Mpc
[LVK+, AjL, 848 (2017)].

- Short Gamma-ray burst and Kilonova allowed
the identification of the source host galaxy **NGC4993**.



$$H_0 = 70.0^{+12.0}_{-8.0} \text{ km s}^{-1} \text{ Mpc}^{-1}$$



Errors:

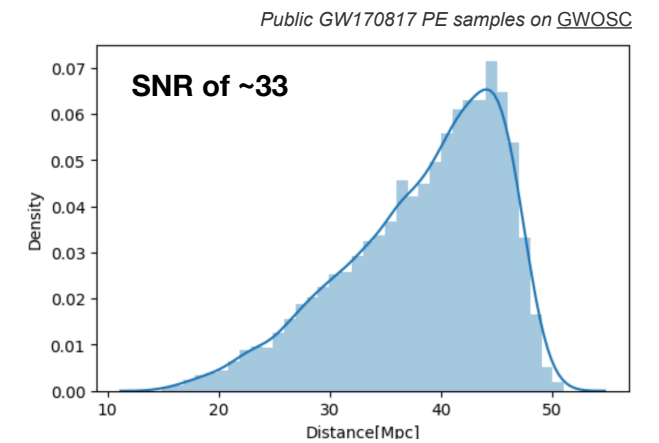
1/ peculiar velocities

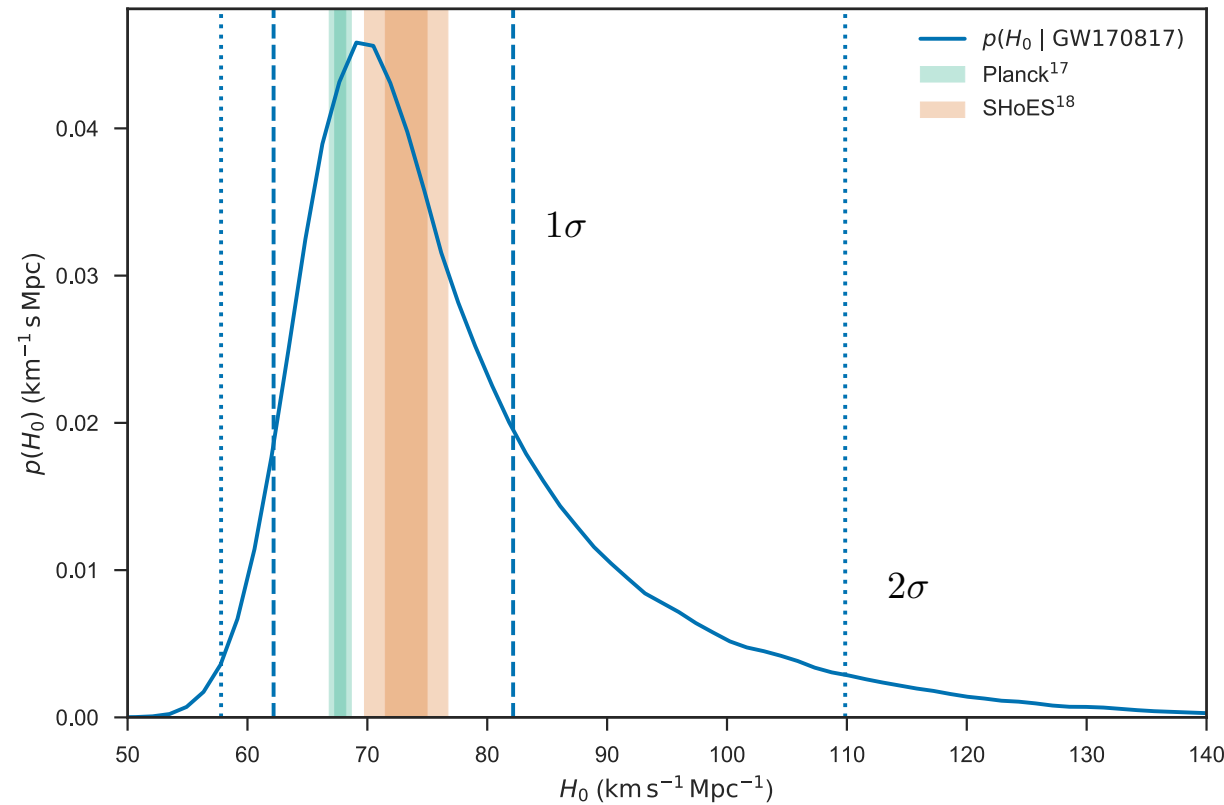
$$v_H = 3017 \pm 166 \text{ km s}^{-1}.$$

2/ distance $d = 43.8^{+2.9}_{-6.9} \text{ Mpc}$

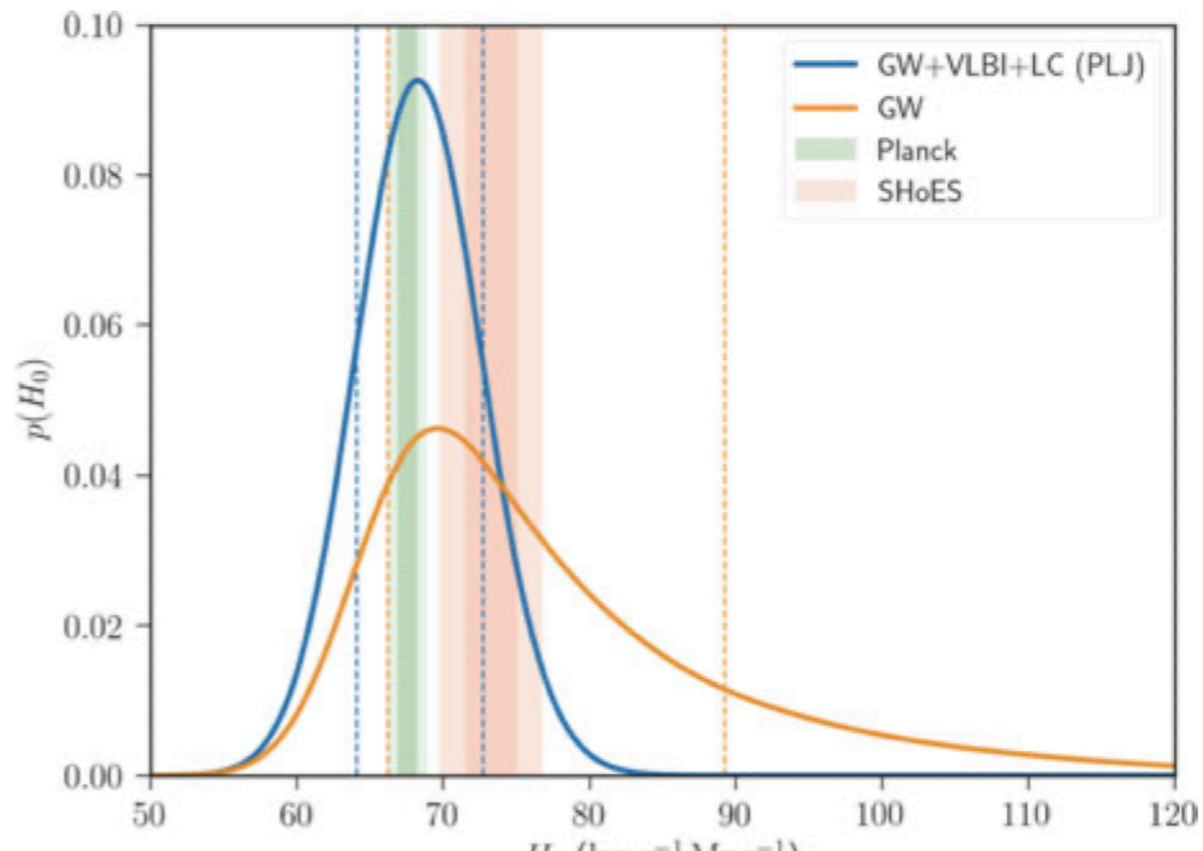
~15% error

3/ statistical measurement error from noise
in detectors instrumentation calibration
uncertainties





- radio band observations with VLBI ==> estimate of inclination
 $15 < \iota (d_L/41\text{Mpc}) < 25$ [Hotokezaka, 2019]



Errors:

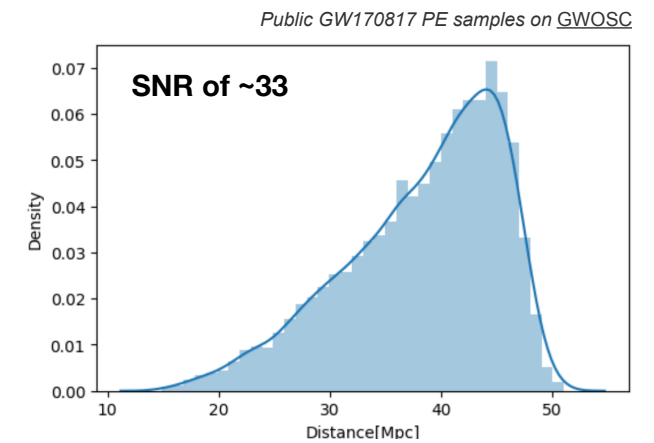
1/ peculiar velocities

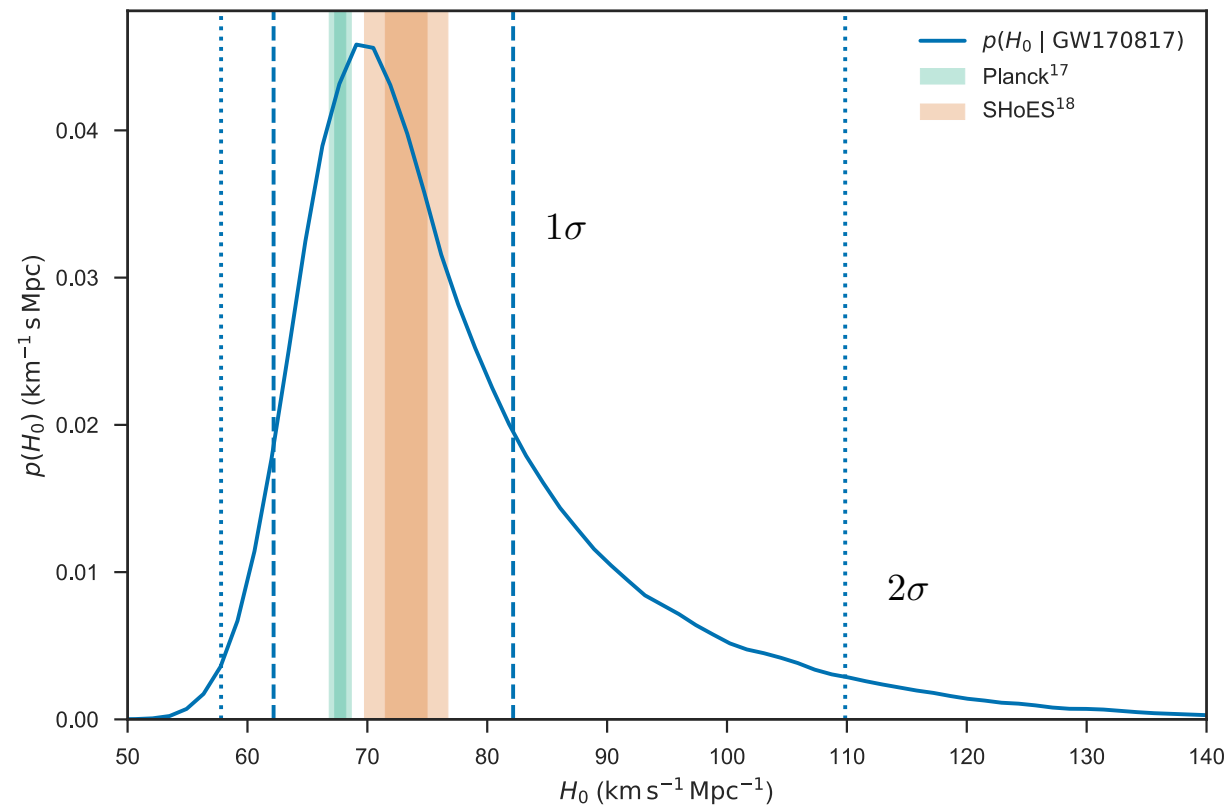
$$v_H = 3017 \pm 166 \text{ km s}^{-1}.$$

2/ distance $d = 43.8^{+2.9}_{-6.9} \text{ Mpc}$

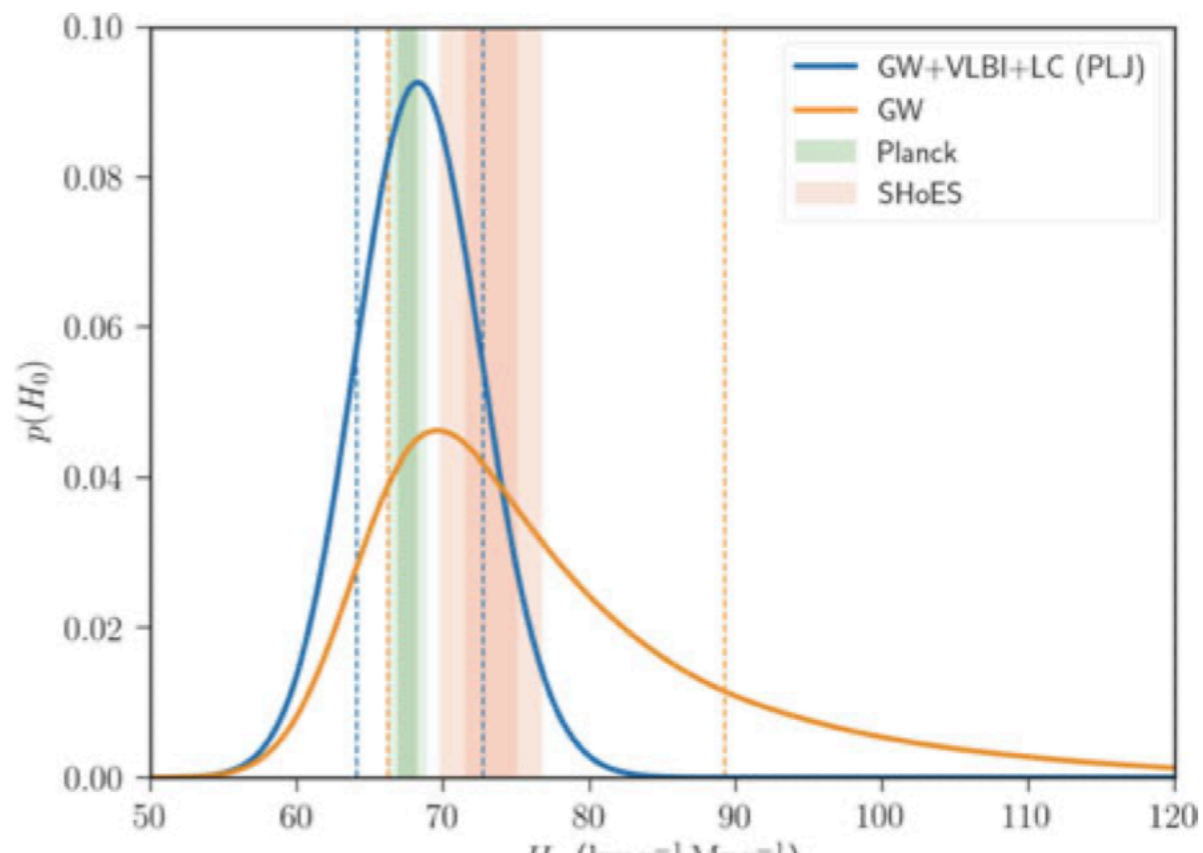
~15% error

3/ statistical measurement error from noise
in detectors instrumentation calibration
uncertainties





- radio band observations with VLBI ==> estimate of inclination
 $15 < \iota (d_L/41\text{Mpc}) < 25$ [Hotokezaka, 2019]



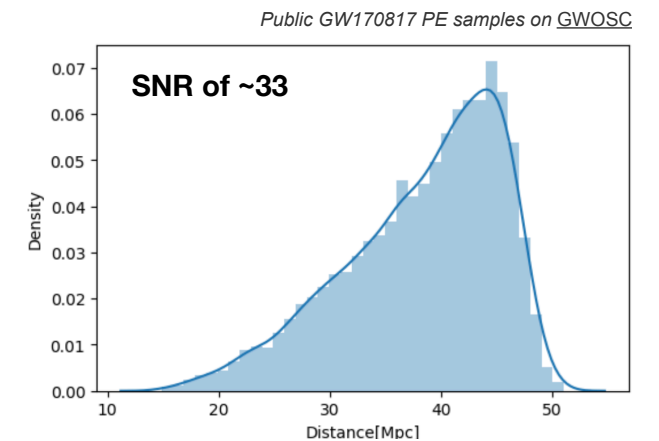
Errors:

1/ peculiar velocities

$$v_H = 3017 \pm 166 \text{ km s}^{-1}.$$

2/ distance $d = 43.8_{-6.9}^{+2.9} \text{ Mpc}$ ~15% error

3/ statistical measurement error from noise in detectors instrumentation calibration uncertainties



But only one such event so far!!!

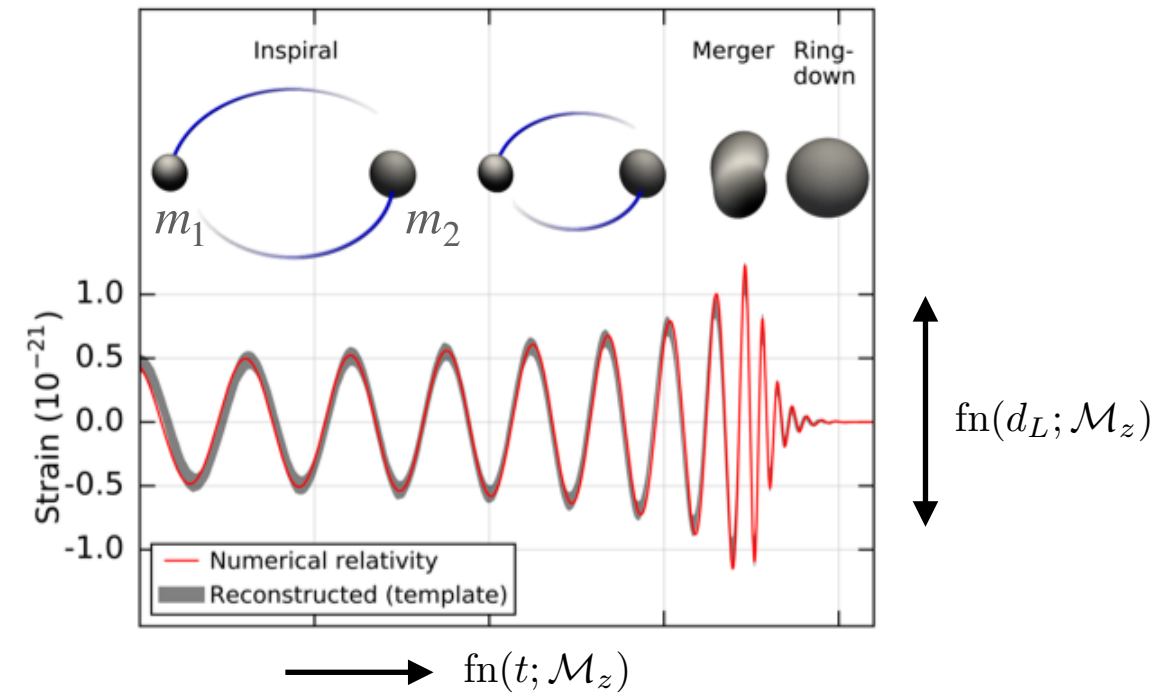
- Pity as errors scale as $1/\sqrt{N}$
- H0 accurate to ~3% with 30 events with counterparts
[Phys.Rev.D 101 (2020) 12, 122001]
- ET: estimates $\sim \mathcal{O}(10^2 - 10^3)/\text{year}$
 with counterparts, depending on EM facilities operating at the time

Spectral siren method = prior knowledge of source frame mass distribution.

- Phase of GW signal depends on the “detector frame” masses which are redshifted relative to the “source frame” masses

$$m_{1,2}^{\text{det}} = [1 + z(d_L, H_0, \dots)]m_{1,2}$$

- knowledge of source mass (for a population or individual source), together with observed “detector” mass can infer z-distribution.

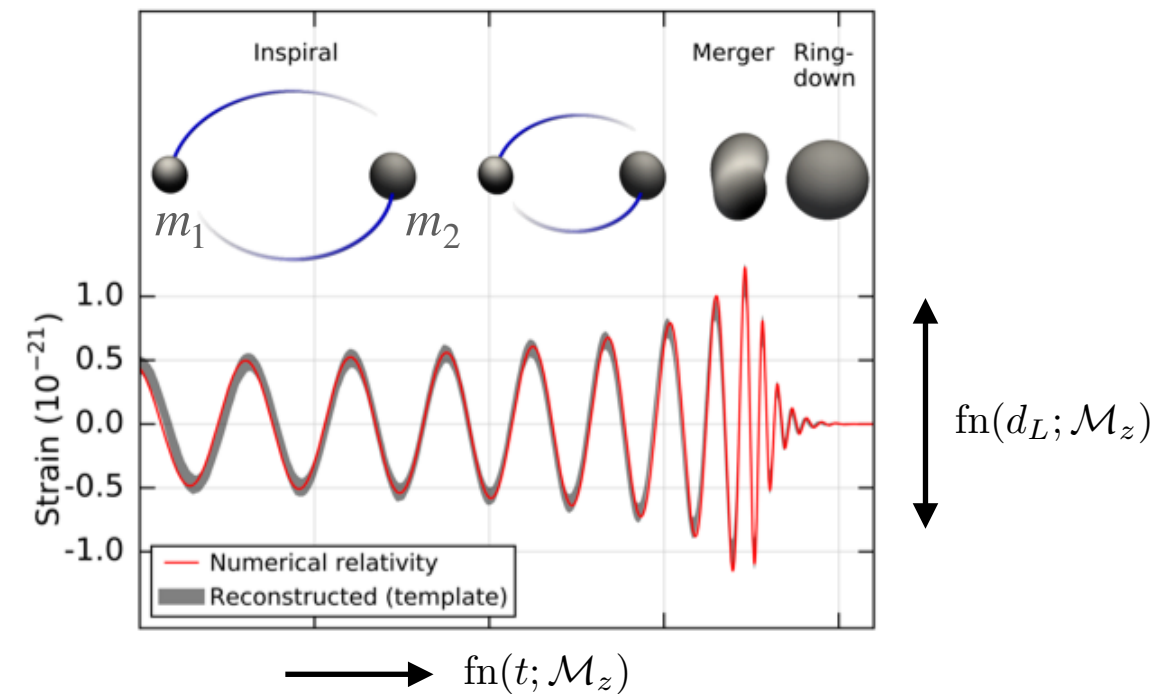


Spectral siren method = prior knowledge of source frame mass distribution.

- Phase of GW signal depends on the “detector frame” masses which are redshifted relative to the “source frame” masses

$$m_{1,2}^{\text{det}} = [1 + z(d_L, H_0, \dots)] m_{1,2}$$

- knowledge of source mass (for a population or individual source), together with observed “detector” mass can infer z-distribution.



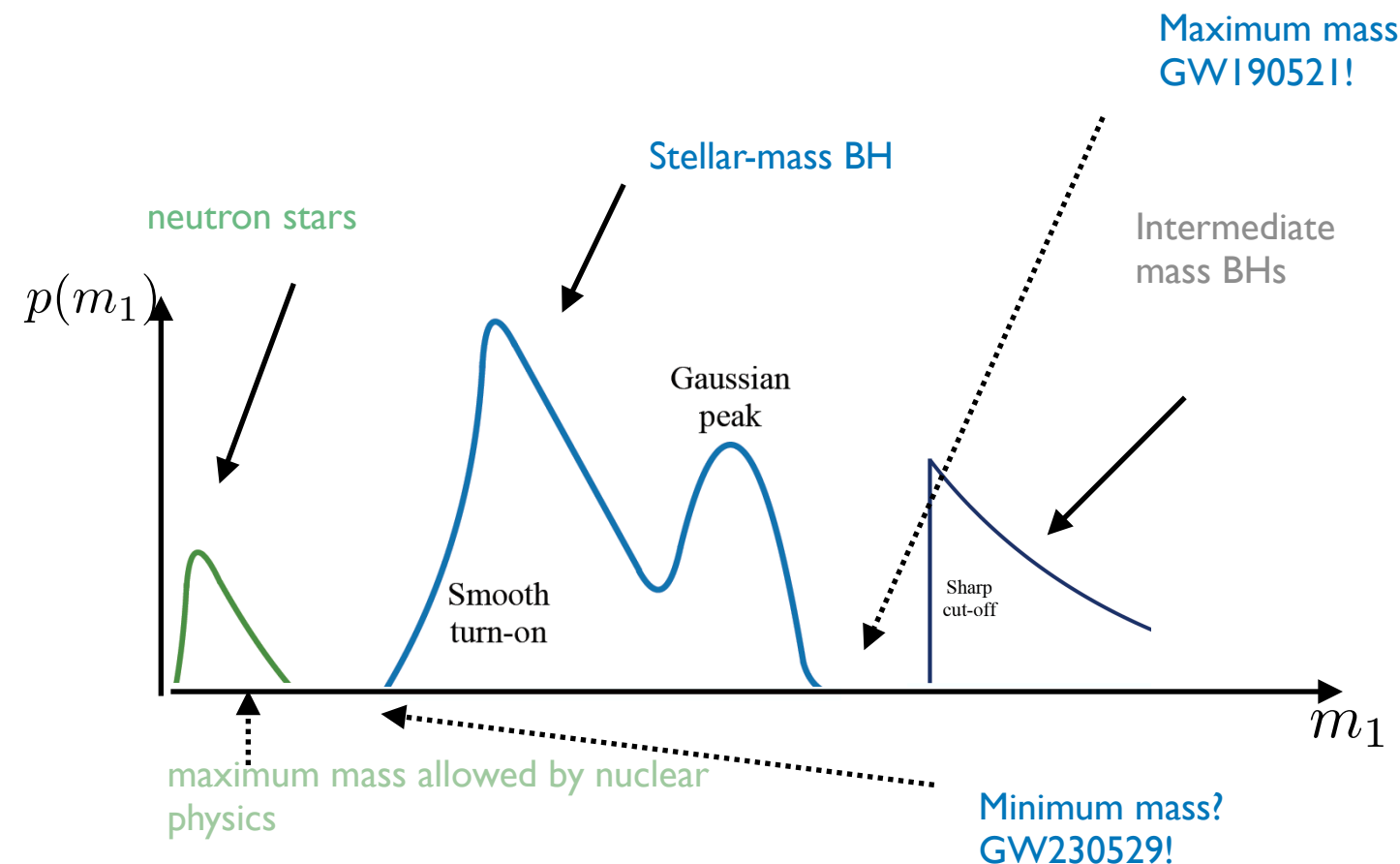
- Cosmological parameters jointly inferred with source-frame population parameters

[Mastrogiovanni et al 2103.14663]

- H_0 error scales as $\sim 1/\sqrt{N}$

ET: BBH $10^5 - 10^6/\text{year}$

BNS $\sim 10^4/\text{year}$



Does it really work and how well? Simulated data

[Mastrogiovanni et al 2103.14663]

- Simulated a set of BBH GW events (*power-law + gaussian peak model*, described by 8 parameters) detected in LVK data assuming sensitivities comparable to the O2 and O3 observing runs

- Use hierarchical Bayesian inference scheme to **estimate jointly the source-frame mass model parameter and cosmological parameters** H_0, Ω_m, \dots

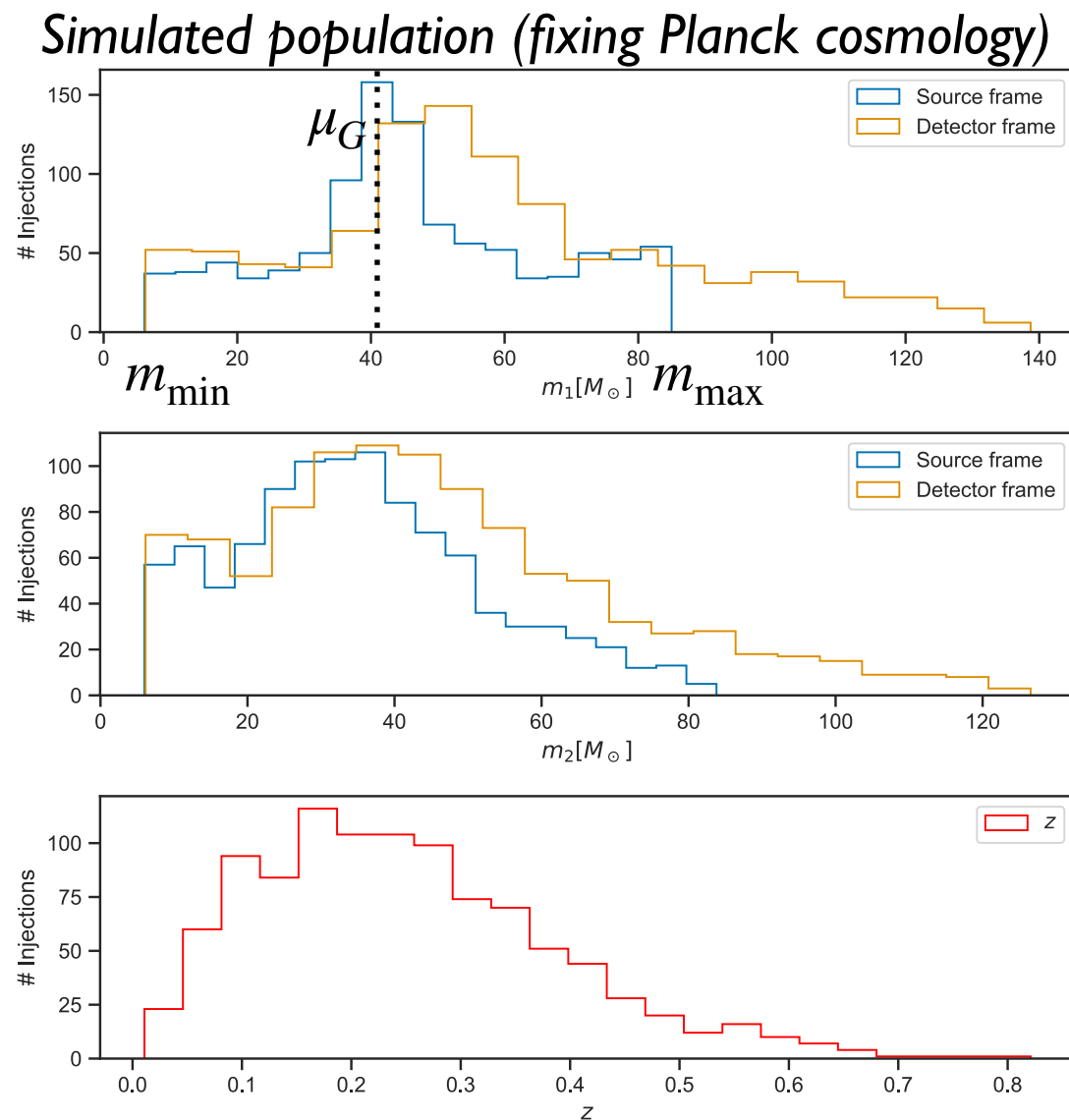
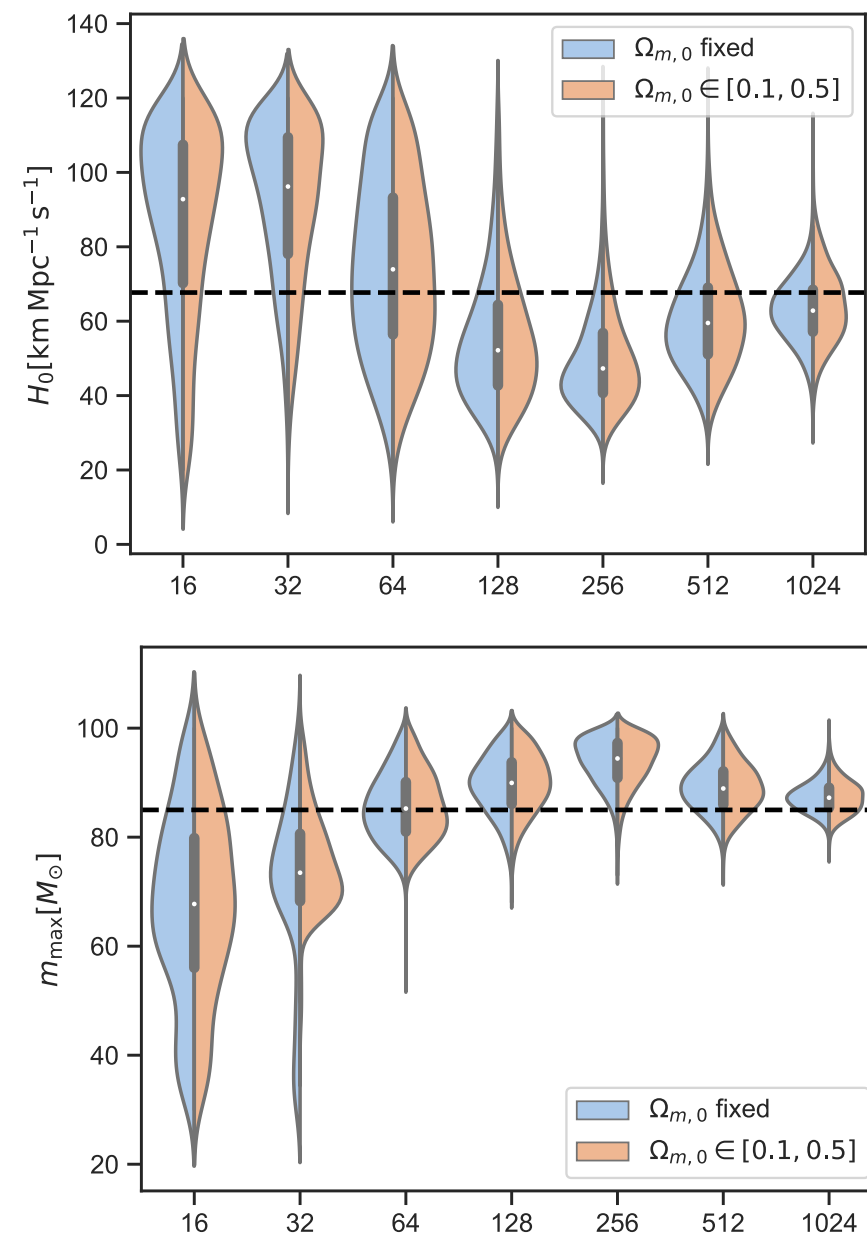


FIG. 1. Simulated population of 1024 observed events, showing the mass distributions (in the detector and source frames) and redshift distribution.



- tight correlation between estimation of source frame mass spectrum + cosmo parameters.

Hubble constant

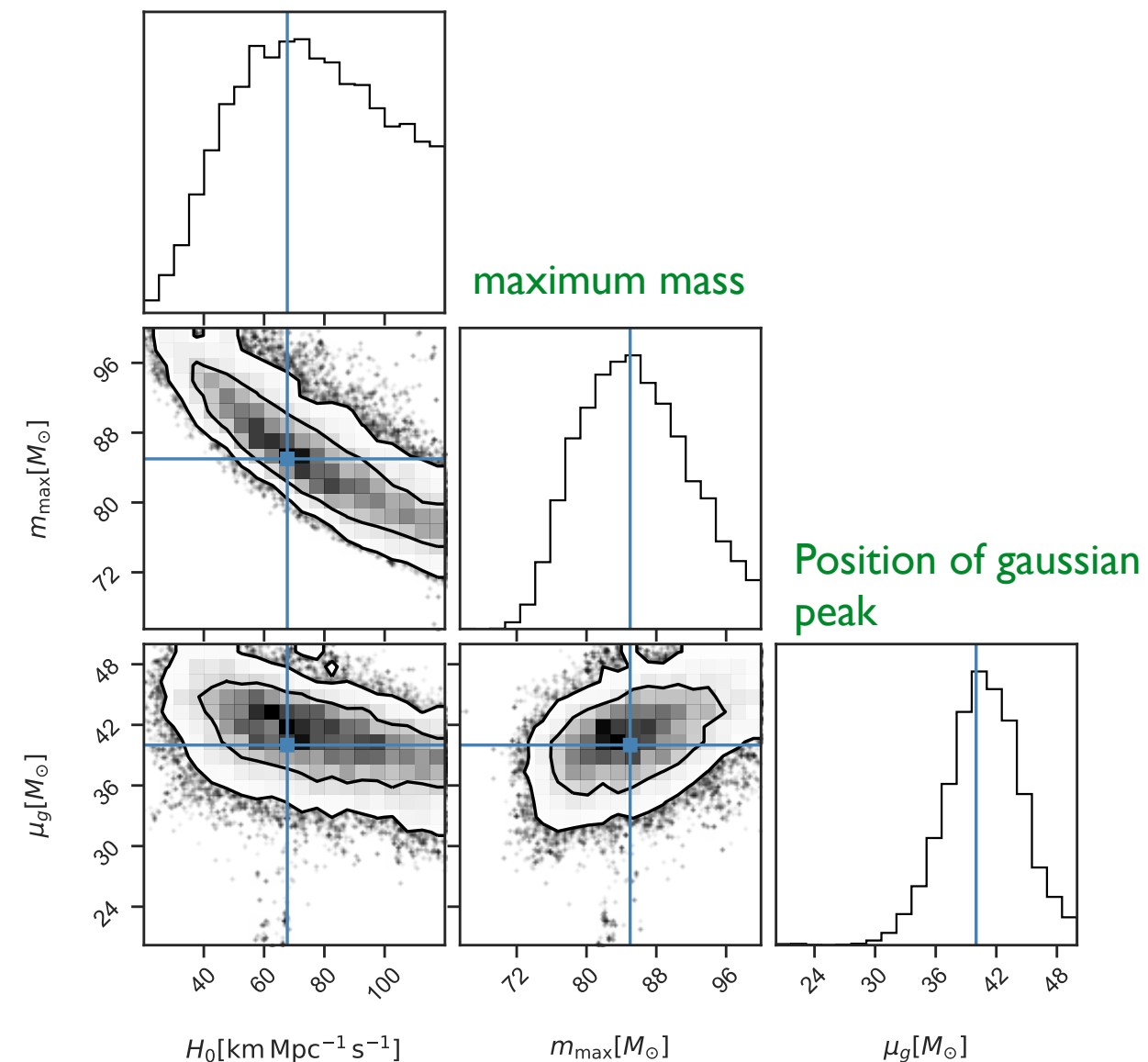


FIG. 6. Posterior distribution on the H_0 , m_{\max} and μ_g for 64 BBH events detected with LIGO and Virgo at current sensitivities. The blue lines show the true parameters. The contours indicate the 1σ and 2σ confidence level intervals.

- If one FIXES the underlying mass model — rather than varying to be estimated together with cosmological parameters — then leads to big errors.

– e.g. m_{\max} fixed to incorrect values in a range around its true value

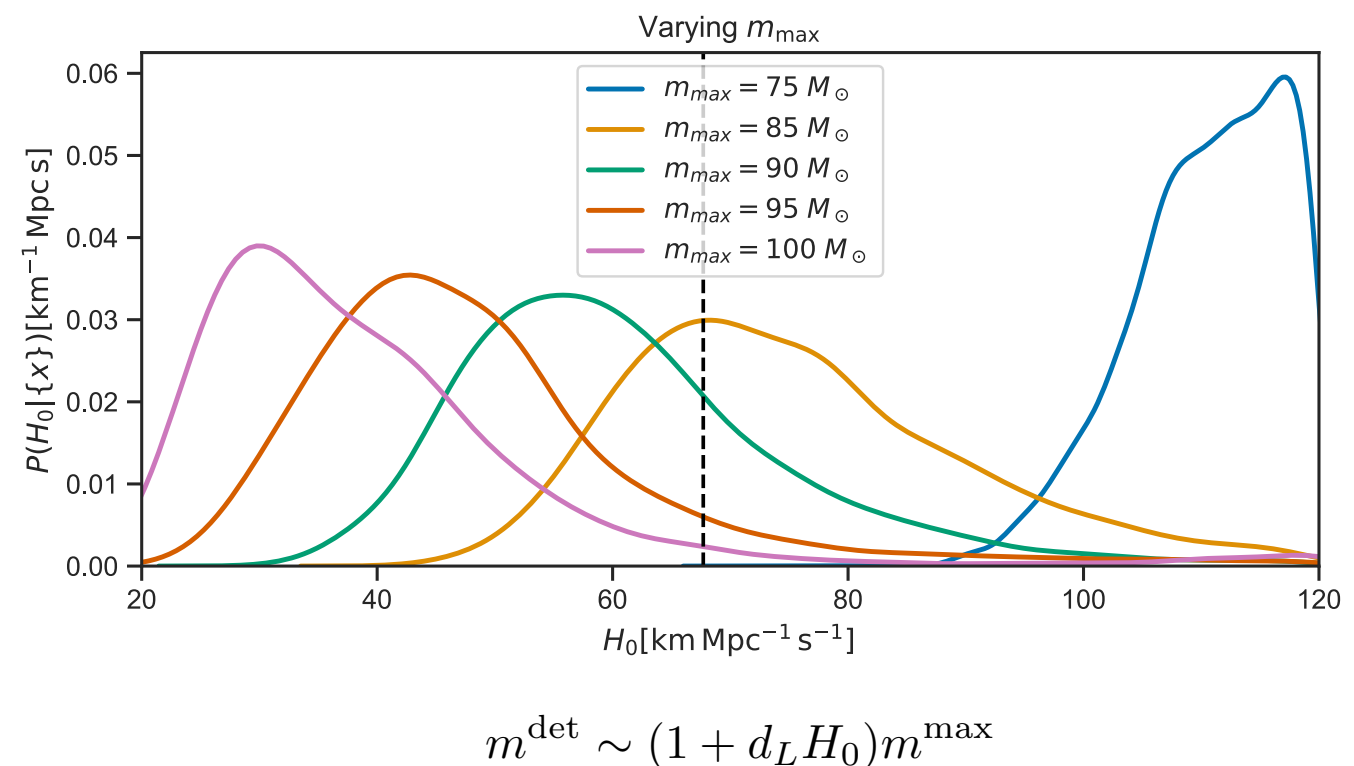
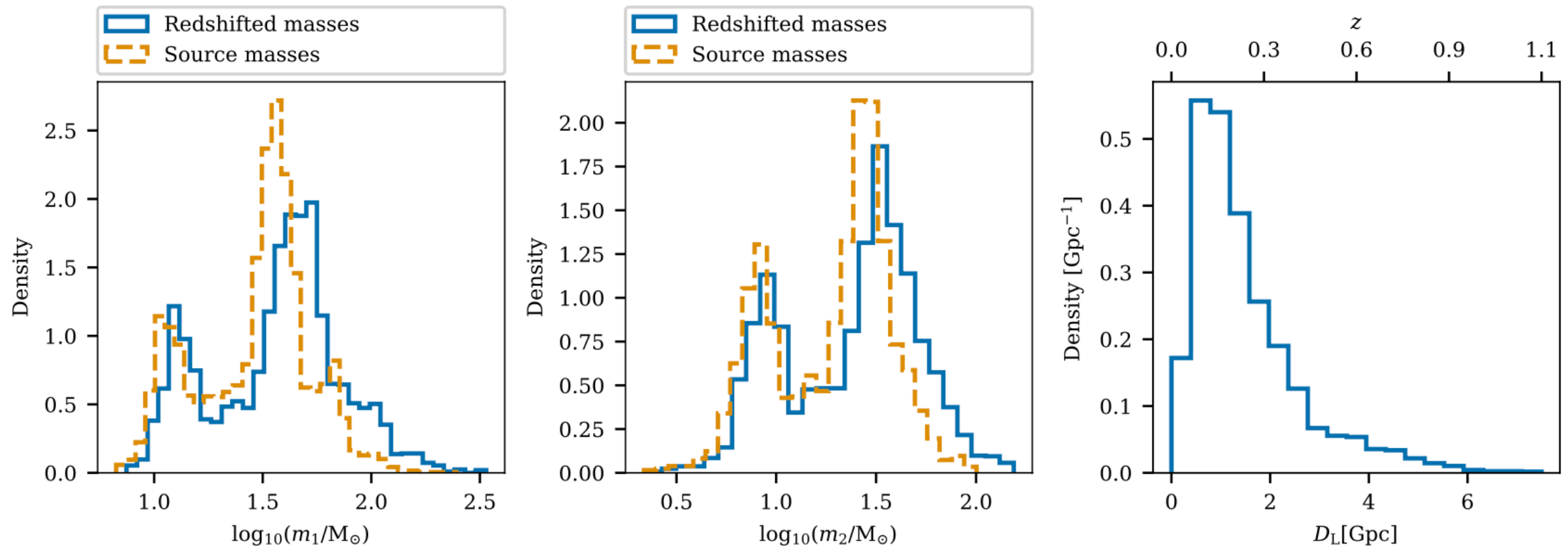


FIG. 7. Posterior distribution for H_0 obtained by fixing m_{\max} and μ_g in a range around their true values $m_{\max} = 85M_{\odot}$ and $\mu_g = 40M_{\odot}$. The black dashed line indicates the true value of H_0 .

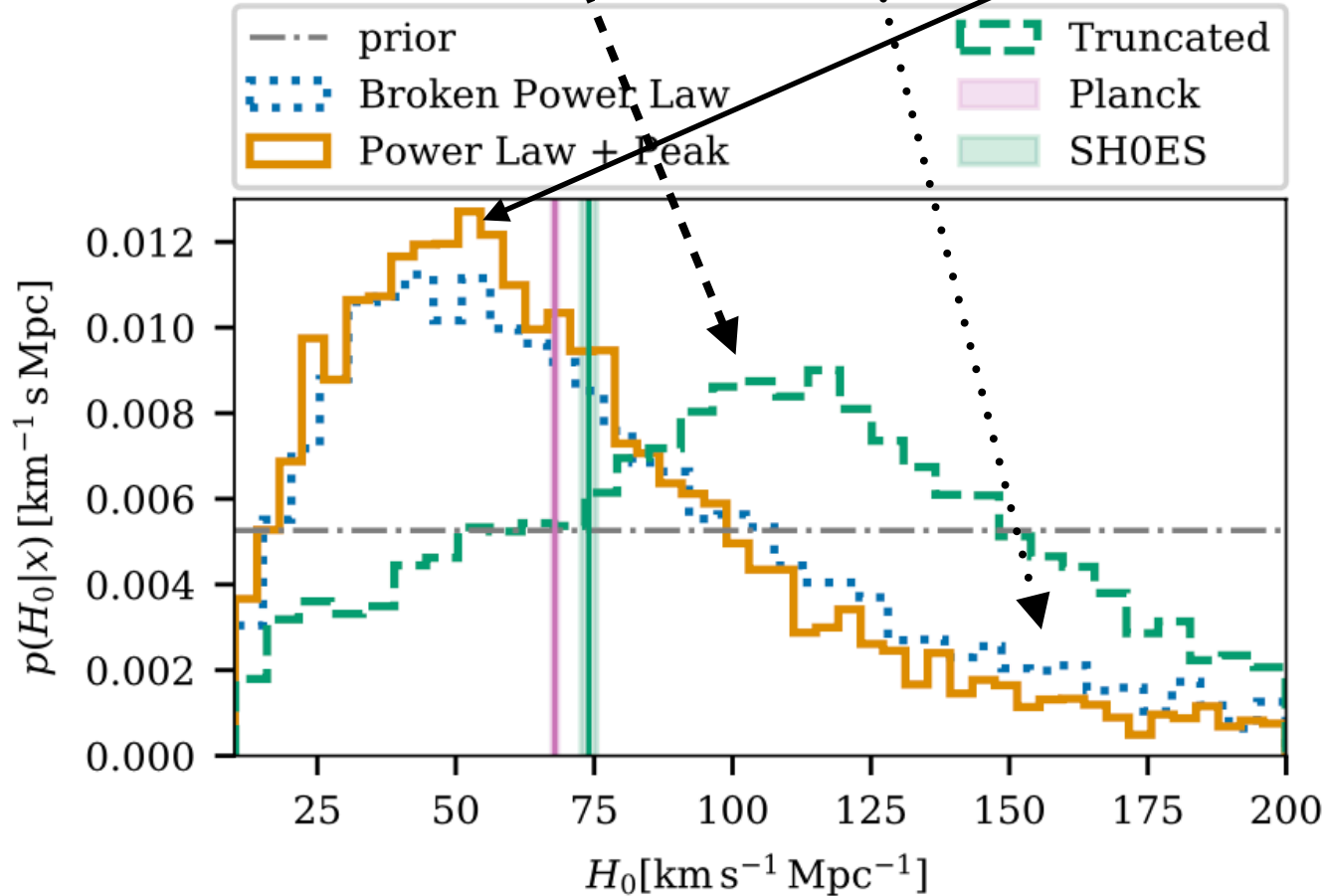
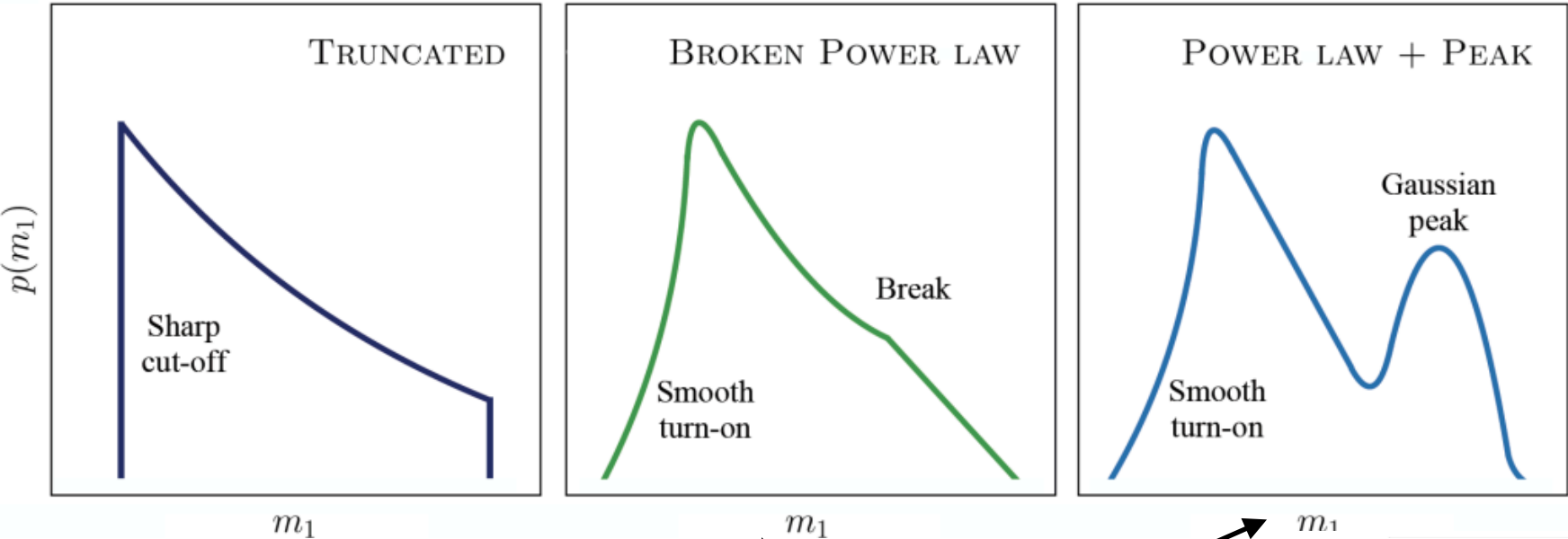
Applied to GWTC3 :

LVK: arXiv:2111.03604

Representative figure of the 42 BBH events with $\text{SNR} > 11$ in GWTC3.
For the figure, COSMOLOGY HAS BEEN FIXED TO PLANCK VALUES!



- 3 parametric mass models considered (assumed to be independent of redshift, see Nicola’s lectures)



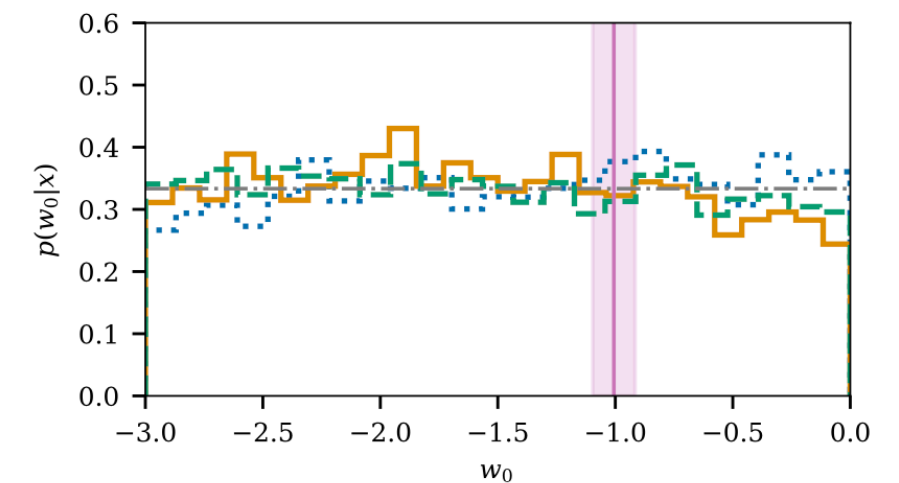
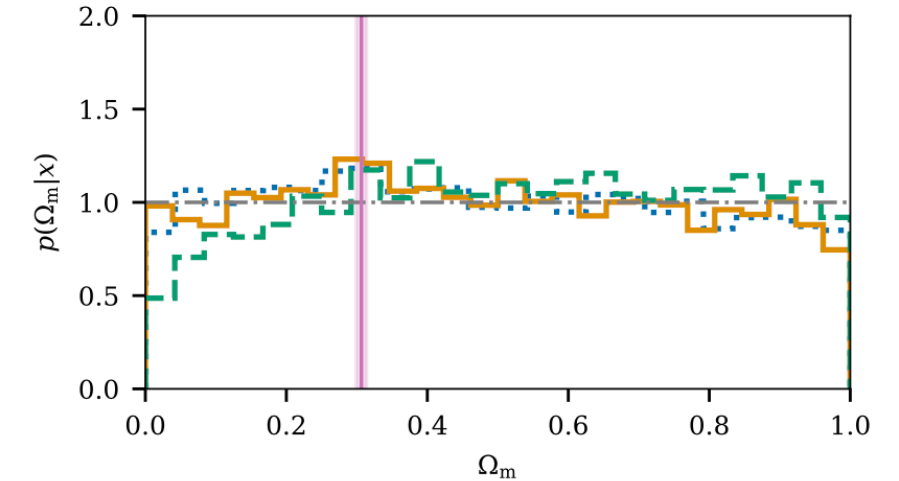
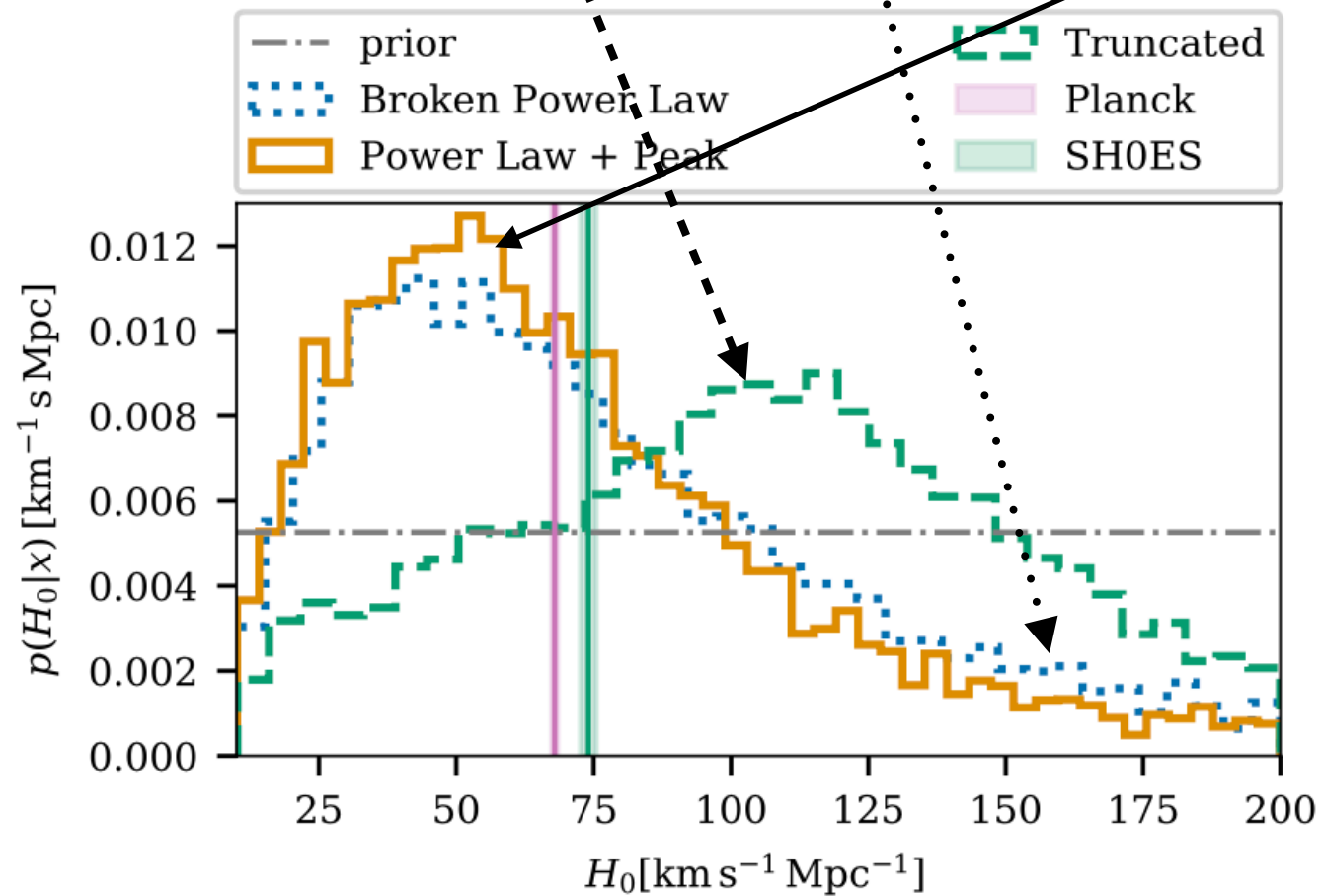
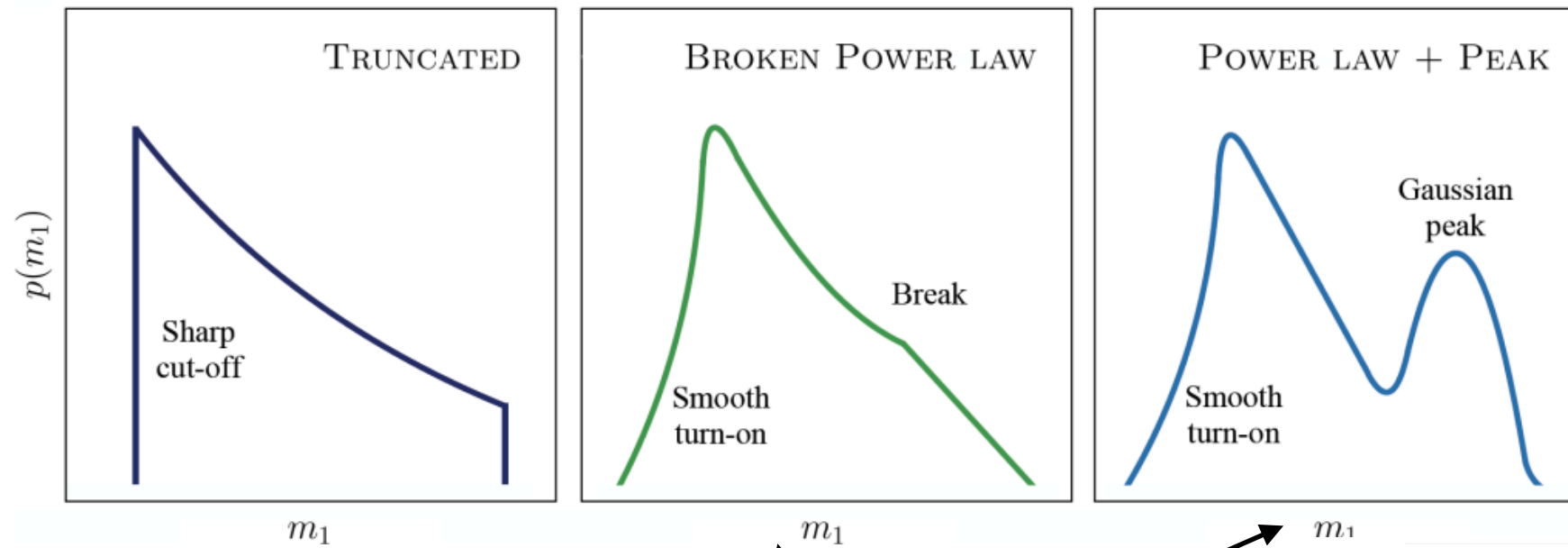
Mass model	$\log_{10} \mathcal{B}$
TRUNCATED	-1.9
POWER LAW + PEAK	0.0
BROKEN POWER LAW	-0.5

Table 3. Logarithm of the Bayes factor between the different mass models and the POWER LAW + PEAK model preferred by the data, for the case of a w_0 CDM cosmology with wide priors.

- truncated disfavoured wrt other two by a factor of ~ 100

Applied to GWTC3 :

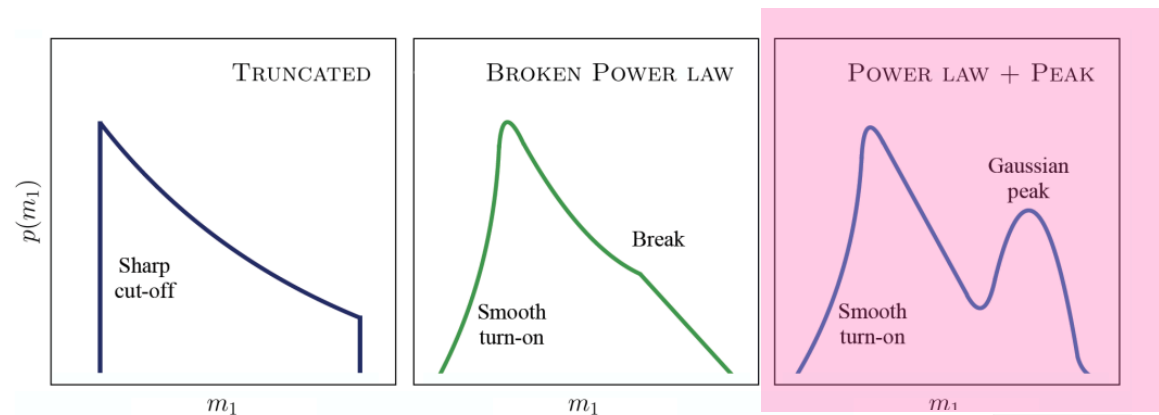
- 3 parametric mass models considered (assumed to be independent of redshift, see Nicola's lectures) [VK: arXiv:2111.03604](#)



Applied to GWTC3 :

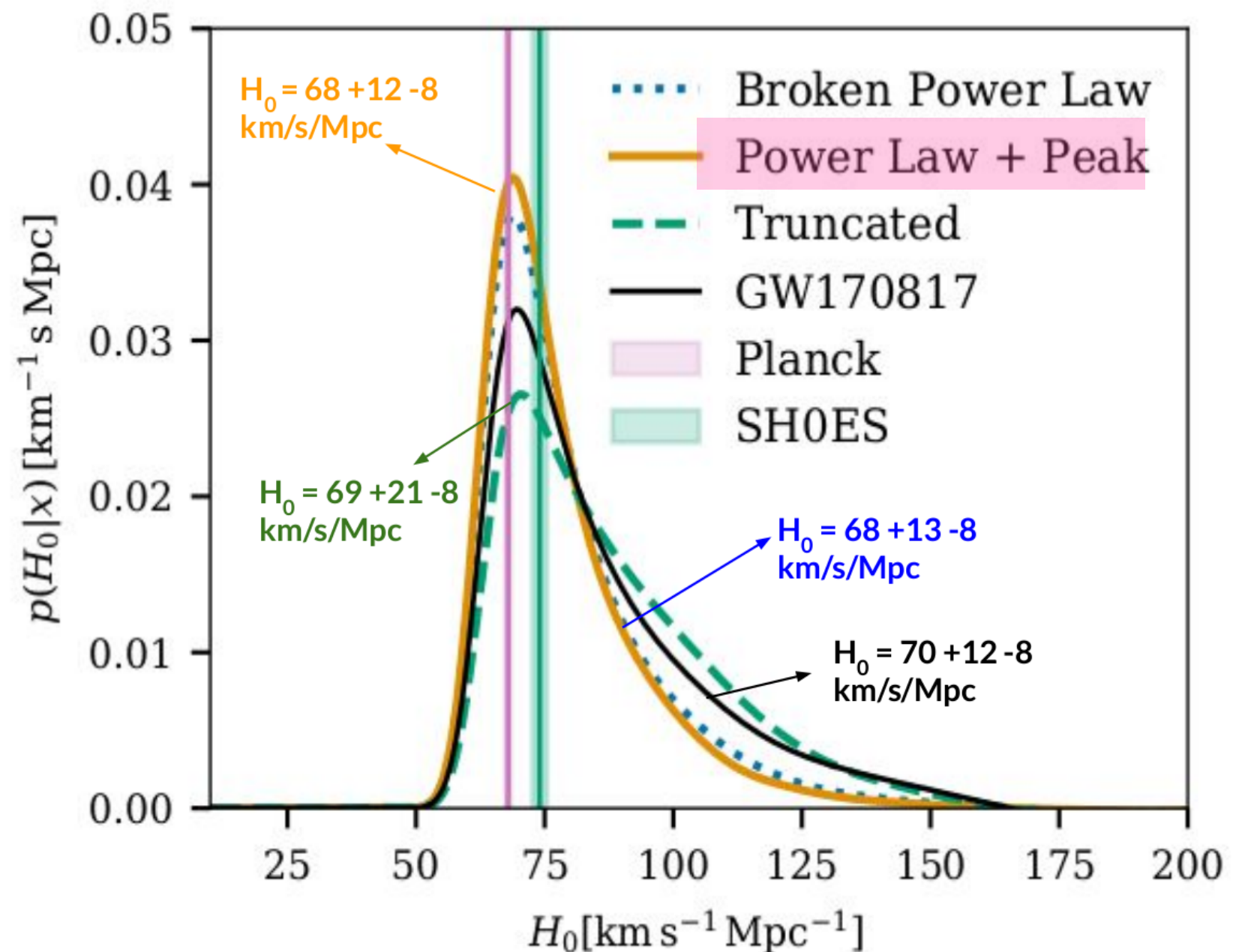
H_0 posterior for 3 mass models combined with GW170817 posterior

LVK: arXiv:2111.03604



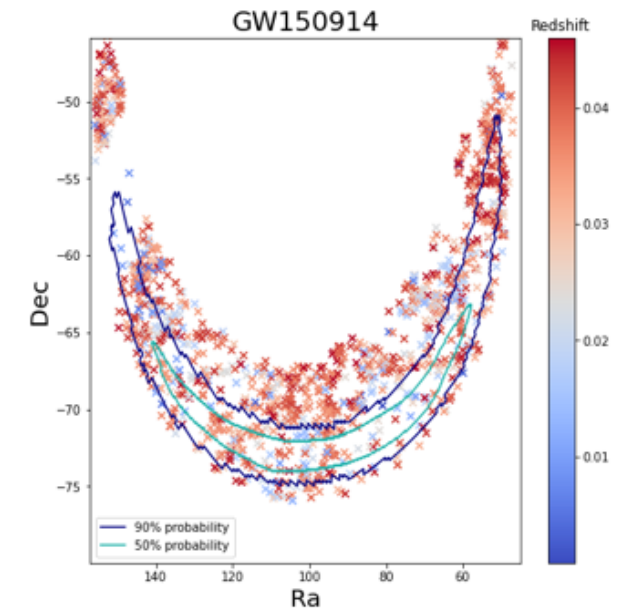
- Parametric mass models

(for studies with non-parametric models, see e.g [2302.07289])



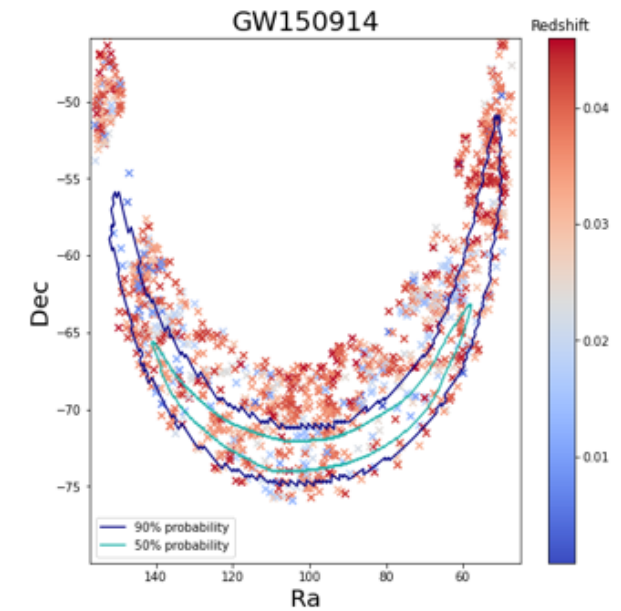
Dark sirens = **Spectral siren** with galaxy catalogue info.

- galaxy catalogues working in optical and IR bands measure billions of galaxies, $z + \delta z$; sky position ;
- How can these be combined with GW observations?

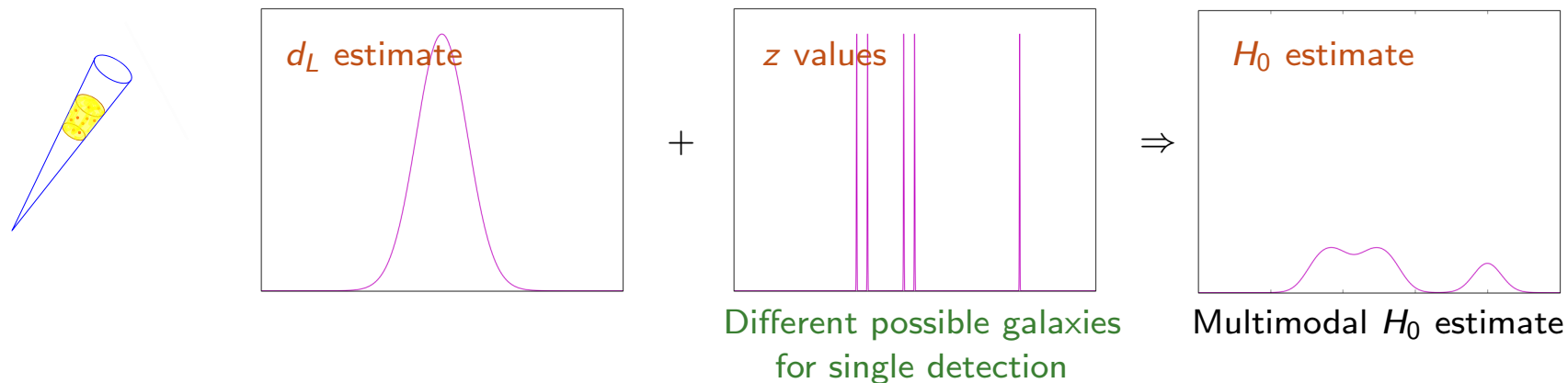


Dark sirens = **Spectral siren** with galaxy catalogue info.

- galaxy catalogues working in optical and IR bands measure billions of galaxies, $z + \delta z$; sky position;
- How can these be combined with GW observations?

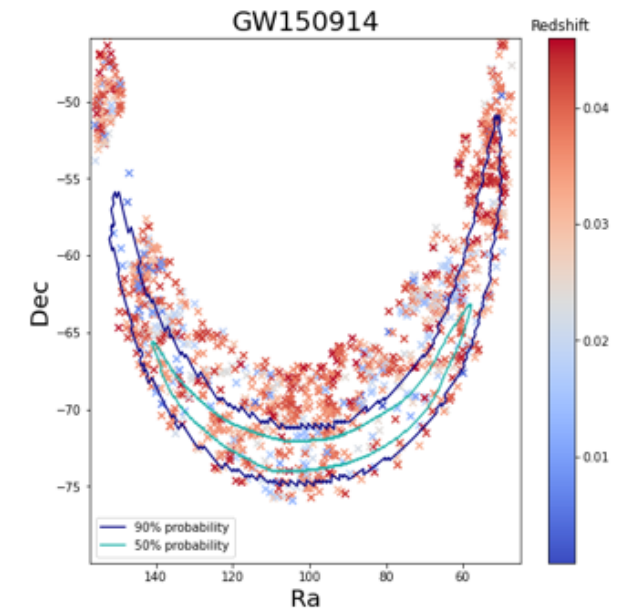


The idea: given some GW event :

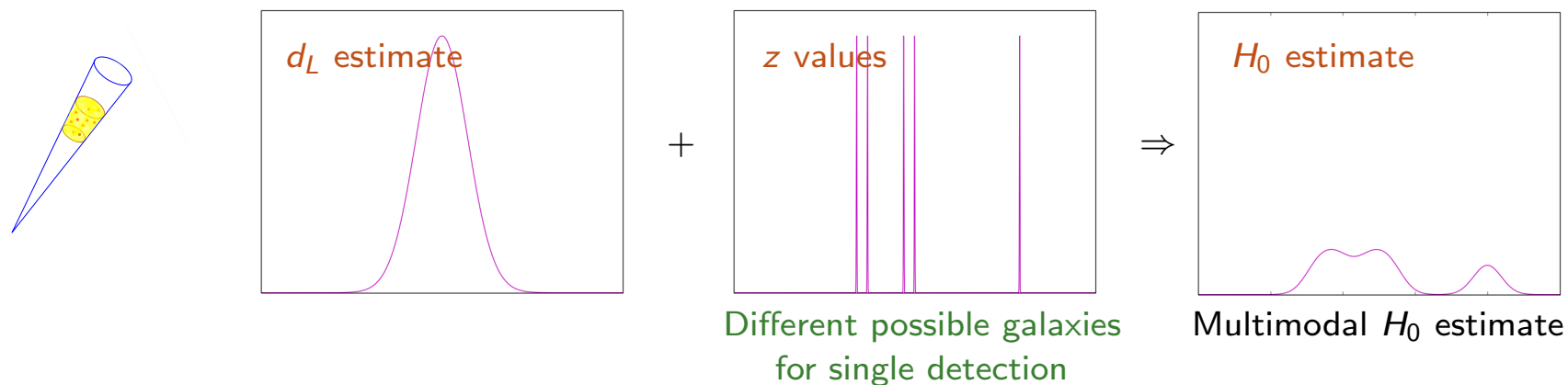


Dark sirens = **Spectral siren** with galaxy catalogue info.

- galaxy catalogues working in optical and IR bands measure billions of galaxies, $z + \delta z$; sky position;
- How can these be combined with GW observations?

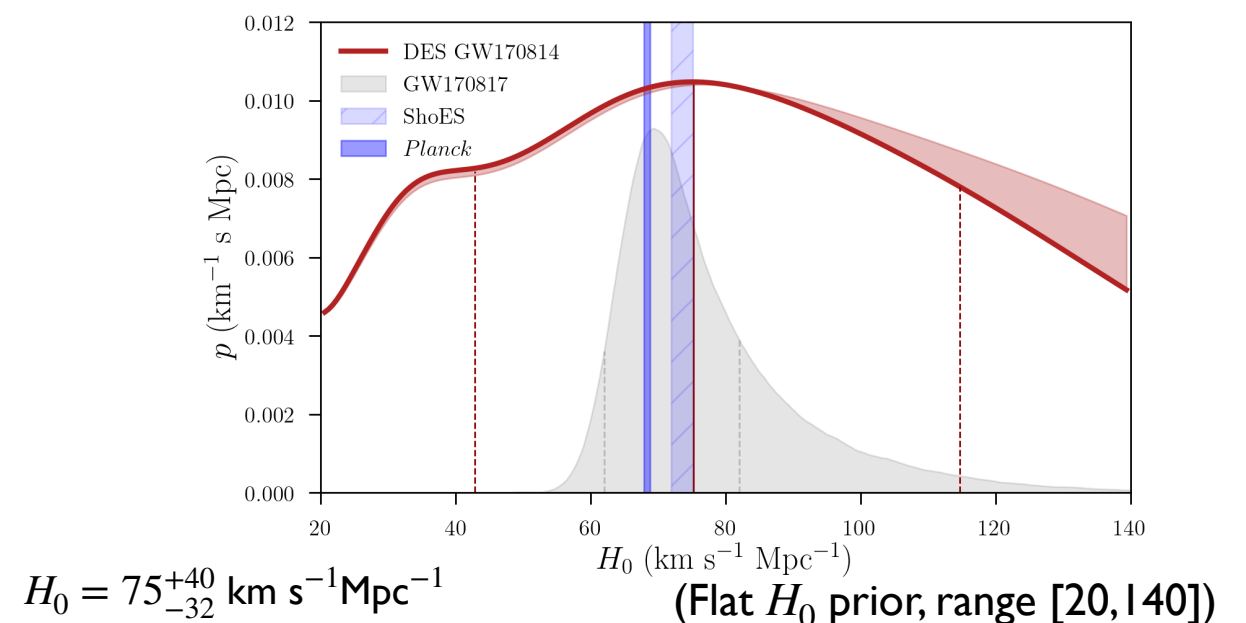


The idea: given some GW event :



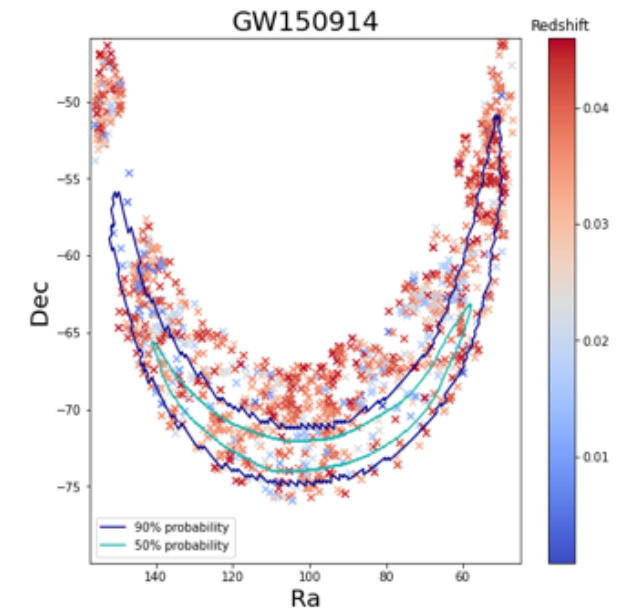
[arXiv: 1909.01540]

Example: GW170814

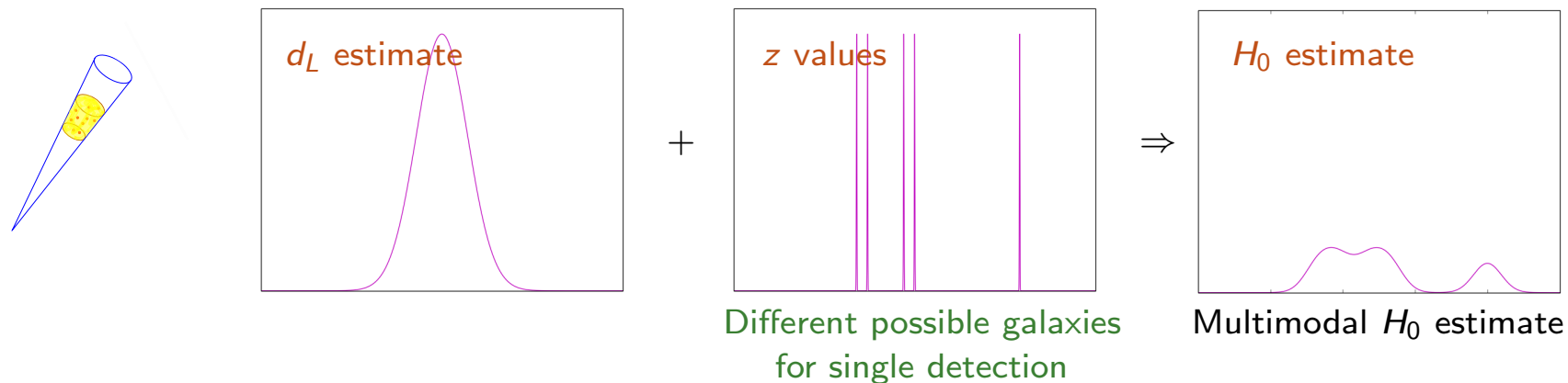


Dark sirens = **Spectral siren** with galaxy catalogue info.

- galaxy catalogues working in optical and IR bands measure billions of galaxies, $z + \delta z$; sky position;
- How can these be combined with GW observations?

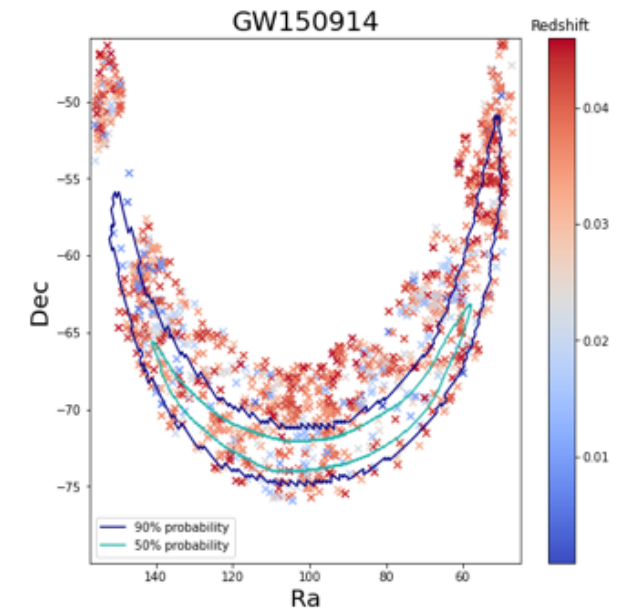


The idea: given some GW event :

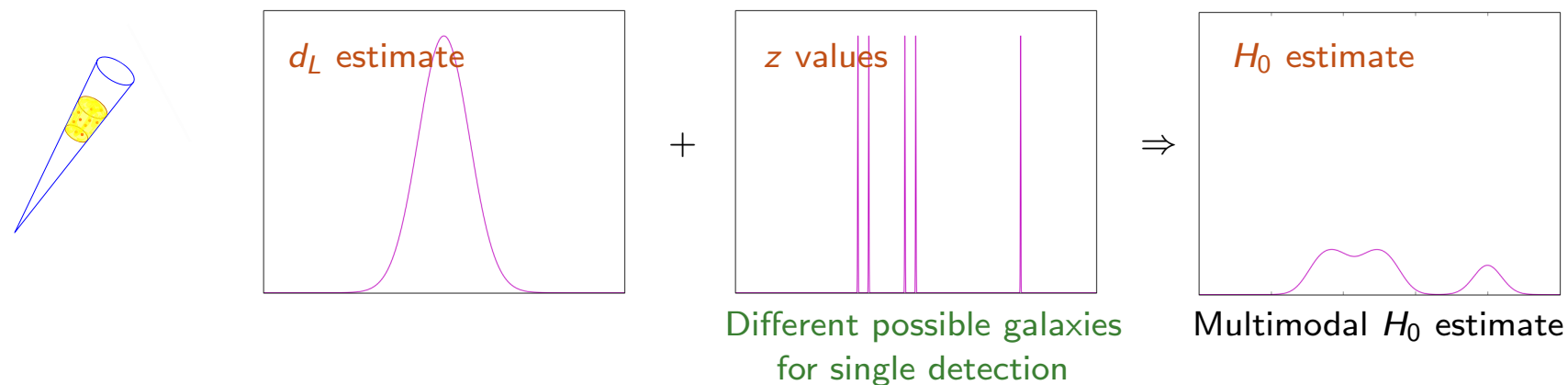


Dark sirens = **Spectral siren** with galaxy catalogue info.

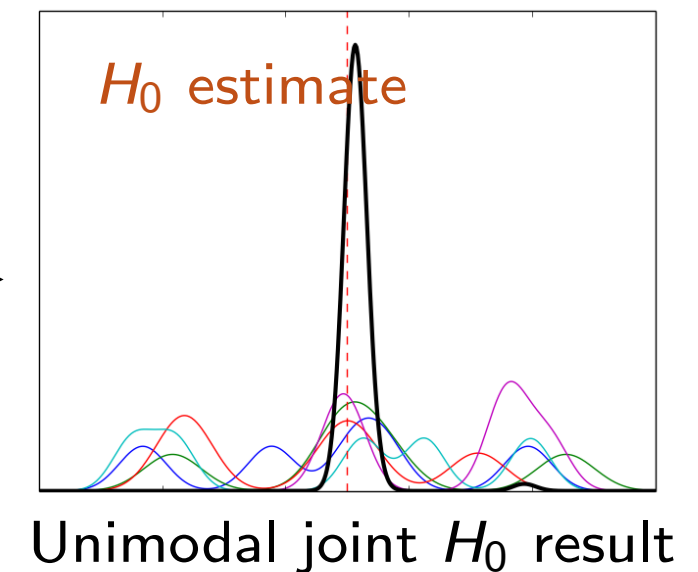
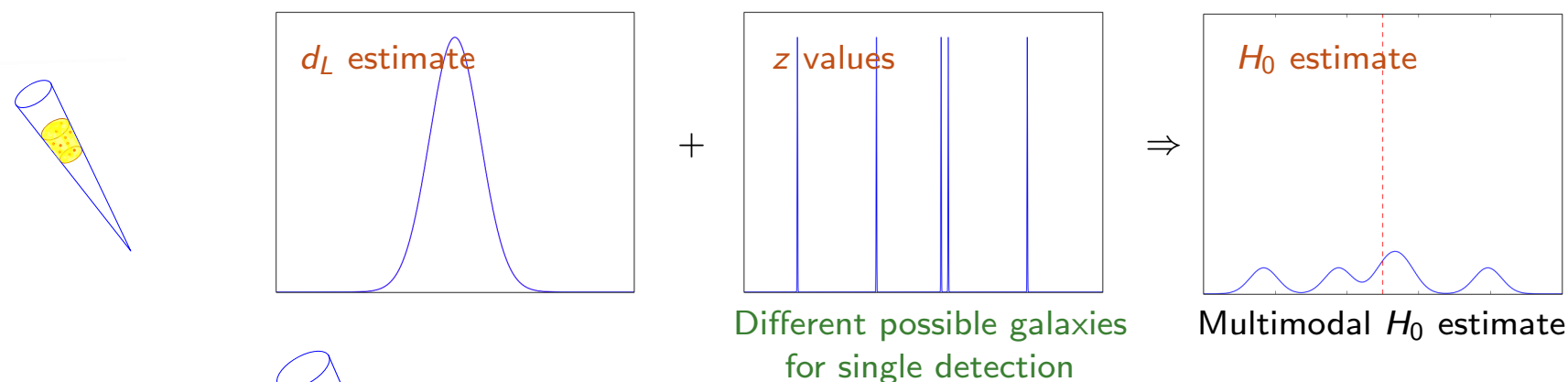
- galaxy catalogues working in optical and IR bands measure billions of galaxies, $z + \delta z$; sky position;
- How can these be combined with GW observations?



The idea: given some GW event :



Now take another GW event



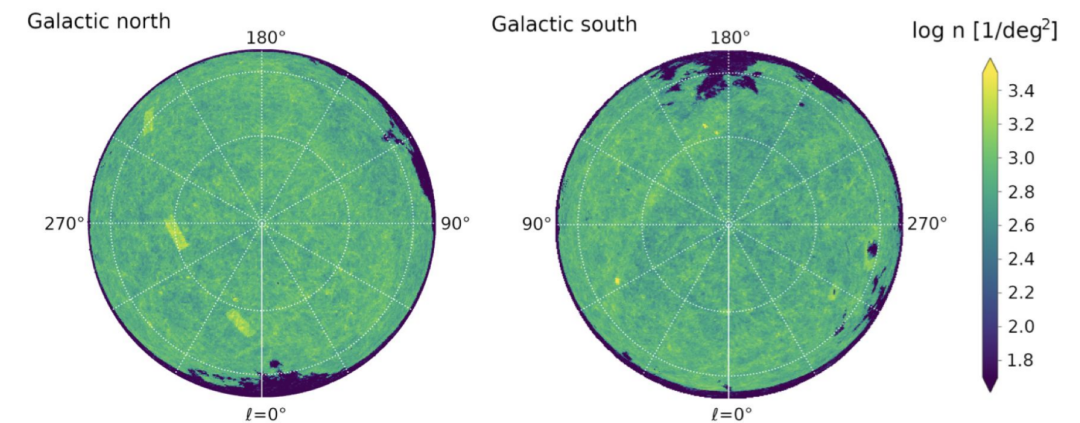
E cosi via for each GW event...

[Courtesy A.Ghosh]

Dark sirens = **Spectral siren** with galaxy catalogue info.

Applied to O3 data:

- Galaxy catalogues:
 - Glade+** all sky
 - 22 million galaxies,
 - 20% completeness up to 800 Mpc since *flux limited*..
 - photometric redshifts with relative errors
 - DES** catalogue
 - Include all galaxies in 99.9% estimated sky area of each GW event.



2/ **DES** catalogue

- BUT method not so powerful yet as :
 - bad localisation of most GW events (best is NS-BH GW190814)
 - many events are outside the range of the galaxy catalogue [galaxies too faint to be observed]
 - and also catalogues don't always cover all the sky

=> this method must be combined with the previous one.
For O3, results dominated by the population; no significant information from the catalogue.

redshift distribution of galaxies in catalogue
Distribution constant in comoving volume

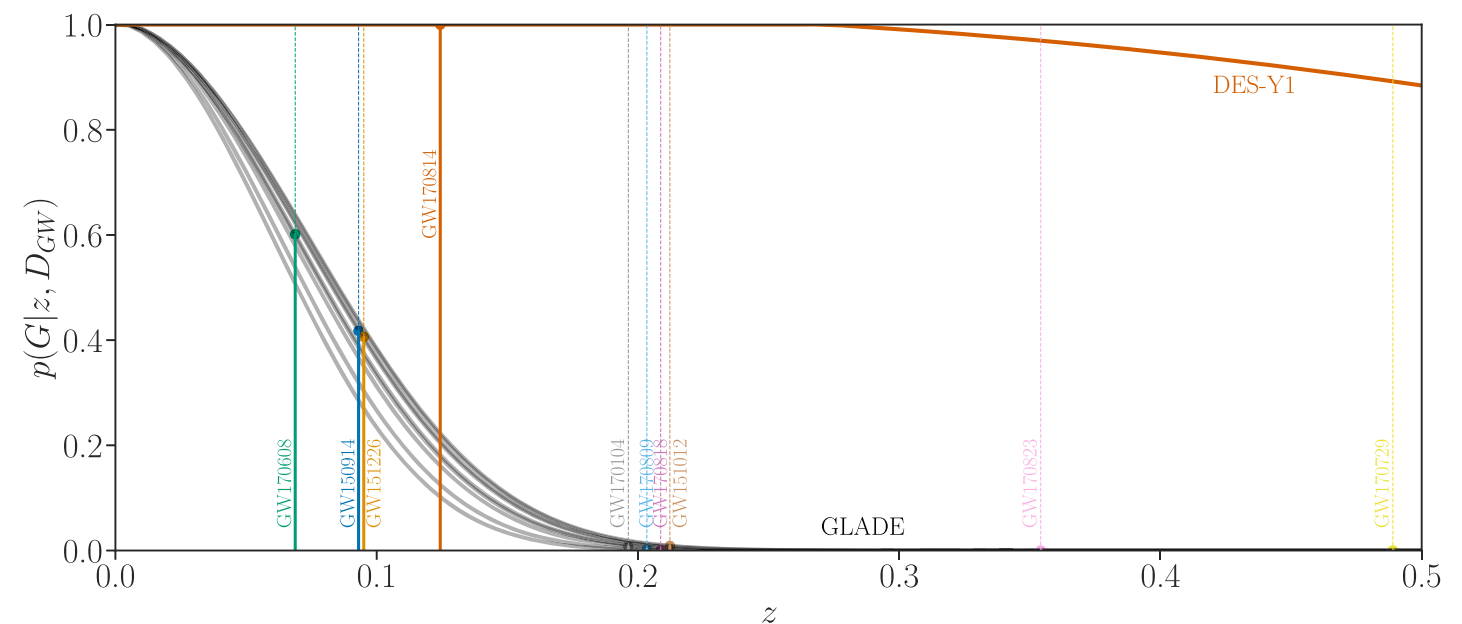
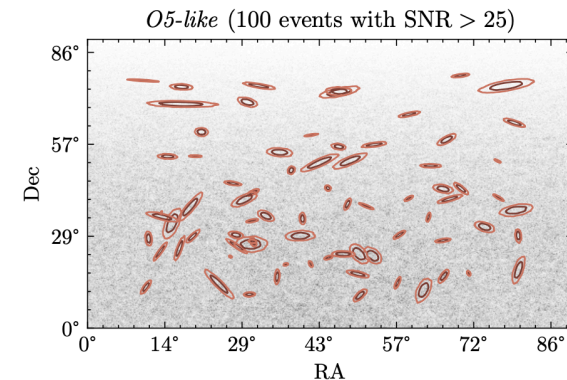
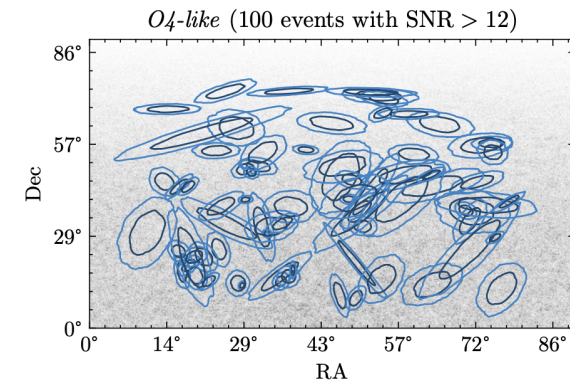


Figure 1. The probability that the host galaxy is inside the galaxy catalog, shown for GLADE (gray curves) and DES-Y1 (orange curve), as a function of redshift. For GLADE, this quantity is calculated for each individual event, using the completeness estimated within each event's sky localization. For DES-Y1, the curve is only valid in the patch of sky covering GW170814. Each curve is independent of the value of H_0 . The vertical lines show the median redshift (assuming a Planck 2015 cosmology) for each event as in Table 1. These lines are thick and solid up to the intercept with the galaxy catalog they are used with, and thin and dashed above.

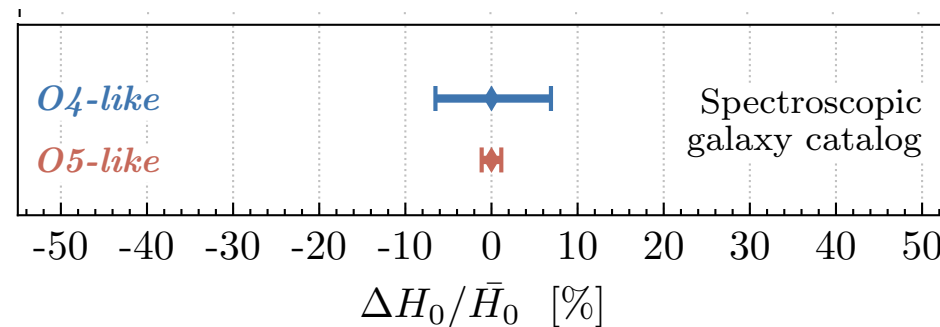
Prospects for cosmological parameter measurements: See Nicola's lecture!

with LVK

- some optimism for O5 (but not shared by all!)
- Better localisation and more complete galaxy catalogues of course help



With complete galaxy catalogue and spectroscopic z uncertainties



~ 6 %

~ 1 %

[arXiv: 2312.05302]

with ET/CE

Assuming galaxy catalogues will be complete up to $z = 1$

– best constraints: ET+CE1+CE2 network, $H_0 \sim 0.7\%$ and Ω_m at 9.0% and 90% confidence level

– Assuming Ω_m known perfectly a priori, a ET+CE1 => 0.3% precision in H_0

[arXiv: 2303.10693]

Extending the methods to constrain late-time modified gravity

$$h'' + 2[1 + \alpha_M(\eta)] \frac{a'}{a} h' + k^2 c_T^2(\eta, k/a) h = 0,$$

- In many modified gravity models, GWs satisfy a modified propagation equation. Typically, can have both a modified friction term, and also $c_T \neq 1$.
- Many theories remain with $c_T = 1, \alpha_M \neq 0$, (e.g. certain Horndeski, DHOST..): can one constrain them
- Modified luminosity distance:

$$d^{\text{GW}}(z) = d_{\text{EM}}(z) \exp \left[\int_0^z \frac{\alpha_M(z)}{1+z} dz \right]$$

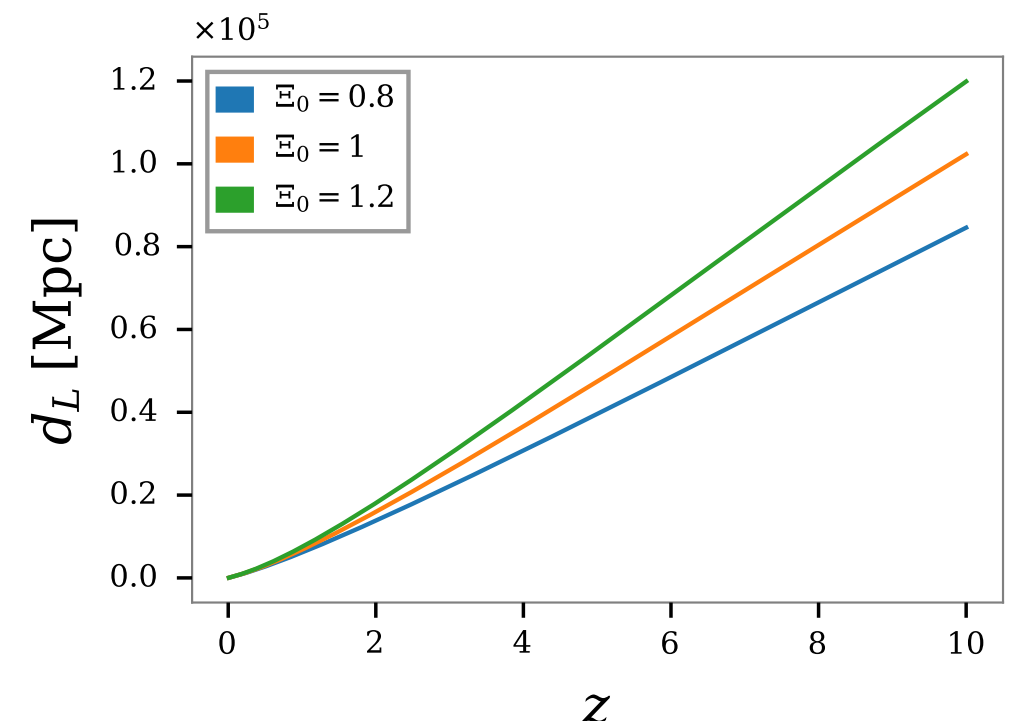
M. Lagos et al Phys. Rev. D 99, 083504 (2019),

Different parametrisations considered

a) Phenomenological model suggested in [1906.01593]

$$d_L^{\text{GW}} = d_L^{\text{EM}} \left(\Xi_0 + \frac{1 - \Xi_0}{(1+z)^n} \right)$$

$$\text{GR: } \Xi_0 = 1$$



b) Assume friction term is linked to dark energy content of the universe [1404.3713...]

$$\alpha_M(z) = c_M \frac{\Omega_\Lambda(z)}{\Omega_\Lambda(0)},$$

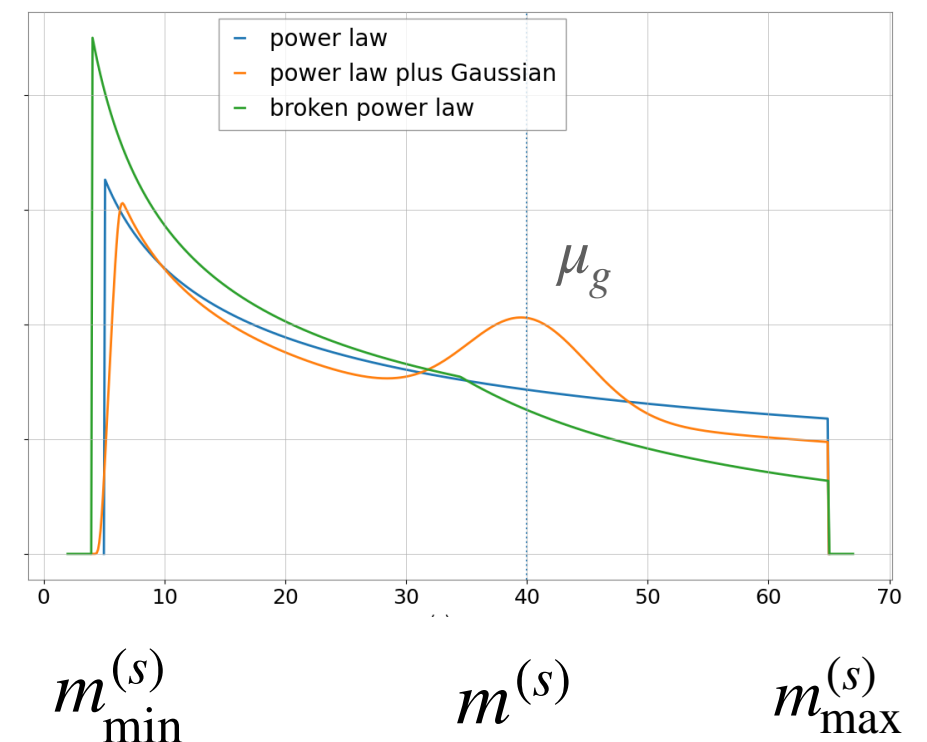
$$d_L^{\text{GW}} = d_L^{\text{EM}} \exp \left[\frac{c_M}{2\Omega_{\Lambda,0}} \ln \frac{1+z}{\Omega_{m,0}(1+z)^3 + \Omega_{\Lambda,0}} \right]$$

c) Model an extra dimensional universe with screening scale, motivated from e.g. [0709.0003, 2109.08748]

$$d_L^{\text{GW}} = d_L^{\text{EM}} \left[1 + \left(\frac{d_L^{\text{EM}}}{(1+z)R_c} \right)^n \right]^{\frac{D-4}{2n}}$$

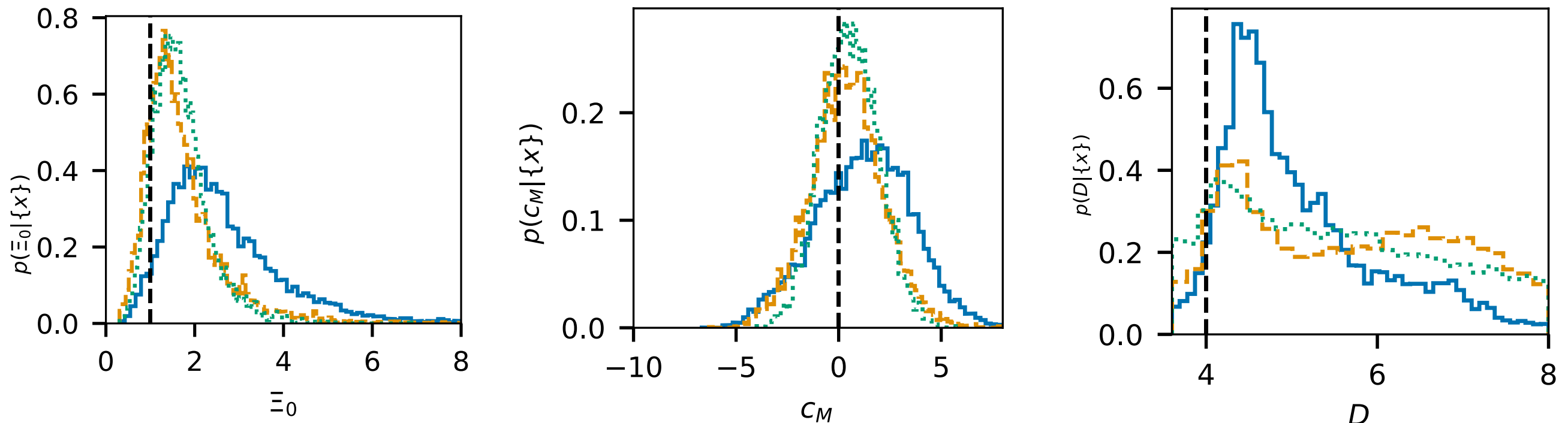
Consider 4 different source mass population models, motivated from 2010.14533, and estimate jointly, using O3 data

- the cosmological parameters (H_0, Ω_m)
- source mass parameters $(m_{\min}^{(s)}, m_{\max}^{(s)}, \dots)$
- parameters describing luminosity distance



Results using O3 data :

- Comparing Bayes factors: GR with multi-peak model is preferred!



Blue: SNR > 11, Orange SNR > 12, green SNR > 10

- For all modified gravity models, values of parameters are compatible with their GR values at 90% confidence level!

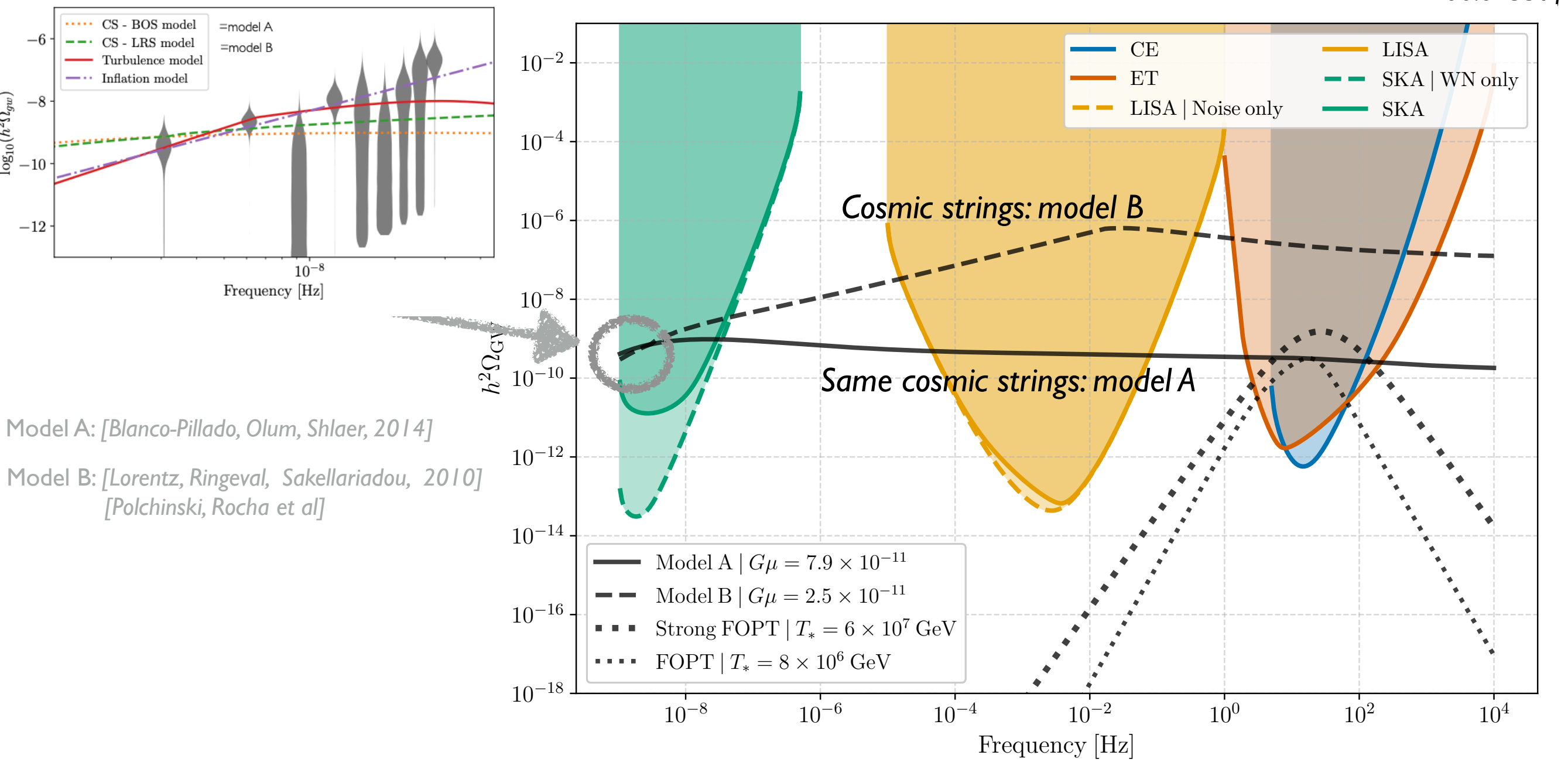
O4 will constrain these models...see set of papers due to come out in the summer.

- Lecture 1: – **Overview** on early- and late-time cosmology with GWs; current and future experiments, – **orders of magnitude**
- Lecture 2: – Late-time cosmology: GWs and $d_L(z)$
 - GWs in theories beyond GR, $d_L^{GW}(z)$
 - **standard sirens I**: Measuring H_0 with GWs and O3 results of LVK
 - Back to early-time universe: an example of what physics we can probe.
- Lecture 3 (Chiara Caprini):
 - *cosmological* stochastic GW background: **early-universe cosmology with GWs**
Solutions of the GW propagation equation in FLRW; its calculation for different sources (inflation, topological defects, first order phase transitions)
- Lecture 4 (Nicola Tamanini):
 - **Standard sirens II**: more details, statistical methods, future prospects
- Lecture 5 (Tania Regimbau):
 - **astrophysical stochastic GW background**: Definition/statistical properties, pulsar timing arrays and background from supermassive BH binaries, LVK results, prospects for the future.

Early universe cosmology,
a few more details on the cosmological SGWB from
cosmic strings

Examples of cosmological SGWB signals: Next generation detectors (SKA, LISA and ET/CE)

[Caprini et al, 2406.02359]

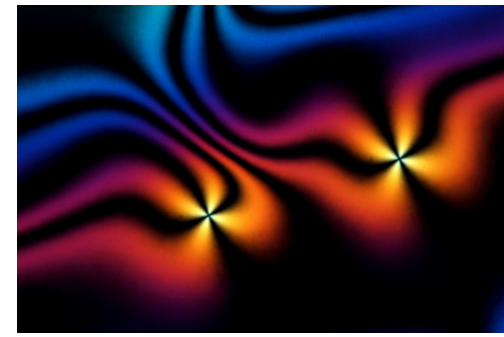


- Models A and B are *meant to describe exactly the same physics!*
- If Model B is the unique source of the SGWB signal in **PTA** then **LVK constraints** actually already *exclude it!*
- Model A would lead to an extremely loud signal in ET, with $\text{SNR} \sim 10^3$

$$\log_{10}(G\mu) = -10.63^{+0.24}_{-0.22}$$

$$G\mu \gtrsim (4.0 - 6.3) \times 10^{-15}$$

Cosmic strings



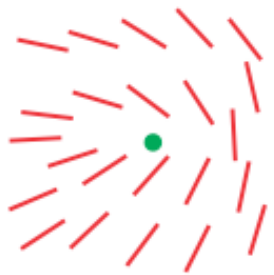
- *Line-like topological defects* which may be formed in symmetry breaking phase transitions....

[Symmetry group G , unbroken symmetry subgroup $H \Rightarrow$
vacuum manifold $\mathcal{M} = G/H$; strings formed if $\Pi_1(\mathcal{M}) \neq 1$]

in condensed matter systems (He3, He4, superconductors, BEC, NLC...), *quantum field theories*,
in soft matter, and in cosmology

[Physics Reports 1075 (2024) 1–137]

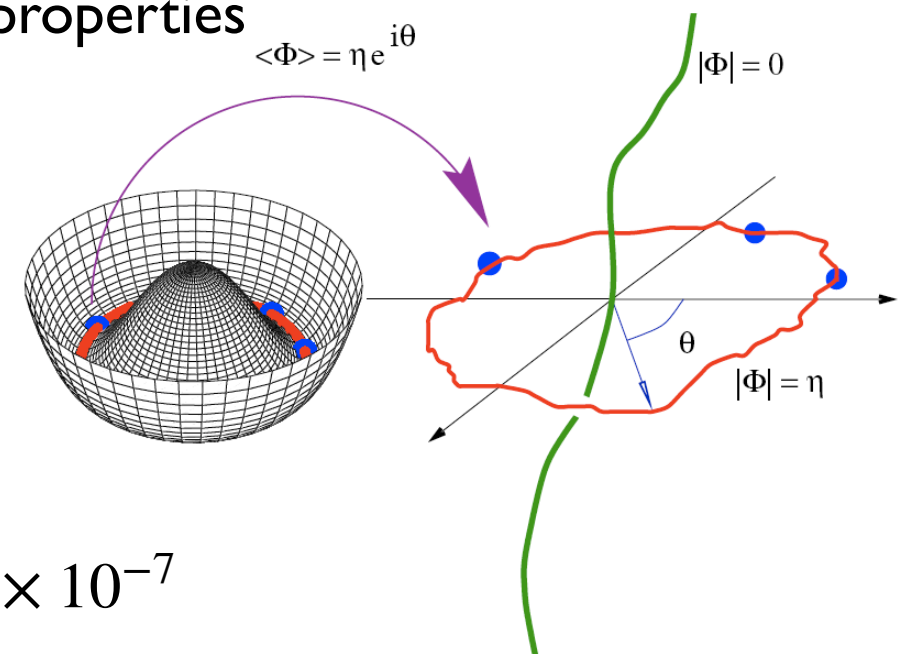
[TWB Kibble 1976]



e.g. – grand unification phase transition
– Peccei-Quinn transition (to explain smallness
of CP violations in QCD), a global $U(1)$ symmetry is broken.)

- If formed, a string network cannot disappear. It will still exist today, and source GWs today
- One parameter only: string tension, and this fixes all gravitational properties

$$G\mu \sim 10^{-6} \left(\frac{\eta}{10^{16} \text{ GeV}} \right)^2$$

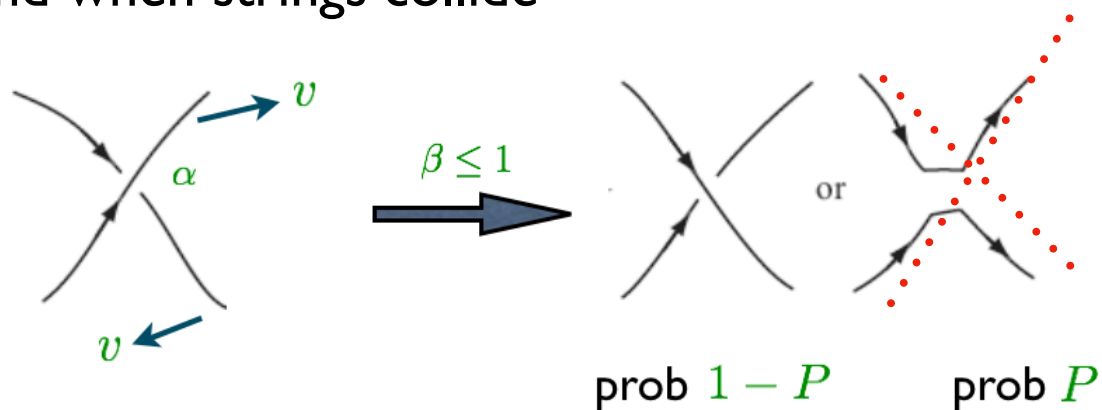


- Most well studied strings are local $U(1)$ strings, CMB: $G\mu \lesssim 1.7 \times 10^{-7}$

- a network of strings forms at the phase transition, and evolves as the universe expands.

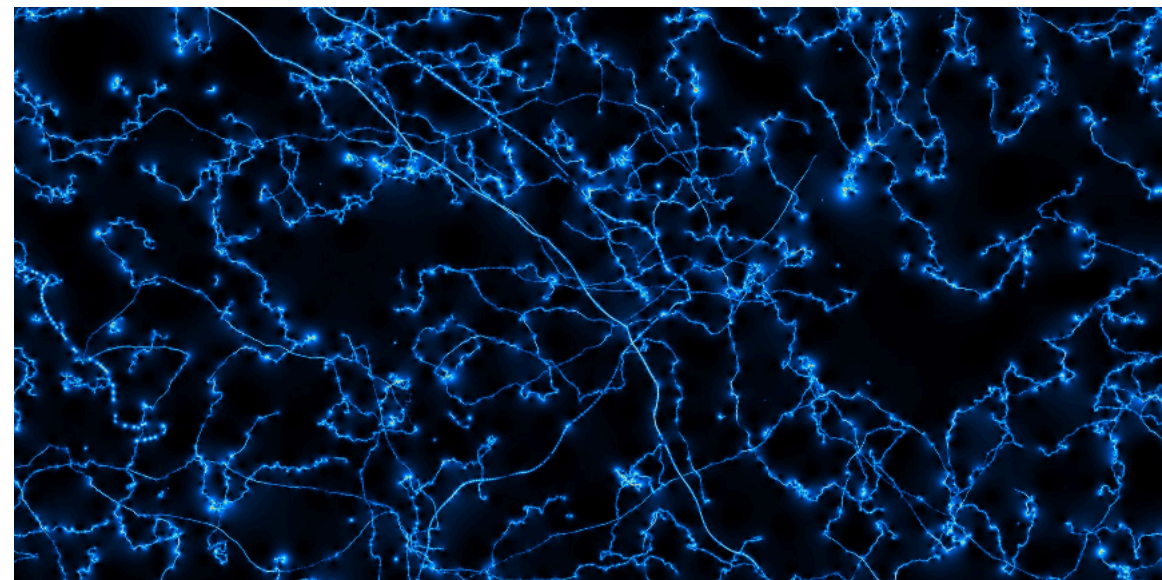
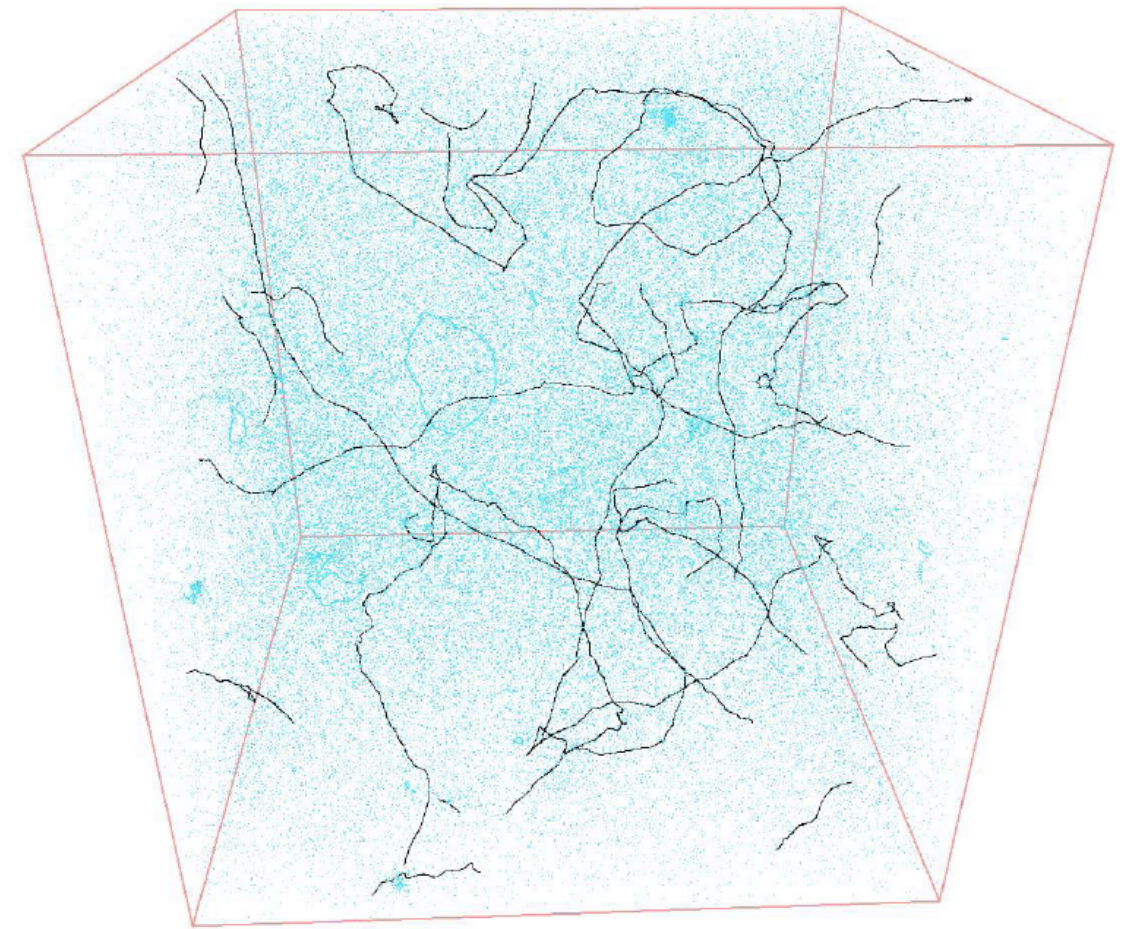
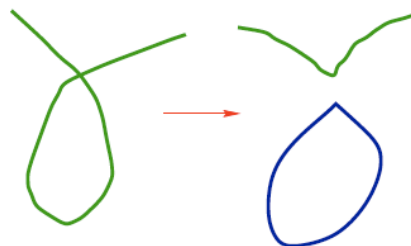
- string width $w \sim 1/\eta \ll$ macroscopic string size \Rightarrow simplified dynamics (Nambu-Goto action = equivalent of the geodesic equation for a particle)

- and when strings collide



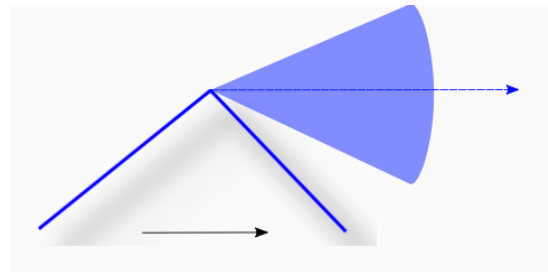
[Shellard et al,...]
[Achucarro and de Putter '06]

- in particular that means loops form

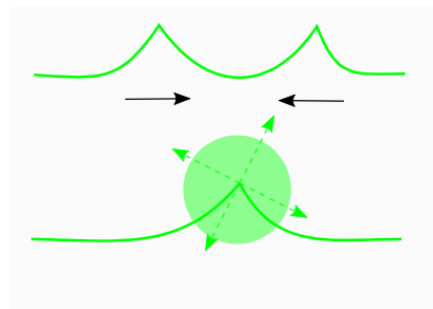


- So have all the ingredients to understand the evolution of the network, but difficult because it's highly non-linear, and a wide range of scales in the problem.
- **Some things are clear.** It's the relativistic loops that source GWs
 - They oscillate periodically in time $T \sim 1/\ell$
 - they emit GWs in harmonics $n = 1, 2, 3 \dots$ of the fundamental mode: loops lose length $\dot{\ell} = -\Gamma G\mu$
 - most emission in the lowest modes. Except...

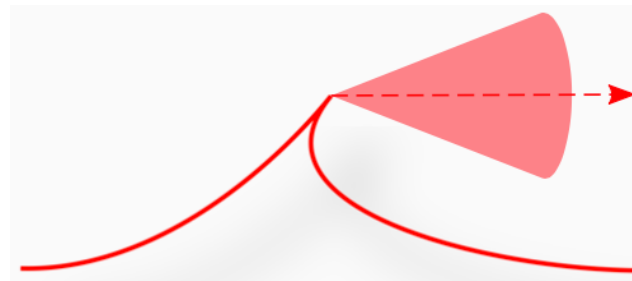
– kinks



– kink-kink collisions



– cusps



GW-form

$$h_i(\ell, z, f) = A_i(\ell, z) f^{-q_i}$$

Amplitude

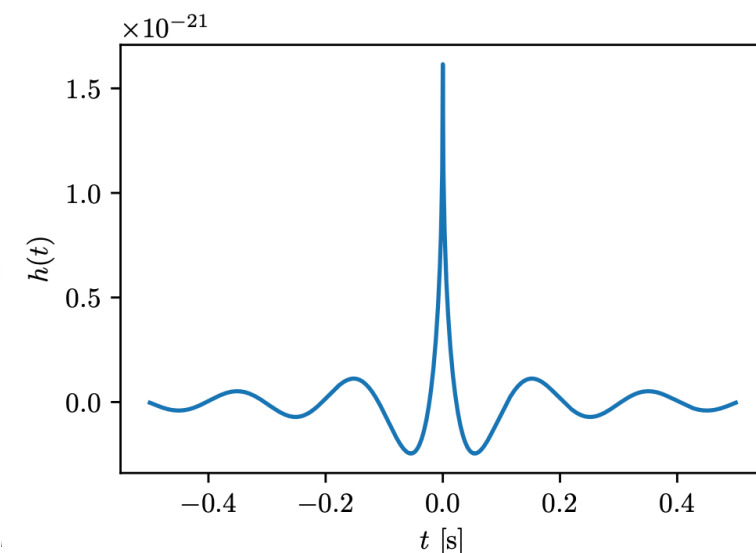
$$A_i(\ell, z) = g_{1,i} \frac{G\mu\ell^{2-q_i}}{(1+z)^{q_i-1} r(z)}$$

$$i = \{c, k, kk\} \quad q_c = 4/3, \quad q_k = 5/3, \quad q_{kk} = 2$$

$$\theta_m(\ell, z, f) = (g_2 f (1+z) \ell)^{-1/3}$$

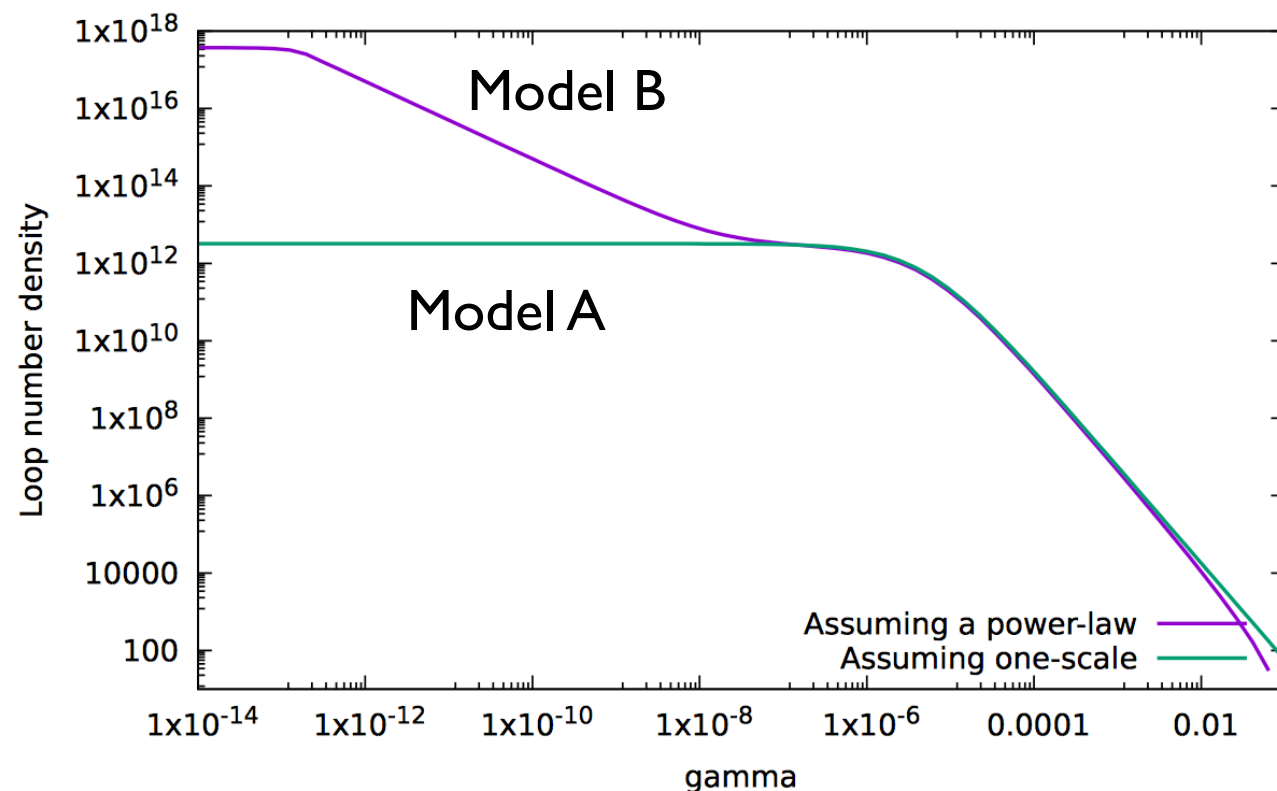
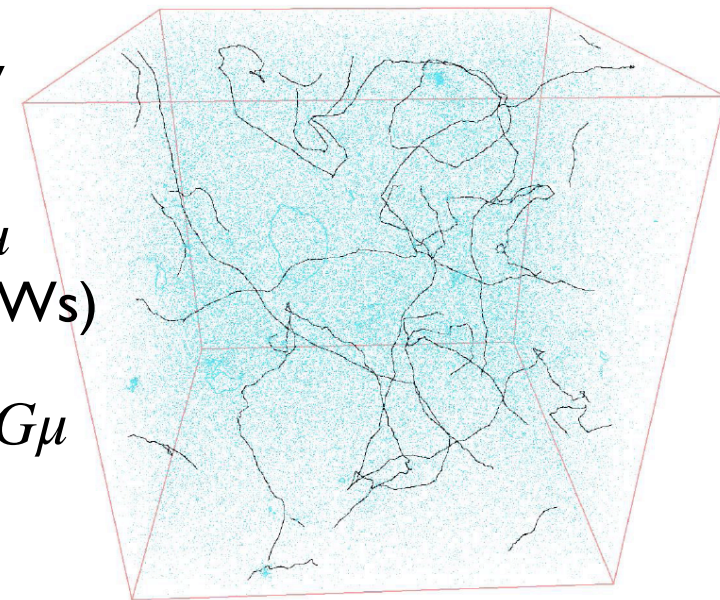
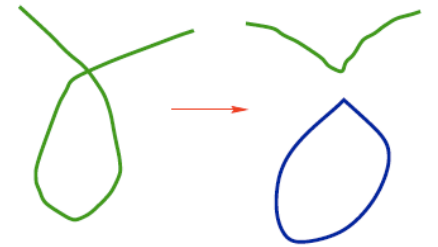
$$\theta_m < 1$$

[Vachaspati+Vilenkin,
Damour+Vilenkin; Siemens et al]

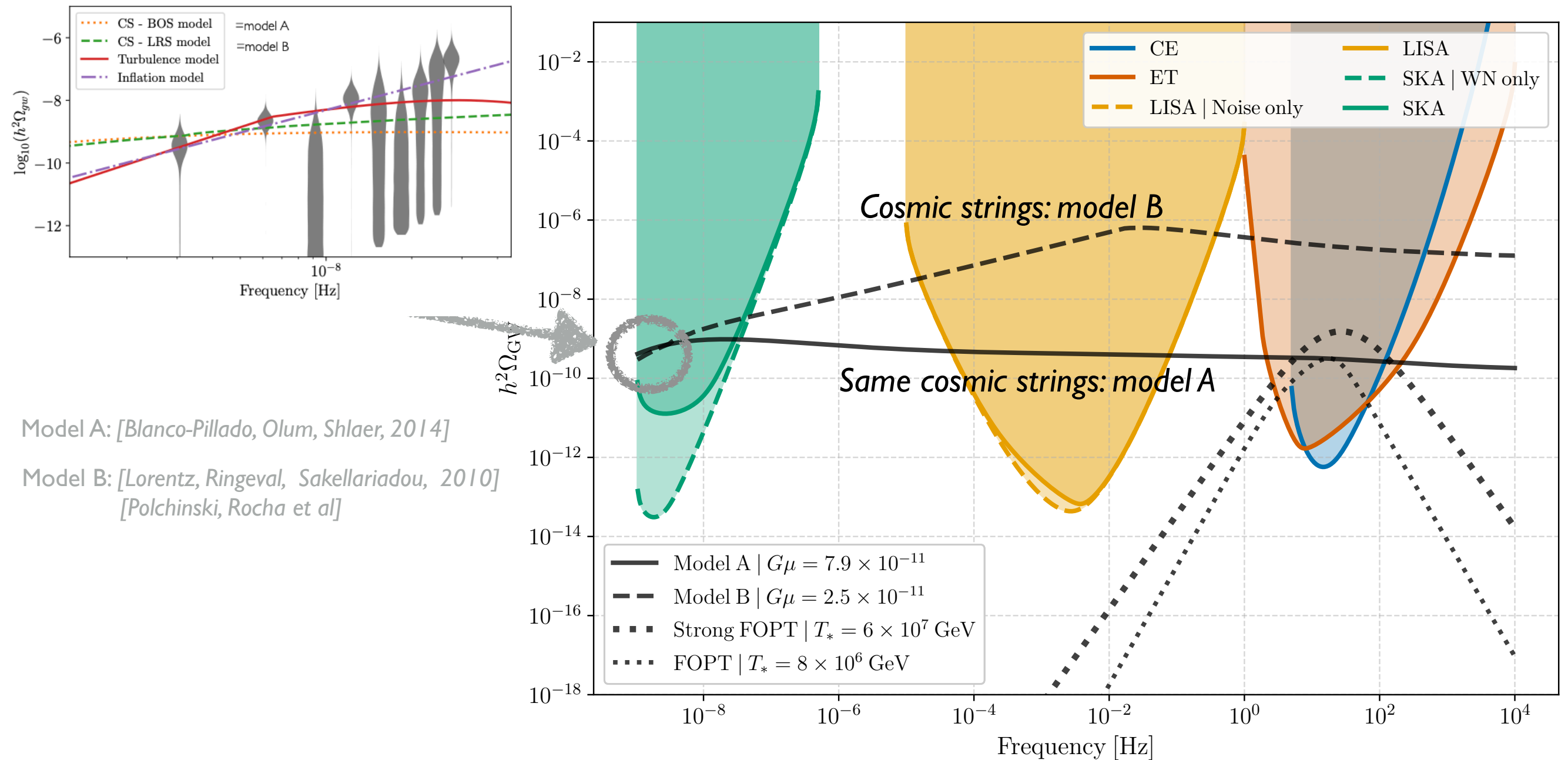


– Some things are not clear.

- How many loops of length ℓ are there at time t ; i.e. the loop density distribution $n(\ell, t)$?
- depends on how many loops (what initial size at time t) are produced via intercommutation
- and here is where the disagreements start!
- To cut a very long story short, there's *agreement* that loops “scale” (their total energy density is a fixed fraction of the energy density of the universe, and this is an attractor solution)
- and there's *agreement* on the shape of $n(\ell, t)$ on scales $\ell \gg \Gamma G\mu$ (which can be probed with numerical simulations that have no GWs)
- but there's *disagreement* on the shape of $n(\ell, t)$ on scales $\ell \ll \Gamma G\mu$



Small loops = high frequencies GWs =
Different predictions for SGWB at
high frequencies.



Model A: [Blanco-Pillado, Olum, Shlaer, 2014]

Model B: [Lorentz, Ringeval, Sakellariadou, 2010]
[Polchinski, Rocha et al]

SGWB : sum over GW emission produced from all oscillating loops produced during the evolution of the string network to today; redshift the frequency; and remove the rare bursts

Rare bursts: none detected by LVK, putting upper constraints on the string tension, but these less stringent than the SGWB constraints from LVK.

– Not a totally crazy thing to think about: in the Peccei-Quinn mechanism (to explain smallness of CP violations in QCD), a global U(1) symmetry is broken.

In some realisations, both strings and domain walls form.

Phenomenological consequences (dark matter, GWs etc) require understanding the evolution of these defect networks.

[Ferreira et al 2107.07542,
Franciolini, Racco, Rompineve,
Rompineve, Pujolas et al
Buchmann et al, 2108.05368,
Servant et al 2307.03121; and
many others.
Also many others from the '80s
Sikivie et al, Battye and Shellard;
AMR simulations A.Drew et al]

Symmetry breaking

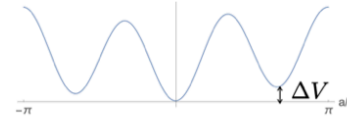
1) Spontaneous breaking
U(1) global

$$V(\phi) \sim (|\phi|^2 - f_a^2)^2$$

2) Spontaneous breaking of a global
 Z_N symmetry,

$$V_a(a) \sim \Lambda^4 \left[1 - \cos \left(\frac{Na}{f_a} \right) \right]$$

3) explicit breaking of Z_N



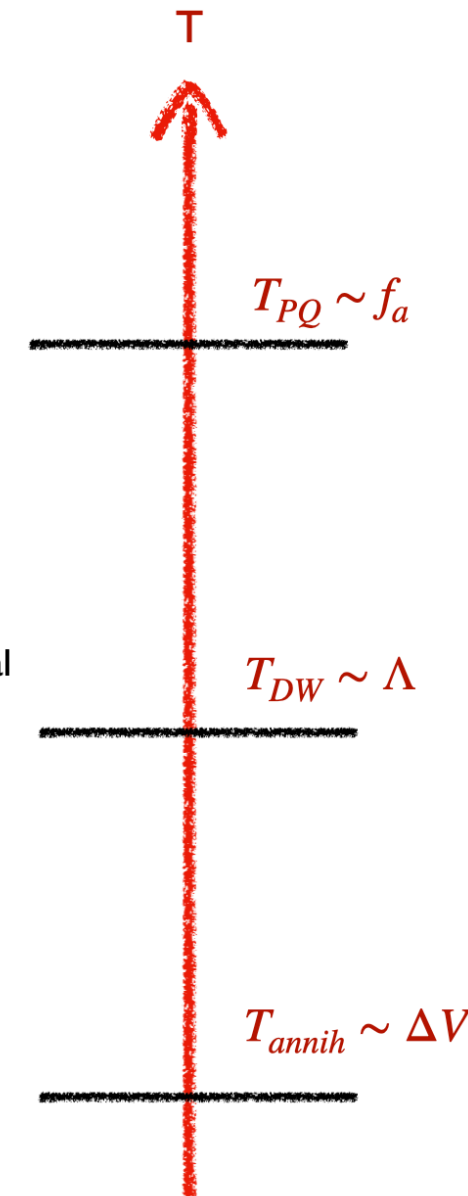
GW sources

Cosmic strings

+ transition possibly also
strongly first order

Domain walls

Domain walls annihilate



- Lecture 1: – **Overview** on early- and late-time cosmology with GWs; current and future experiments, – **orders of magnitude**
- Lecture 2: – Late-time cosmology: GWs and $d_L(z)$
 - GWs in theories beyond GR, $d_L^{GW}(z)$
 - **standard sirens I**: Measuring H_0 with GWs and O3 results of LVK
 - Back to early-time universe: an example of what physics we can probe.
- Lecture 3 (Chiara Caprini):
 - *cosmological* stochastic GW background: **early-universe cosmology with GWs**
Solutions of the GW propagation equation in FLRW; its calculation for different sources (inflation, topological defects, first order phase transitions)
- Lecture 4 (Nicola Tamanini):
 - **Standard sirens II**: more details, statistical methods, future prospects
- Lecture 5 (Tania Regimbau):
 - **astrophysical stochastic GW background**: Definition/statistical properties, pulsar timing arrays and background from supermassive BH binaries, LVK results, prospects for the future.